

**A THEORETICAL INVESTIGATION
OF ORGANIC REARRANGEMENTS**

by

GEORGE LANCE HEARD, B.Sc. (Hons.)

Submitted in fulfilment of the requirements for the degree of

DOCTOR OF PHILOSOPHY

UNIVERSITY OF TASMANIA

HOBART

OCTOBER, 1995

to the memory of my grandfather,

Lance Vernon Steel

This thesis contains no material which has been accepted for a degree or diploma by the University or any other institution, except by way of background information, and duly acknowledged in the thesis. To the best of my knowledge and belief no material previously published or written by another person except where due acknowledgement is made in the text of the thesis.

George Heard

October 1995

This thesis may be made available for loan and limited copying in accordance with the Copyright Act 1968.

Abstract

Ab initio and semi-empirical molecular orbital methods have been used to study the rearrangement pathways of ammonium ylides. There are two primary competing rearrangements of ammonium ylides, a [1,2] migration (Stevens rearrangement) and a [3,2] rearrangement (usually followed by rearomatisation as the Sommelet-Hauser rearrangement).

The mechanism of the Stevens rearrangement has been determined by an investigation of twelve model rearrangements. A dissociative radical mechanism is predicted to be the true mechanism in all cases of alkyl migration. There is no competition from the formally symmetry-forbidden concerted mechanism, or from an ion-pair dissociative pathway. The interaction of lithium ions from the bases used to generate ammonium ylides does not affect the mechanism. The effects of solvation have been taken into account using polarisable continuum models, supermolecule calculations (at PM3) and a hybrid polarisable continuum-supermolecule model (in an effort to take into account both electrostatic and specific solvent-solute interactions). Incorporation of solvent effects does not change the prediction of a radical pair pathway for the Stevens rearrangement.

The concerted transition geometry for the [3,2] rearrangement has been characterised for fifteen model rearrangements. The important factor in the activation energy of the [3,2] rearrangement is in aligning the carbanion lone pair to be in a favourable position to interact with the vacant π^* orbital of the double bond. This requires rotation about the N-C and C-C bonds.

The competition between the [1,2] and [3,2] rearrangements for a prototype ylide, N-methyl-3-propenyl ammonium methyllide, has been investigated. The activation energies for the two processes are remarkably close, separated by 2 kJ mol⁻¹ at ROMP2/6-311+G(d,p). Increasing the size of the basis set leads to a relative stabilisation of the [3,2] transition geometry, while higher levels of electron correlation

(such as CCSD(T)) favour the [1,2] rearrangement. Incorporation of solvent effects via the SCRF polarisable continuum model leads to a lowering of the energy barrier of the concerted [3,2] rearrangement, but have little effect on the radical [1,2] rearrangement.

The activation energies of both pathways have been calculated for ylides bearing substituents on the ammonium nitrogen and the double bond. Substituents at nitrogen lead to an ylide which is sterically unstable, and hence a preference for the dissociative [1,2] rearrangement. Electron-withdrawing substituents on the double bond show a preference for the [3,2] rearrangement, mildly electron-donating alkyl substituents have very little effect on activation energies.

The sulfonium ylide is shown to have a much smaller barrier to the [3,2] rearrangement than its nitrogen analogue, and there is no competition from the Stevens rearrangement, which, in the sulfonium case, has a similar barrier to dissociation as in the nitrogen case.

Acknowledgements

To Dr Brian Yates I wish to express my immense gratitude. I could not wish for a more co-operative, competent and helpful supervisor.

I would like to thank the staff of the Chemistry Department of the University of Tasmania for their assistance throughout my project, in particular Anne Kelly, for her organisational skills and assistance.

I would like to thank Vicky Barnett, Catherine Rowland, Jason Hoare and Barry O'Grady for proofreading sections of this thesis.

Funding of a Postgraduate Award by the ARC is gratefully acknowledged, as are the grants of computer time provided by the Australian National University Supercomputing Facility (ANUSF) and Australian Supercomputing Technology (ANSTO). I also thank the University of Tasmania Information Technology Services for access to their computer facilities.

I would like to thank Richard Wong, Peter Gill, Arvi Rauk, Wesley Allen and the late Eddie Schipper for stimulating discussions during the course of my PhD.

I would like to thank my family and friends for support, in particular my close friends Andrew Butt, Michael Hardie, Peter O'Neill, Angela Richardson, Peter Traill, and Damien Foster.

The computational chemistry research group at the University of Tasmania has been a great environment - thanks to all the students who have been a part of it: Mark Mackey, Robert Martin, Bruce Reardon, Andrew Clippingdale, Paul Anderson, Yos Ginting, and particularly the long-suffering Katrina Frankcombe.

Glossary of terms

AMI	Austin Model I
CC	Coupled-Cluster
CCSD	Coupled Cluster (Singles and Doubles)
CI	Configuration Interaction
CIDNP	Chemically Induced Dynamic Nuclear Polarisation
COSMO	Conductor-Like Screening Model
DBU	1,8-diazobicyclo[5.4.0]undec-7-ene
DFT	Density Functional Theory
DMF	Dimethyl formamide
EF	Eigenvector Following
HF	Hartree-Fock
HMPA	Hexamethyl phosphoramide
LCAO	Linear Combination of Atomic Orbitals
MINDO	Modified Intermediate Neglect of Differential Overlap
MNDO	Modified Neglect of Differential Overlap
MP	Møller-Plesset
NMR	Nuclear Magnetic Resonance spectroscopy
PCM	Polarisable Continuum Model
PES	Potential Energy Surface
PM3	Parameterised Model 3
PUMP	Projected Unrestricted Møller-Plesset
RHF	Restricted Hartree-Fock
ROHF	Spin-Restricted Open-shell Hartree-Fock
ROMP	Restricted Open-shell Møller-Plesset
SCF	Self-Consistent Field
SCRf	Self-Consistent Reaction Field

Glossary (cont.)

UHF	Unrestricted Hartree-Fock
UMP	Unrestricted Møller-Plesset

Atom Legend (for all perspective diagrams)



Hydrogen



Carbon



Nitrogen



Oxygen



Lithium (Chapter 5)



Sulfur (Chapter 8)

List of Publications

Heard, G.L.; Marsden, C.J.; Scuseria, G.E. "The trifluoride anion: a difficult challenge for quantum chemistry" *J. Phys. Chem.* **1992**, *96*, 4359-4366

Heard, G.L.; Frankcombe, K.E.; Yates, B.F. "A theoretical study of the Stevens rearrangement of methylammonium methylide and methylammonium formylmethylide" *Aust. J. Chem.* **1993**, *46*, 1375-1388

Heard, G.L.; Yates, B.F. "Theoretical studies of the Stevens rearrangement of alkylammonium ylides" *J. Mol. Struct. (Theochem)* **1994**, *310*, 197-204

Heard, G.L.; Yates, B.F. "Steric and electronic effects on the mechanism of the Stevens rearrangement - large organic ylides of unusually high symmetry" *Aust. J. Chem.* **1994**, *47*, 1685-1694

Heard, G.L.; Yates, B.F. "Theoretical evaluation of alternative pathways in the Stevens rearrangement" *Aust. J. Chem.* **1995**, *48*, 1413-1423

Heard, G.L.; Yates, B.F. "A hybrid supermolecule-PCM approach to solvation - application to the mechanism of the Stevens Rearrangement" *J. Comp. Chem.*
(accepted)

Table of contents

Chapter 1. Introduction	1
1.1. Ammonium ylides	1
1.2. The Stevens [1,2] Rearrangement	4
1.3. Sommelet-Hauser [3,2] rearrangement	8
1.4. Hofmann Elimination of ammonium ylides	11
1.5. Competition between the [1,2] and [3,2] rearrangements	11
1.6. The Project	19
Chapter 2. Theoretical Methods	21
2.1. Introduction	21
2.2. Quantum theory of molecules	21
2.3. Semi-empirical molecular orbital theory	25
2.4. Ab initio molecular orbital theory	26
2.5. Ab initio basis sets	26
2.6. Electron Correlation Methods	27
2.6.1. Møller-Plesset Perturbation Theory	27
2.6.2. Coupled-Cluster Theory	29
2.7. Geometry optimisation	29
2.8. Theoretical description of solvation effects	30
2.8.1. Supermolecule Calculations	32
2.8.2. Self Consistent Reaction Field (SCRF) theory	32
2.8.3. Conductor-Like Screening Model (COSMO)	33
2.8.4. Hybrid methods	33
2.9. Computational details	34
2.10. Conclusions	34

Chapter 3. The Stevens [1,2] rearrangement	37
3.1. Introduction	37
3.2. The Stevens rearrangement of methylammonium methylene	38
3.2.1. Ethylamine (1)	38
3.2.2. Methylammonium methylene (2)	38
3.2.3. Aminomethyl radical (3)	45
3.2.4. Concerted Transition structure for 2a → 1 (4)	47
3.3. The Stevens rearrangement of methylammonium formylmethylene (6)	50
3.3.1. 2-aminopropanal (5)	50
3.3.2. Methylammonium formylmethylene (6)	50
3.3.3. Aminoformylmethyl radical (7)	54
3.3.4. Concerted transition geometry for 6 → 5 (8)	57
3.4. Energy profile of the prototype Stevens rearrangement	59
3.5. Conclusions	60
Chapter 4. Effects of substitution on the Stevens rearrangement	65
4.1. Introduction	65
4.2. Ab initio studies of substitution	70
4.2.1. Effect on amine geometries	70
4.2.2. Effect on ylide geometries	74
4.2.3. Effect on radical intermediates	78
4.2.4. Effect on concerted transition geometries	83
4.2.5. Effect on the reaction profile	87
4.3. Semi-empirical studies of more complex ylides	89
4.3.1. Geometries of species predicted by semi-empirical theory	89

4.3.2. The use of a halogen to approximate the steric effect of a phenyl group	102
4.3.3. Relative energies of species	102
4.3.4. Comparison with ab initio predictions	104
4.4. Single-point MP2/6-31G(d) calculations on optimised semi-empirical geometries	107
4.5. Conclusions	109
Chapter 5. Evaluation of alternative pathways in the Stevens rearrangement.	110
5.1. Introduction.	110
5.2. The ion-pair pathway	111
5.3. Interaction of lithium ions	115
5.3.1. Lithium ion interaction with methylammonium methylene	115
5.3.2. Interaction of a lithium ion with methylammonium formylmethylene	116
5.4. Conclusions	119
Chapter 6. The effects of solvation on the Stevens rearrangement	131
6.1. Introduction	131
6.2. Supermolecule studies of the Stevens rearrangement of methylammonium formylmethylene	132
6.2.1. Geometries of complexed species	132
6.2.2. Complexation energies of supermolecules	141
6.3. SCRF studies of ylide rearrangements	142
6.4. COSMO studies of methylammonium formylmethylene	144

6.5.	Hybrid COSMO-supermolecule studies of solvation.	146
6.5.1.	Geometries of solvated clusters	146
6.5.2.	Interactions of solvent molecules with the solute	153
6.5.3.	Complexation energy of solvated clusters	154
6.6.	Comparison of solvation methods on the Stevens rearrangement.	155
6.7.	Conclusions	157
Chapter 7.	Competing rearrangements of ammonium ylides	158
7.1.	Introduction	158
7.2.	The rearrangement ylide and product amine	160
7.2.1.	N-methyl-3-propenyl ammonium methyllide (1)	160
7.2.2.	N-methyl-4-butenylamine (2)	162
7.3.	The Stevens [1,2] rearrangement of N-methyl-3-propenyl ammonium methyllide	164
7.4.	The Sommelet-Hauser [3,2] rearrangement of N-methyl-3-propenyl ammonium methyllide	166
7.5.	Relative energies of competing pathways	168
7.5.1.	Effect of level of theory on activation energies	168
7.5.2.	Effect of basis set on activation energies	169
7.5.3.	Effect of solvation on activation energies	170
7.6.	Effect of substitution on competing rearrangements	171
7.6.1.	Effects of substitution at nitrogen	177
7.6.2.	Effects of substitution at the double bond	178
7.6.3.	ab initio studies of solvation	179
7.7.	Conclusions	180

Chapter 8. Sulfonium ylides	182
8.1. Introduction	182
8.2. The Stevens [1,2] rearrangement of S-methyl-S-propenylsulfonium methylide	183
8.3. The [3,2] rearrangement of S-methyl-S-propenylsulfonium methylide	183
8.4. Conclusions	186
 References	 187

Chapter 1. Introduction

1.1. Ammonium ylides¹

An ammonium ylide consists of a formally quaternary nitrogen bound to a carbanion, as shown in Figure 1.1. This inherently unstable species undergoes spontaneous rearrangement to a more stable amine via one of a number of possible pathways. The high degree of substitution in the product amine, and the fact that the rearrangement pathways allow for a great deal of stereo- and regio- control makes ammonium ylides important precursors in organic synthesis.

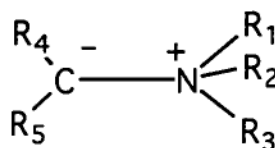


Figure 1.1. The structure of an ammonium ylide.

There are many routes to the synthesis of ammonium ylides. The most common is the deprotonation of an ammonium salt by a strong base, as shown in Figure 1.2. The salt is generally generated by an active alkylating agent, usually an alkyl or aryl halide, and the ylide by a strong lithium base.

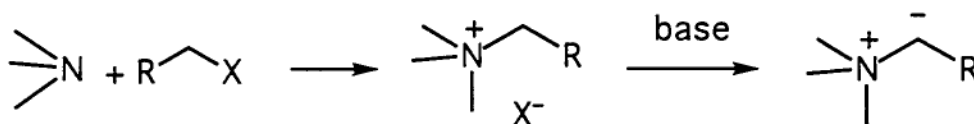


Figure 1.2. The salt method for generation of ammonium ylides.

Ammonium ylides may also be generated by direct addition of a carbene or benzyne to an amine² (Figure 1.3). Carbenes generated from diazonium salts by irradiation or by metal catalysis will react with organic amines if there are no other available substrates. This is most easily accomplished by using intramolecular attack to form a cyclic ylide^{3,4} (Figure 1.4).

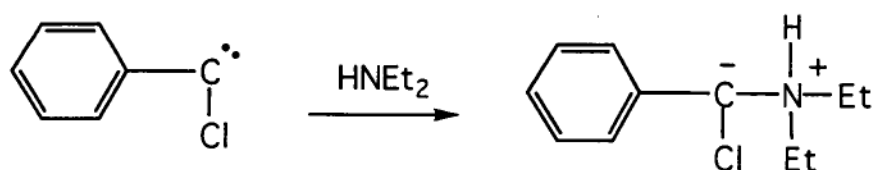


Figure 1.3. Formation of an ammonium ylide by addition of an amine to a carbene.

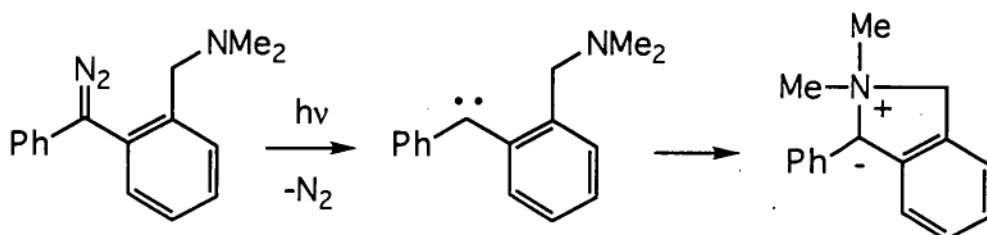


Figure 1.4. Formation of an ammonium ylide by intramolecular rearrangement of a carbene.

Desilylation of trimethylsilyl ammonium salts by fluoride ion (Figure 1.5) also produces ammonium ylides⁵⁻⁷. This method is particularly useful since the carbanion can be localised, an advantage over the base generation method where there may be a choice of abstractable protons.



Figure 1.5. Formation of ammonium ylides by fluoride anion induced desilylation of trimethylsilyl ammonium salts.

Another novel method of generating ammonium ylides involves alkyne insertion into chromium-stabilised aminocarbenes⁸ (Figure 1.6). This produces ylides that are difficult to demetallate, however, and their synthetic uses are limited.

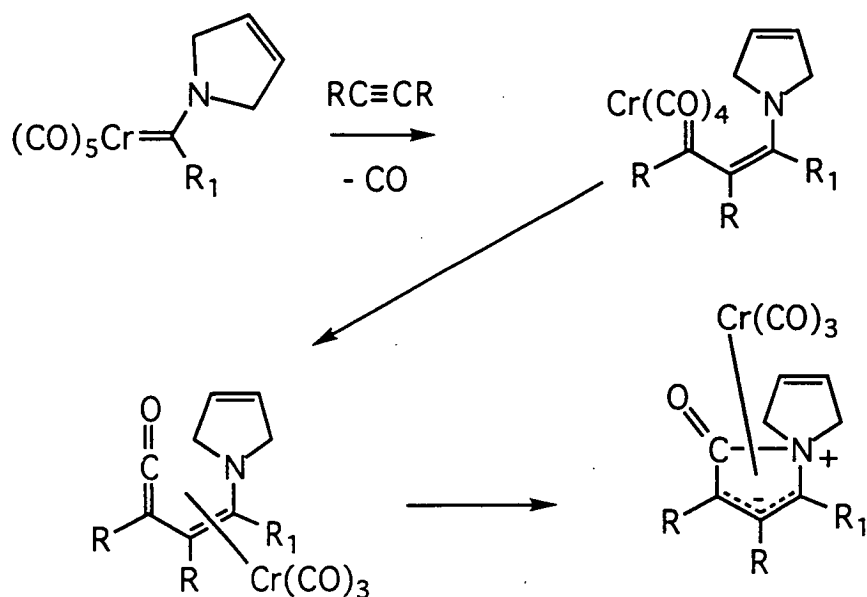


Figure 1.6. Ammonium ylides prepared by alkyne insertion into chromium-stabilised aminocarbenes.

1.2. The Stevens [1,2] Rearrangement

The Stevens rearrangement of ammonium ylides involves migration of one of the nitrogen substituents (typically the largest) to the carbanion, as shown in Figure 1.7. It was first reported by Stevens in 1928, with the conversion of phenylacetylbenzyltrimethylammonium bromide to 1-benzoyl-2-benzyl dimethylamine⁹ (Figure 1.8).



Figure 1.7. The Stevens [1,2] rearrangement of ammonium ylides.

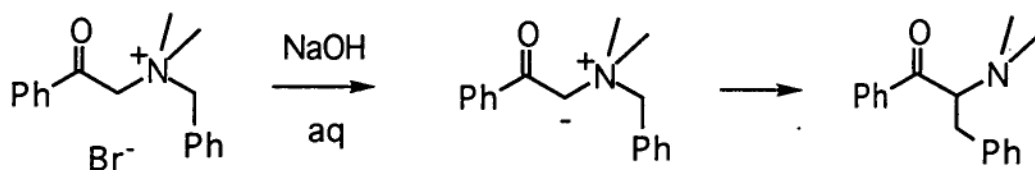


Figure 1.8. The first reported Stevens rearrangement.

Synthetically, the Stevens rearrangement of ammonium ylides has been used for ring expansion of pyrroles to pyridines¹⁰ (Figure 1.9), and more recently it has been applied to the synthesis of α -amino carbonyl moieties¹¹ (Figure 1.10), substituted piperidines³ (Figure 1.11) and unnatural α -amino acid derivatives such as morpholin-2-ones¹² (Figure 1.12).

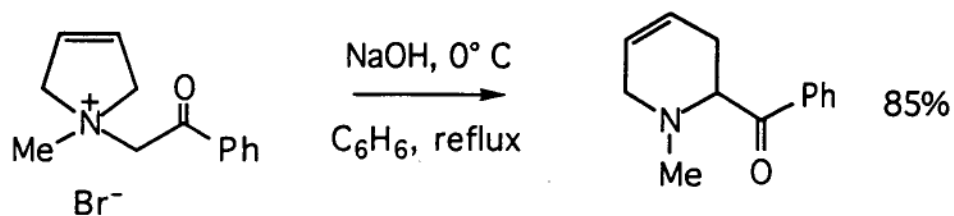


Figure 1.9. Preparation of pyridine by Stevens rearrangement of pyrroles.



Figure 1.10. Synthesis of α -aminocarbonyl moieties by Stevens rearrangement of ammonium ylides.

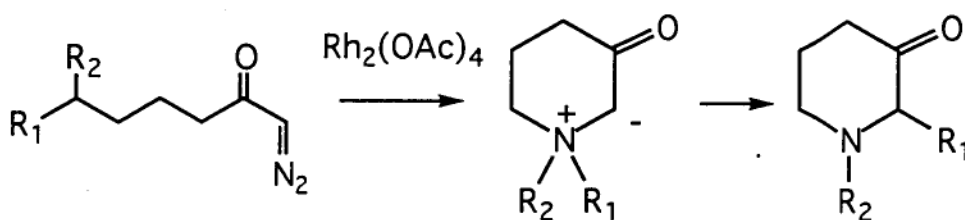


Figure 1.11. Synthesis of 2-substituted piperidin-3-ones by Stevens rearrangement

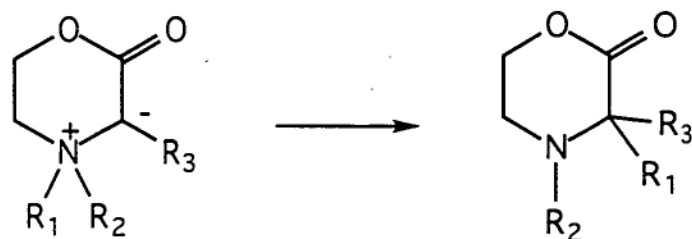


Figure 1.12. Synthesis of morpholin-2-ones by Stevens rearrangement.

The mechanism of the Stevens rearrangement has been a point of some debate in the literature. The original prediction of Stevens¹³, based on the effects of substitution on the migrating benzyl group, was that the ylide dissociated heterolytically to a benzylic anion and an iminium ion, as shown in Figure 1.13. Later

studies on migration of chiral groups indicated a retention of chirality¹⁴, and Wittig¹⁵ and Hauser¹⁶ proposed that the rearrangement was a concerted intramolecular process, as shown in Figure 1.14. A concerted pericyclic mechanism, however, would be a violation of the rules of Woodward and Hoffmann regarding conservation of orbital symmetry¹⁷.

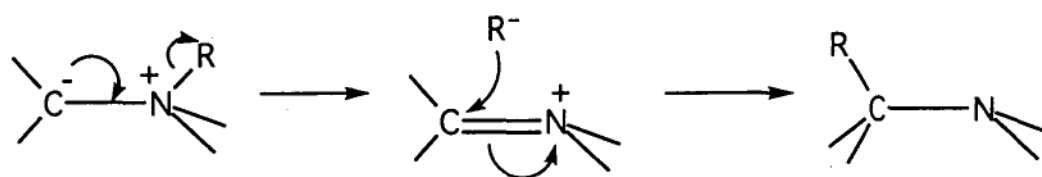


Figure 1.13. Proposed ion-pair mechanism for the Stevens rearrangement.

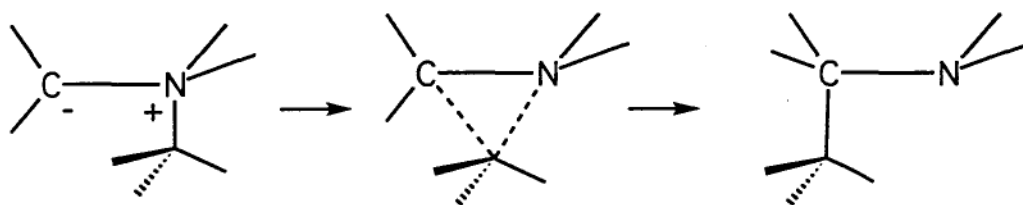


Figure 1.14. Proposed concerted pathway for the Stevens rearrangement, showing retention of chirality.

In 1969, Jemison and Morris¹⁸ followed the Stevens rearrangement of *N,N*-dimethyl-*p*-nitrobenzylamine acetamide by NMR and noted a CIDNP effect on benzylic protons consistent with a benzyl radical. They postulated that this Stevens-type rearrangement of a benzyl group from an ammonium centre to a negatively-charged nitrogen centre occurred via a homolytic dissociation pathway, and that radical pairs were involved. The radical pair mechanism for the ammonium ylide radical pathway is given in Figure 1.15. In 1974, Dewar and Ramsden¹⁹ performed semi-empirical MINDO/3 calculations on the Stevens rearrangement of an alkylammonium ylide, trimethylammonium methylide, in an effort to characterise the concerted transition geometry and determine if this mechanism is energetically feasible. They predicted a small barrier to the concerted process, but found that dissociation to radical pairs was exothermic, and concluded that a concerted

mechanism may be in effect in polar solvents where formation of radicals is not favoured.

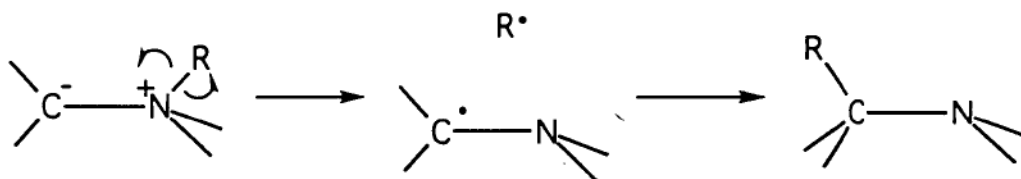


Figure 1.15. The proposed biradical pathway for the Stevens rearrangement.

Studies of Stevens rearrangements of alkylammonium ylides by Closs, Ollis and co-workers^{20,21} concentrating on chiral migrating groups showed that there was a slight decrease in stereoselectivity if a solvent of low viscosity was used, but there was no noticeable effect on the stereoselectivity by changing the solvent polarity. The conclusion of this study was that the radical pair pathway was the primary route for the Stevens rearrangement, but there may be a contribution from a competing concerted pathway; alternatively the radicals formed have too short a lifetime to rotate or separate. Distinction between these two possibilities is difficult.

Stamegna and McEwen²² noted the presence of minor products such as α -benzamidostilbenes from the Stevens rearrangement of analogues of Reissert compounds. These minor products could be formed by recombination of radicals formed by homolysis. Further evidence for this was provided in that the minor products were observed for radical intermediates one would predict to be relatively stable (such as benzyl radicals), yet they were not observed if the radical intermediate was not expected to be stable (such as aryl radicals).

Further experimental studies on base catalysed Stevens rearrangements by Ollis, Rey and Sutherland²³ found that minor products were formed from random couplings of radical intermediates, and that the degree of stereoselectivity could be partly related to solvent viscosity and temperature. The possibility of a concerted mechanism is not totally ruled out, but it was suggested the evidence was mostly in favour of a radical pair pathway.

Recent studies on the enantioselective synthesis of pentahelicene²⁴ have suggested that there may be competition between a concerted suprafacial and nonconcerted antarafacial mechanism, due to the retention of configuration along a usually labile binaphthyl bond. The system studied is highly unusual, involving a macrocycle in which a radical pathway would still be unimolecular in nature, and the assignment of pathway is entirely based on the rate of reaction and retention of configuration arguments.

1.3. Sommelet-Hauser [3,2] rearrangement

The [3,2] sigmatropic rearrangement of ammonium ylides is a concerted symmetry allowed process. The general mechanism is shown as Figure 1.16. Due to the high selectivity of the rearrangement, it has been used extensively in synthesis.

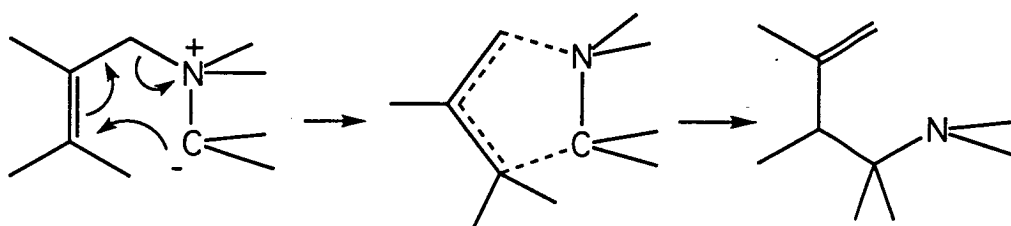


Figure 1.16. The [3,2] rearrangement of ammonium ylides.

The [3,2] rearrangement is a useful synthetic step in the synthesis of β,γ -unsaturated aldehydes²⁵ (Figure 1.17). It is also an attractive method for ring expansion of nitrogen heterocycles²⁶ (Figure 1.18).

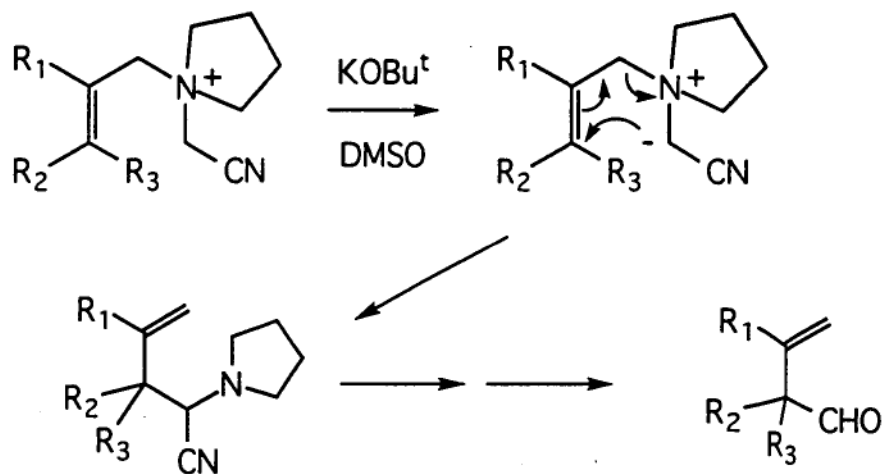


Figure 1.17. Preparation of unsaturated aldehydes with the [3,2] rearrangement as a crucial step.

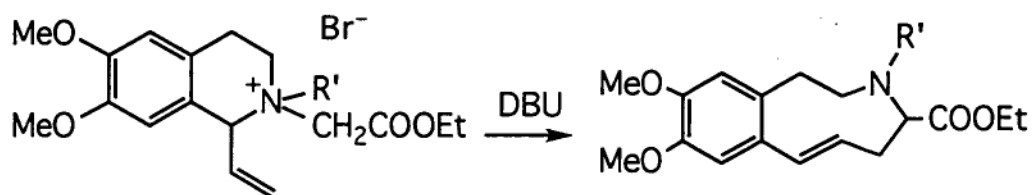


Figure 1.18. The [3,2] rearrangement in ring expansion of nitrogen heterocycles.

If the double bond involved in the [3,2] rearrangement is part of an aromatic system, then there is usually a rearomatisation following the [3,2] shift, the complete process being known as the Sommelet-Hauser rearrangement, shown in Figure 1.19. This is a useful synthetic tool towards highly substituted benzylamines²⁷ (Figure 1.20). The [3,2] intermediate can sometimes be isolated (particularly in the case where there is no abstractable hydrogen to complete the rearomatisation)⁷, and hence the factor determining whether the Sommelet-Hauser rearrangement will occur is the facility of the initial [3,2] concerted shift.

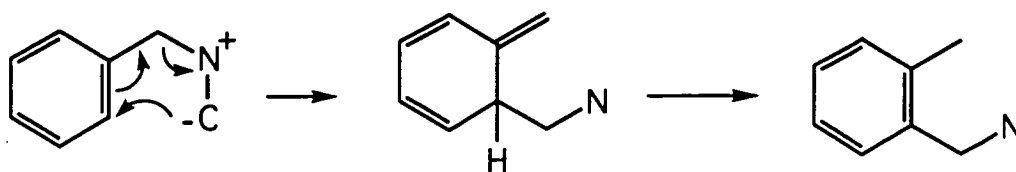


Figure 1.19. The Sommelet-Hauser rearrangement of benzylammonium ylides.

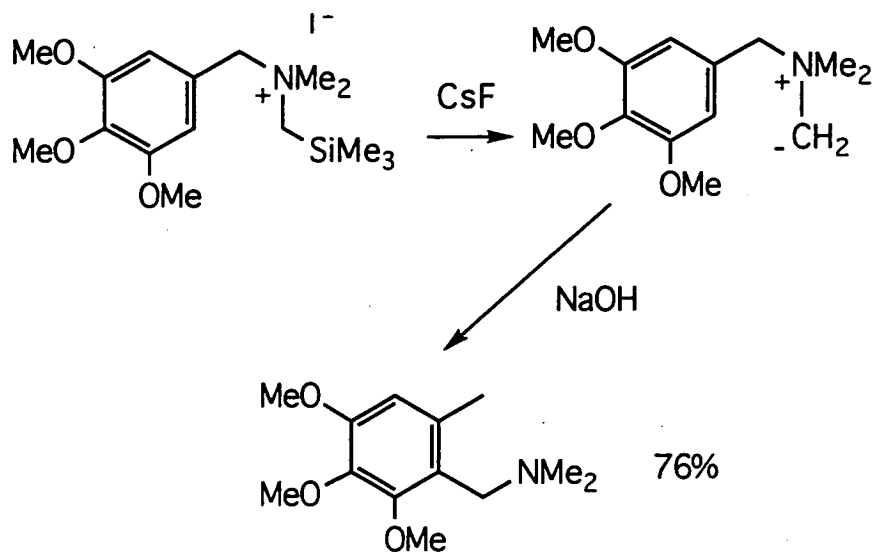


Figure 1.20. Highly substituted benzylamines prepared by the Sommelet-Hauser rearrangement.

1.4. Hofmann Elimination of ammonium ylides

In cases where there is an abstractable hydrogen in a position β to the ammonium centre, there is a possibility of the ylide decomposing to an amine and an unsaturated fragment via the Hofmann elimination²⁸, shown in Figure 1.21. The Hofmann elimination is avoidable by choosing an ylide without the necessary β -hydrogen, however since this is not usually the case, there is typically some competition from the elimination reaction in synthesis.

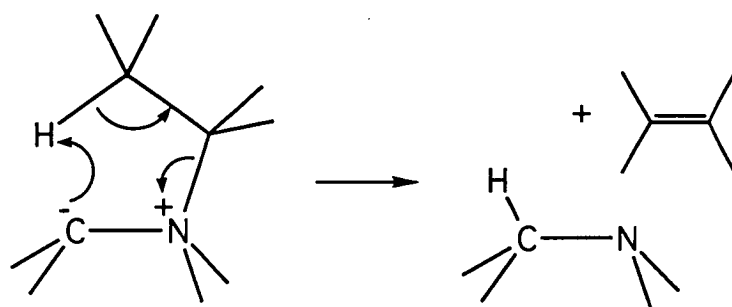


Figure 1.21. The Hofmann elimination reaction of ammonium ylides.

1.5. Competition between the [1,2] and [3,2] rearrangements

The major drawback in the application of ammonium ylides to synthesis is the competition between the rearrangements. Recently, there has been numerous experimental studies of the range and ratios of products formed from ylide rearrangement, and a review of synthetic aspects of the Sommelet-Hauser rearrangement in competition with the Stevens rearrangement has recently been published in Japanese²⁹.

In experiments aimed at ring expansion of nitrogen macrocycles, Bailey found competition between both the [1,2] and [3,2] pathways, as well as β -elimination of 1-vinyl tetrahydroisoquinoline derivatives²⁶. The competition between rearrangements is summarised in figure 1.22.

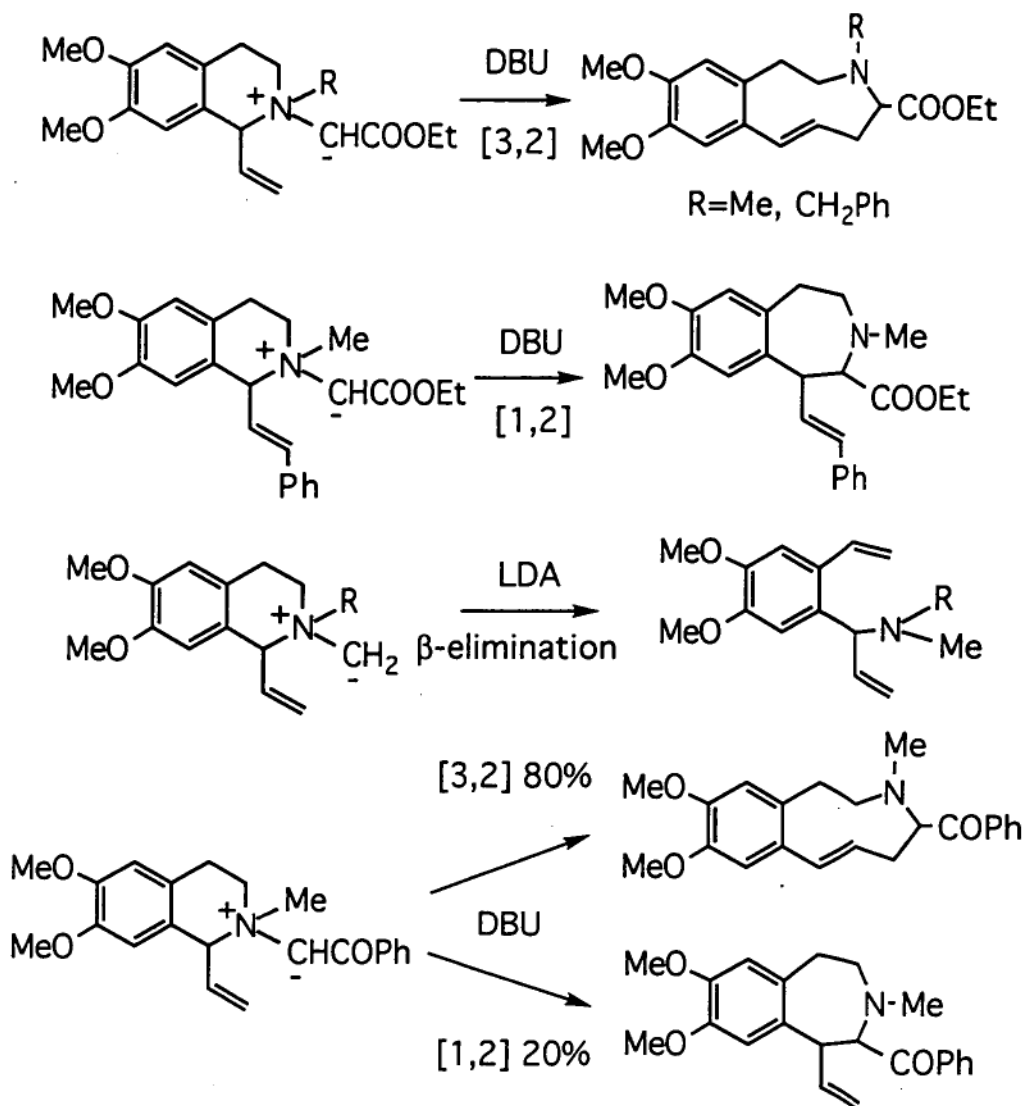


Figure 1.22. Competition between rearrangements in the ring expansion of nitrogen macrocycles.

The addition of a phenyl group to the double bond changes the preferred rearrangement from the [3,2] to the [1,2], while replacing the ester group with a phenylketone brings in competition from the [1,2] pathway. Removal of ylide protection groups gave rise to the elimination pathway.

Competition between the Stevens and the Sommelet-Hauser rearrangement has been the focus of much study. Shirai⁷ reported the effects of substitution at the 3 and 4 position of benzylammonium N-methylides and determined the relative yields of

Sommelet-Hauser and Stevens products in HMPA at room temperature. Results are summarised in Table 1.1.

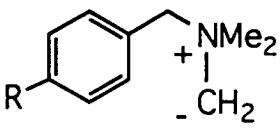
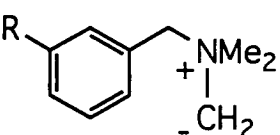
ylide	R	% [1,2]	% [3,2]	% yield
	OMe	100	0	66
	Me	96	4	77
	AcO	99	1	72
	H	97	3	84
	COOCMe ₃	86	14	79
	NO ₂	12	88	77
	OMe	98	2	86
	Me	99	1	76
	OAc	98	2	52
	COOCMe ₃	100	0	71
	NO ₂	88	12	22

Table 1.1. Effect of substitution at the 3 and 4 position of benzylammonium N-methylides on ratio of products.

Substitution of a nitrile or butoxycarbonyl group at the 3 position promotes the Stevens rearrangement, however similar substitution at the 4 position does not have as significant an effect.

Further studies of substitution on the carbanion by Tanaka³⁰ show the effect of the solvent and additives on the preferred rearrangement. The effects of addition of the strong base DBU to the solvents HMPA and DMF are summarised in Table 1.2. The two systems described show a preference for the Stevens rearrangement in the relatively non-basic solvent, however addition of the base promotes the Sommelet-Hauser rearrangement. This study also considers substitution at the 2 position by methyl and methoxy groups, however substitution at this position had no real effect on

the ratio of products. The addition of UV radiation gave great enhancement to the Stevens rearrangement, presumably by promoting radical formation.

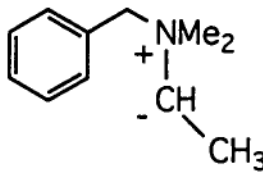
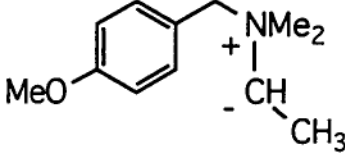
	additive	% [1,2]	% [3,2]	% yield
	HMPA	88	8	32
	HMPA/DBU	16	84	65
	DMF	92	4	39
	DMF/DBU	32	68	59
	HMPA	99	1	53
	HMPA/DBU	12	88	71
	DMF	99	1	51
	DMF/DBU	70	30	58

Table 1.2. The effect of adding strong base on preferred rearrangement.

Studies on the Sommelet-Hauser rearrangements of furylmethylammonium ylides and thienylmethylammonium ylides by Usami³¹ showed some small competition from the Stevens rearrangement in the case of 2-furyl and 2-thienyl substitution, however 3-furenyl and 3-thienyl methylammonium ylides rearranged exclusively to the Sommelet-Hauser product, as shown in Table 1.3.

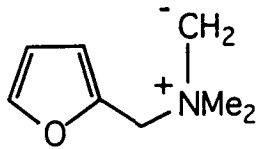
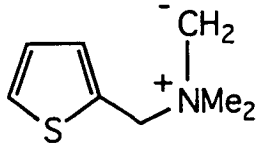
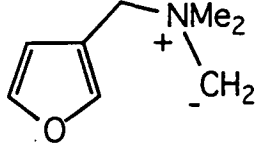
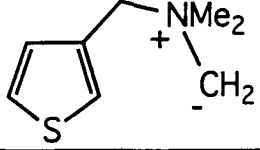
	% [3,2]	% [1,2]	% yield
	90	10	83
	92	8	85
	100	0	73
	100	0	71

Table 1.3. Ratios of products formed from the rearrangement of dimethyl(furylmethyl)ammonium and dimethyl(thienylmethyl)ammonium N-methylides.

Experimental attempts to accomplish ring expansion of piperazines by Kitano³² ran into difficulty with the competing rearrangements. The three piperazinium 1-methylides investigated are shown in Figure 1.23. **1** rearranged to the Sommelet-Hauser product in the presence of DBU, however the rearrangement of **2** gave a mixture of Sommelet-Hauser and Hofmann elimination products in a ratio of 6:1. **3** rearranged exclusively to the Stevens product, even in the presence of DBU.

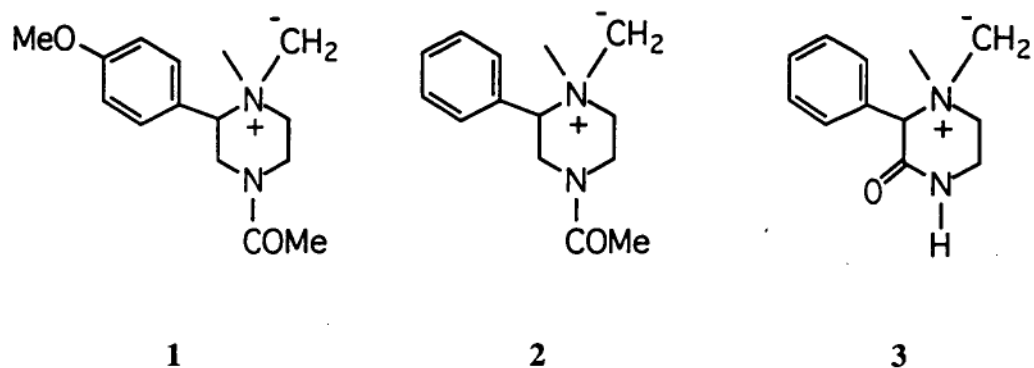


Figure 1.23. Piperazinium 1-methylides showing different rearrangement behaviour.

Sato³³ found that the rearrangement of isoquinolinium 2-methylides produced varying amounts of the Sommelet-Hauser and Stevens rearrangement dependent not only upon the substituents, but also the stereochemistry of the ylide (Table 1.4). Further experimental work on the effects of isomerisation³⁴ show that for isoindolinium methylides, the Sommelet-Hauser rearrangement is considerably disfavoured in the case where the double bond is *trans* to the carbanion across a cyclic system, and hence a concerted rearrangement would be sterically prohibitive. Table 1.5 summarises their findings for a series of mixtures of *cis*- and *trans*- ylides.

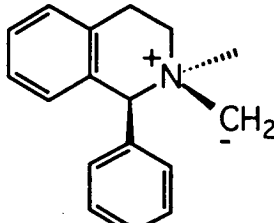
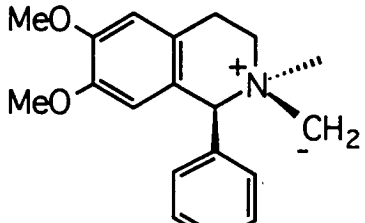
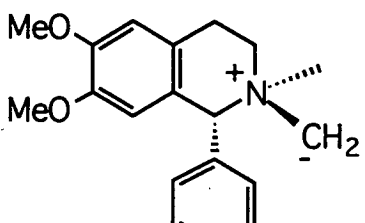
	% Stevens	% Sommelet-Hauser
	77	18
	46	49
	45	36

Table 1.4. Relative yields of competing rearrangements of isoquinolinium 2-methylides.

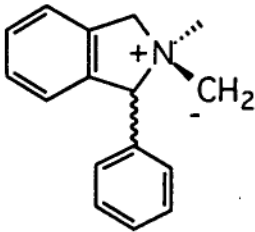
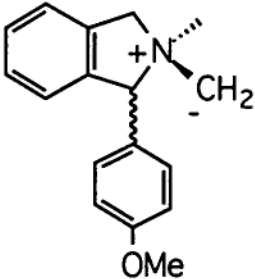
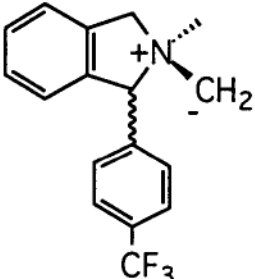
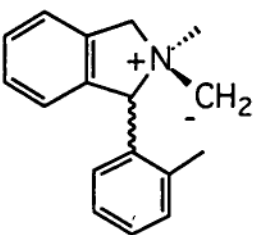
	ratio <i>cis:trans</i>	ratio S-H:Stevens
	92:8	82:18
	70:30	63:37
	37:63	35:65
	25:75	20:75
	13:87	7:84
	15:85	13:85
	45:55	40:59
	70:30	66:34
	90:10	82:18
	3:97	3:94
	51:49	45:53
	80:20	66:34
	97:3	81:19
	55:45	48:52
	75:25	56:44
	95:5	68:32

Table 1.5. Effects of isomerisation on ratio of Stevens and Sommelet-Hauser (S-H) products for substituted isoindolinium ylides.

Although most of these studies indicate that the Sommelet-Hauser rearrangement is promoted by addition of strong alkali and by including electron-donating groups in the phenyl ring, this may not be the answer for successful synthesis. Recent experimental work on (polymethoxybenzyl)ammonium

N-methylides²⁷ led to [3,2] rearrangement intermediates that were intensely hygroscopic, and the major reaction products were methoxytoluenes.

1.6. The Project

The mechanism of the Stevens rearrangement is generally accepted to be a dissociative radical pathway, however none of the experimental evidence has ruled out the possible competition from a concerted process. It is proposed to theoretically model prototype ylides and their respective transition geometries and Stevens rearrangement products for both the radical and concerted mechanisms. An investigation of several ylides encompassing a range of steric and electronic effects should give an indication of whether there is any chance of a concerted symmetry-forbidden process causing the high degree of stereoretention seen in the Stevens rearrangement.

There has been no theoretical study to date of the transition geometry for the [3,2] rearrangement. It is thus necessary to characterise the concerted transition state theoretically before a comparison can be made between the [1,2] and the [3,2] rearrangements. The transition state is anticipated to be a concerted five-center process with formation of the bond between the two carbon centres occurring simultaneously to the breaking of the nitrogen-carbon bond.

Having determined the transition geometries for each process, a comparison of the two should give an indication of the amount of competition between the two processes. Substituent effects of both a steric and electronic nature need to be investigated for both transition geometries. Inspection of the effects of substitution should give an indication of why particular ylides favour certain rearrangements, and how, if possible, to avoid the case of close competition between the rearrangement processes. The importance of electronic substitution on the stability of ylides and transition geometries will be investigated during the course of this, as there is no point aiming for an ammonium ylide that may be too difficult or unstable to synthesise.

The effects of solvation on the activation barrier of each rearrangement are to be investigated. It has been well-documented that DBU suppresses the [1,2] rearrangement almost totally, but milder solvents such as HMPA and acetonitrile may have some effect in promoting or suppressing one rearrangement over the other.

It is hoped that the findings of this study can be brought back to the laboratory in the form of an increased understanding of the driving force behind each rearrangement. It may be possible to improve yields of the desired product through application of the predictions of these theoretical studies to optimising the conditions for chemical synthesis.

Chapter 2. Theoretical Methods

2.1. Introduction

Molecular orbital theory is rapidly becoming a prominent method in chemistry, and is being applied to a number of systems, due to the ability to predict many spectroscopic and energetic properties from direct manipulation of the molecular wavefunction. There are many fine references available on molecular orbital methods³⁵⁻³⁸; below is presented a brief overview of the theory, followed by a discussion of the essential differences between the methods used in this study.

2.2. Quantum theory of molecules

The basis of molecular orbital theory is the molecular wavefunction, Ψ , which is an approximation to the true solution of the Schrödinger equation

$$\hat{H}\Psi = E\Psi \quad (2.1)$$

where \hat{H} is the Hamiltonian operator and E is the molecular energy of the system. In atomic units, the Hamiltonian for a molecule of N electrons and M nuclei is

$$\hat{H} = -\sum_i^N \frac{1}{2} \nabla_i^2 - \sum_A^M \frac{1}{2M_A} \nabla_A^2 - \sum_i^N \sum_A^M \frac{Z_A}{r_{iA}} + \sum_i^N \sum_{j>i}^N \frac{1}{r_{ij}} + \sum_A^M \sum_{B>A}^M \frac{Z_A Z_B}{R_{AB}} \quad (2.2)$$

In order to simplify this calculation, we invoke the Born-Oppenheimer approximation that the motion of the nuclei is very slow when compared to the electrons, and hence may be considered to be stationary. This means that the second term of equation 2.2 is equal to zero, and the last term is a constant. The Hamiltonian operator can be further separated into electronic and nuclear components, which can be treated separately.

$$\hat{H} = \hat{H}^{el} + \hat{H}^{nuc} = \left(-\sum_i^N \frac{1}{2} \nabla_i^2 - \sum_i^N \sum_A^M \frac{Z_A}{r_{iA}} + \sum_i^N \sum_{j>i}^N \frac{1}{r_{ij}} \right) + \left(\sum_A^M \sum_{B>A}^M \frac{Z_A Z_B}{R_{AB}} \right) \quad (2.3)$$

The electronic wavefunction Ψ^{el} , which we are interested in calculating is an eigenfunction of the electronic Hamiltonian operator, with eigenvalue equal to the electronic energy of the molecule

$$\hat{H}^{el}|\Psi^{el}\rangle = E^{el}|\Psi^{el}\rangle \quad (2.4)$$

In molecular orbital theory, each electron exists in a one-electron spin orbital χ which is the product of a spatial component ψ and a spin function (α or β). A molecular wavefunction can be constructed from a normalised antisymmetric determinant formed from products of these spin orbitals. This is known as a Slater determinant.

$$\Psi = (N!)^{-1/2} \begin{vmatrix} \chi_i(x_1) & \chi_j(x_1) & \cdots & \chi_k(x_1) \\ \chi_i(x_2) & \chi_j(x_2) & \cdots & \vdots \\ \vdots & \vdots & \ddots & \vdots \\ \chi_i(x_N) & \chi_j(x_N) & \cdots & \chi_k(x_N) \end{vmatrix} \quad (2.5)$$

$$= |\chi_i \chi_j \cdots \chi_k\rangle$$

The Hartree-Fock approximation involves using a single Slater determinant as the ground state wavefunction and the variation principle to determine the optimal spin orbitals by minimising the electronic energy for this determinant. The electronic energy is given by

$$E_0 = \langle \Psi_0 | \hat{H} | \Psi_0 \rangle$$

$$= \sum_a^N \langle \chi_a | h | \chi_a \rangle + \frac{1}{2} \sum_{ab} (\langle \chi_a \chi_b | \chi_a \chi_b \rangle - \langle \chi_a \chi_b | \chi_b \chi_a \rangle) \quad (2.6)$$

Where h is the one electron operator

$$h_i = -\frac{1}{2} \nabla_i^2 - \sum_A \frac{Z_A}{r_{iA}} \quad (2.7)$$

And the two-electron operators are given by

$$\langle \chi_i \chi_j | \chi_k \chi_l \rangle = \langle ij | kl \rangle$$

$$= \int dx_1 dx_2 \chi_i^*(x_1) \chi_j^*(x_2) \frac{1}{r_{12}} \chi_k(x_1) \chi_l(x_2) \quad (2.8)$$

The spin orbitals are further constrained to be orthonormal, which leads to the eigenvalue Hartree-Fock equation.

$$\left[h(1) + \sum_b (J_b(1) - K_b(1)) \right] \chi_a(1) = \varepsilon_a \chi_a(1) \quad (2.9)$$

Where the Coulomb operator J is given by

$$J_b(1) = \int dx_2 |\chi_b(2)|^2 r_{12}^{-1} \quad (2.10)$$

and the exchange operator K is given by

$$K_b(1) \chi_a(1) = \left[\int dx_2 \chi_b^*(2) r_{12}^{-1} \chi_a(2) \right] \chi_b(1) \quad (2.11)$$

The operator on the left of equation 2.9 is the one-electron Fock operator

$$f(1) = h(1) + \sum_b (J_b(1) - K_b(1)) \quad (2.12)$$

and thus we obtain the Hartree-Fock equation

$$f|\chi_a\rangle = \varepsilon_a|\chi_a\rangle \quad (2.13)$$

To solve the Hartree-Fock equation, we need to define the spatial components of the spin orbitals χ_i . For practical reasons, the spatial molecular orbitals ψ_i are expressed as linear combinations of a set of one-electron functions, ϕ_μ , known as basis functions.

$$\psi_i = \sum_\mu c_{\mu i} \phi_\mu \quad (2.14)$$

The basis functions resemble the atomic orbitals of individual atoms, and hence Ψ_i is a linear combination of atomic orbitals (LCAO). For closed-shell molecules, the spatial components of both α and β orbitals are the same, and hence we have doubly-occupied molecular orbitals. The orbital coefficients, $c_{\mu i}$ are optimised to give the lowest energy in the Hartree-Fock equation. This leads to the Roothaan-Hall equation

$$\sum_\nu \mathbf{F}_{\mu\nu} \mathbf{C}_{\nu i} = \varepsilon_i \sum_\mu \mathbf{S}_{\mu\nu} \mathbf{C}_{\nu i} \quad (2.14)$$

where $\mathbf{F}_{\mu\nu}$ is the matrix of the Fock operator in the basis ϕ_μ

$$\begin{aligned}
 \mathbf{F}_{\mu\nu} &= \int dr_1 \phi_\mu^*(1) f(1) \phi_\nu(1) \\
 &= \mathbf{H}_{\mu\nu}^{core} + \sum_a \sum_{\lambda\sigma}^{N/2} \mathbf{C}_{\lambda a} \mathbf{C}_{\sigma a}^* [2(\mu\nu|\sigma\lambda) - (\mu\lambda|\sigma\nu)] \quad (2.15)
 \end{aligned}$$

and $\mathbf{S}_{\mu\nu}$ is the overlap matrix of the basis functions

$$\mathbf{S}_{\mu\nu} = \int dr_1 \phi_\mu^*(1) \phi_\nu(1) \quad (2.16)$$

This needs to be solved iteratively for \mathbf{C}_{ui} , since $\mathbf{F}_{\mu\nu}$ is dependant on \mathbf{C}_{ui} - this approach is known as the self-consistent field (SCF) theory.

For open-shell systems, the approach of treating pairs of electrons is inappropriate. Unrestricted Hartree-Fock (UHF) theory treats α and β electrons separately, with a discrete set of spatial orbitals for each spin, which are allowed to be different, yet are generated from the same set of basis functions. This leads to the Pople-Nesbet equations

$$\begin{aligned}
 \sum_\nu \mathbf{F}_{\mu\nu}^\alpha \mathbf{C}_{\nu j}^\alpha &= \epsilon_j^\alpha \sum_\nu \mathbf{S}_{\mu\nu} \mathbf{C}_{\nu j}^\alpha \\
 \sum_\nu \mathbf{F}_{\mu\nu}^\beta \mathbf{C}_{\nu j}^\beta &= \epsilon_j^\beta \sum_\nu \mathbf{S}_{\mu\nu} \mathbf{C}_{\nu j}^\beta \quad (2.17)
 \end{aligned}$$

Due to the differences in spatial orbitals for α and β electrons, the UHF procedure does not produce a pure spin state. The degree of spin contamination can be quantified by calculating the expectation value of the S^2 operator. A pure spin state would have the value $s(s+1)$ where s is the quantum number of total spin ($s = 0, \frac{1}{2}, 1, \frac{3}{2}, 2, \dots$).

Spin-restricted open-shell Hartree-Fock theory (ROHF)³⁹ involves a molecular wavefunction in which α and β orbitals have different spatial components, but the β spatial orbitals are restricted to be a linear combination of the spatial components of α orbitals. This approach leads to pure spin states, but is computationally more expensive and provides an unsatisfactory starting point for a perturbation treatment of electron correlation (explained later).

2.3. Semi-empirical molecular orbital theory

In semi-empirical theory, many of the more computationally expensive aspects of the SCF method have been approximated by simpler expressions. This leads to a molecular orbital theory that can be applied easily to systems with a very large number of atomic orbitals.

The basis set for semi-empirical calculations has the form of one s orbital and three p orbitals per atom. The Roothaan equation is simplified by ignoring the overlap matrix $S_{\mu\nu}$ entirely, and hence the following remains to be solved

$$\sum_{\mu}^N (\mathbf{F}_{\mu\nu} - \varepsilon_i) \mathbf{C}_{\nu i} = 0 \quad (2.18)$$

Further simplifications are made to the Fock matrix by ignoring integrals of the type $(\mu\nu|\sigma\lambda)$ where ϕ_{μ} and ϕ_{ν} are on different centres. Having removed three- and four-centre integrals, the one- and two-centre two-electron integrals are derived either from experiment or theory. The one-electron integrals are parameterised (the overlap matrix actually being re-introduced), and the core-core repulsion integrals are approximated by modified parameterised two-centre integrals. The three semi-empirical methods used in this study vary mainly in the parameterisation.

MNDO (Modified Neglect of Differential Overlap)⁴⁰ uses experimentally derived parameters for the two-electron repulsion integrals, optimised theoretical parameters for atomic orbital exponents, core-core repulsion integrals and one-electron integrals.

AM1 (Austin Model 1)⁴¹ includes modification to the core terms to account for Van der Waals attractions between nuclear centres at relatively large separations.

PM3 (Parameterised Model 3)⁴² uses two-electron integral parameters which have been optimised to reproduce experimental molecular properties.

2.4. Ab initio molecular orbital theory

In ab initio molecular orbital theory, the only further approximation to the SCF equation made is in the basis set. Each atomic orbital is described by a basis function, which in turn is formed from a linear combination of Gaussian functions

$$\phi_{\mu} = \sum_k d_{\mu k} g_k \quad (2.19)$$

Each Gaussian primitive, g_k is of an approximate form to the spatial component of an atomic orbital (s, p, d...), and the basis function is hence a contracted Gaussian.

The use of Gaussians makes each two-electron integral reasonably easy to calculate, however as the Gaussians are still only approximations to the true spatial atomic orbitals, a large number are needed to obtain a good molecular wavefunction, and hence ab initio methods are computationally expensive for treatments of large systems.

2.5. Ab initio basis sets⁴³⁻⁴⁶

The collection of Gaussian primitives and their contractions is known as a basis set. In this study, basis sets created using the contractions of Pople are used. All basis sets are of split valence quality, i.e. one basis function per core atomic orbital, and two or more per valence orbital. The three primary basis sets used in this study are 3-21G, which involves three primitives contracted to one for core orbitals, and the inner and outer valence shell defined by two and one Gaussian primitives. The 6-31G basis set differs by having six primitives on the core electrons and the valence basis functions described by three and one primitive, and the 6-311G basis set involves the valence orbitals being split into three basis functions, described by three, one and one primitive Gaussians.

Basis sets are augmented by polarisation functions, which are of higher angular momentum quantum number than the valence shell. The amount and type of polarisation is shown in parentheses after the basis set definition, i.e. 6-31G(d) includes d-type polarisation functions added to non-hydrogen atoms and 6-311G(2d,p) involves two sets of d-type functions on non-hydrogen atoms, and p-type polarisation on hydrogen atoms. These allow for concentration of charge away from atomic centres, and are important in describing chemical bonding.

Basis sets may be further augmented by diffuse functions, which are Gaussians with a very low exponent, and hence allow for electron density far from the atomic centres. In this study, the use of diffuse s and p functions in the basis set is indicated by a + at the end of the contraction description, i.e. 6-31+G(d).

2.6. Electron Correlation Methods

The use of the theory thus far described produces an energy which is an upper bound to the exact energy of the system. The difference between the SCF energy and the exact energy is called the correlation energy, as it arises from neglect of correlation of electron motion (which is only treated for electrons with parallel spins, in the K term of the Fock operator). In this study, two methods of incorporating electron correlation have been used, both with the Hartree-Fock wavefunction as a starting point.

2.6.1. Møller-Plesset Perturbation Theory

In perturbation theory, the Hamiltonian is separated into two parts, a zeroth-order Hamiltonian \hat{H}_0 (in Møller-Plesset theory, this is the Hartree-Fock Hamiltonian), and a perturbation v . The exact Hamiltonian is then given by

$$\hat{H} = \hat{H}_0 + \lambda v \quad (2.20)$$

and the exact eigenfunctions (the complete wavefunction) and eigenvalues (total correlated energy) of \hat{H} can be expanded as a Taylor's series in λ .

$$\begin{aligned} E_\lambda &= E^{(0)} + \lambda E^{(1)} + \lambda^2 E^{(2)} + \lambda^3 E^{(3)} + \dots \\ |\Psi_\lambda\rangle &= |\Psi^{(0)}\rangle + \lambda |\Psi^{(1)}\rangle + \lambda^2 |\Psi^{(2)}\rangle + \lambda^3 |\Psi^{(3)}\rangle + \dots \end{aligned} \quad (2.21)$$

This series should converge as the higher-order terms become smaller and smaller. Terminating this series at $E^{(n)}$ produces the n-th order energy, the second-order energy is commonly referred to as MP2, the third as MP3 and so on.

Open-shell systems show poor convergence behaviour using conventional Møller-Plesset theory due to the low-lying doubly excited determinants entering the UHF wavefunction. It is possible to use a projection operator to remove spin contamination at the MP2 level, leading to the Projected Second-order Møller-Plesset energy, PUMP2.

A treatment of perturbation based on removing spin contamination from the wavefunction before commencing the energy perturbation is the Restricted Open-Shell Møller-Plesset treatment (ROMP)⁴⁷. In this method, the Fock matrix is transformed into occupied and virtual orbital sets: this is necessary as Brillouin's theorem does not hold for these open-shell wavefunctions (i.e. $F_{ov}^\alpha, F_{ov}^\beta \neq 0$). Using this method, the perturbation treatment commences from a pure spin state (analogous to the ROHF wavefunction) and the energy should converge at a lower order of perturbation.

2.6.2. Coupled-Cluster Theory⁴⁸⁻⁵²

Coupled Cluster (CC) theory belongs to the configuration interaction (CI) methods of dealing with electron correlation. In CI, the molecular wavefunction is a linear combination of all possible Slater determinants which can be generated from the basis set, i.e.

$$|\Phi_0\rangle = c|\Psi_0\rangle + \sum_a c_a^r |\Psi_a^r\rangle + \sum_{\substack{a<b \\ r<s}} c_{ab}^{rs} |\Psi_{ab}^{rs}\rangle + \sum_{\substack{a<b<c \\ r<s<t}} c_{abc}^{rst} |\Psi_{abc}^{rst}\rangle + \dots \quad (2.22)$$

If we ignore single, triple... excitations (which do not mix with $|\Psi_0\rangle$), we approximate the full CI wavefunction by the following intermediate normalised wavefunction.

$$|\Phi_0\rangle = |\Psi_0\rangle + \sum_{\substack{a<b \\ r<s}} c_{ab}^{rs} |\Psi_{ab}^{rs}\rangle + \sum_{\substack{a<b<c<d \\ r<s<t<u}} c_{abcd}^{rstu} |\Psi_{abcd}^{rstu}\rangle + \dots \quad (2.23)$$

The coupled-cluster approximation is that the coefficients of the quadruple excitations are a function of the coefficients of the double excitations

$$c_{abcd}^{rstu} \cong c_{ab}^{rs} * c_{cd}^{tu} \quad (2.24)$$

where the * indicates all possible combinations of exciting a and b into r and s , and c and d into t and u . This leads to interactions between quadruple and double excitations being defined by this expression for the coefficients and the interaction between the Hartree-Fock ground state and a doubly-excited determinant. Inclusion of singly-excited determinants in this equation leads to CCSD, and an approximate method can be used to calculate the effects of triple excitations (CCSD(T)).

2.7. Geometry optimisation

The energy obtained from all methods discussed thus far is a function of the internuclear co-ordinates R_{AB} , and hence the energy may be defined as a potential surface (however, energy is only calculated for one geometry at a time). At a

stationary point on the potential energy surface (PES), the gradient of the energy with respect to nuclear co-ordinates is zero.

$$\frac{\delta E}{\delta R_i} = 0 \quad i=1,2,\dots,(3N-6) \quad (2.25)$$

Geometry optimisation in most cases is handled analytically, by calculating gradients of the energy from the molecular wavefunction, and then using an efficient optimisation algorithm until the desired stationary point conditions are reached.

Algorithms which have been used in this study are the Berny optimisation algorithm, the eigenvector following (EF)⁵³ algorithm, which calculates eigenvectors and eigenvalues of the Hessian matrix (second derivatives of energy with respect to geometry) at each step, making it particularly useful in the optimisation of transition states, and the Fletcher-Powell algorithm for geometry optimisation at ROMP2, where analytical geometries are unavailable.

There are two important types of stationary points, local minima, and transition geometries. At a local minimum the Hessian matrix has all positive eigenvalues, and all calculated vibrational frequencies are real. A transition state between two local minima is characterised by one negative eigenvalue in the Hessian matrix, and hence one imaginary frequency, indicating that distortion along a normal mode will result in a lowering of energy. Transition geometries in this study have been further characterised by performing a geometry optimisation after a slight distortion of the molecule along the appropriate normal mode: this ensures that the transition geometry is appropriate for the reaction being studied.

2.8. Theoretical description of solvation effects

The methods described thus far give the energy of an isolated gas-phase molecule at equilibrium. While this is an extremely important quantity and is useful for describing many chemical effects, the application of this model to organic synthesis could be questionable, since the chemical environment of the molecule is not

taken into account. It would be advantageous to have the effects of solvation incorporated in the quantum description of the molecule.

There are two important aspects of solvation which need to be considered. The electrostatic effects of solvation arise from the interaction of the solute with the electric field generated by a polar solvent. Electrostatic effects take two forms, the relaxation of the solute molecules as an effect of a polar solvent, and the polarisation of the solvent by the solute. Specific solvent-solute effects are more difficult to define, they range from specific co-ordination of solvent molecules to the solute, to hydrogen bonding and other dispersion effects, to solvent cage effects in the case of a particularly viscous solvent.

In theoretical chemistry, there are four general approaches to describing solvation effects. Conceptually, the simplest of these is the explicit incorporation of solvent molecules into the molecular wavefunction. This addresses many of the specific solvent-solute interaction, but is limited by the number of solvent molecules which can be described. It is also possible to use a molecular dynamics approach such as a Monte-Carlo simulation of solute molecules interacting with number of solvent molecules, thus addressing the electrostatic effects and some of the dispersion and cage effects of the solvent. The Born model of treating the solvent as a series of spheres interacting with the solvent accessible surface is employed routinely in molecular mechanics and is being developed in the semi-empirical SMX series of algorithms. Most ab initio treatment of solvation has centred around the polarisable continuum model (PCM), which involves placing the solute in an arbitrarily defined cavity, and then describing the solvent either by a bulk dielectric (the SCRF method), or by a series of surface charge densities (the Langevin Dipole method, for example). The PCM method only treats electrostatic effects of solvation, and is highly dependent on the description of the cavity.

A recent review⁵⁴ has covered the range of solvation methods currently available, and compared them for the case of aqueous solvation of organic molecules.

Below is a brief description of the essential differences between the three models of solvation used in this thesis.

2.8.1. Supermolecule Calculations

The explicit incorporation of solvent molecules is a common method of describing solvation in molecular mechanics, however in molecular orbital calculations, it is only possible to include a small number of solvent molecules, particularly if the solvent itself has a complex molecular structure. In calculating the energy of the supermolecule, it is imperative that one use a size-consistent theory, i.e. one where the energy of a system of N noninteracting molecules scales as N . This is true for semiempirical calculations, and also the Hartree-Fock and Møller-Plesset theories.

2.8.2. Self Consistent Reaction Field (SCRF) theory⁵⁵

SCRF is one of the family of polarisable continuum models. The solute is assumed to reside in a spherical cavity in a solvent which is described by its dielectric constant ϵ . Onsager determined that the electric field \mathbf{R} of a dipole μ in a spherical cavity of radius a_0 is

$$\mathbf{R} = \frac{2(\epsilon - 1)\mu^2}{(2\epsilon + 1)a_0^3} = g\mu \quad (2.26)$$

This reaction field is incorporated in the Fock matrix

$$\mathbf{F}_{\lambda\sigma} = \mathbf{F}_{\lambda\sigma}^0 - g\mu \langle \phi_\lambda | \mu | \phi_\sigma \rangle \quad (2.27)$$

and the SCF procedure as outlined earlier is followed using this modified Fock matrix. This method allows for geometry optimisation within the cavity, and the only parameter introduced is the cavity radius a_0 . The radius is generally determined from

he extremes of an isodensity surface of the solute generated from the gas-phase molecular wavefunction.

The SCRF method is essentially a self-consistent method inside another self-consistent method, as the reaction field magnitude g is dependent upon the dipole moment, μ which is used to calculate it and is determined by the molecular wavefunction.

2.8.3. Conductor-Like Screening Model (COSMO)⁵⁶

The COSMO method, developed by Klamt and Schüürmann is a novel approach to solvent reaction field from the surface charge density. In this method, the attention is on the cavity surface S , and the screening densities $\sigma(r)$, defined by

$$\sigma(r) = \frac{1-\epsilon}{4\pi\epsilon} \frac{\delta}{\delta\mathbf{n}} [\phi_\rho(r) + \phi_\sigma(r)]_S \quad (2.28)$$

where \mathbf{n} is the surface normal vector, ϕ_ρ is the electrostatic potential due to the solute charge distribution and ϕ_σ is a potential due to the surface charges. COSMO assumes $\epsilon=0$ (conductor-like screening), and uses a Greens function approach to solve $\sigma(r)$ as a function of the charge distribution $\rho(r)$. The effects of a finite dielectric constant are then corrected for empirically. Using this approach, one can optimise the energy of large systems within the cavity. The cavity itself is defined by a set of interlocking spheres around the centres of the atoms of the solute.

2.8.4. Hybrid methods

For the problem of a solute with a small dipole in a solvent with a relatively low dielectric constant, the specific solvent-solute interactions may be the largest contributions of the solvation energy. The question then arises - how can we know which approach is appropriate, and is there a way of incorporating both electric field and specific solvent-solute effects in a quantum chemical calculation, with as little

extra parameterisation as possible. In this study, we investigate the possible solution of describing individual solvent molecules in the molecular wavefunction, treating the remainder of the solvent as a bulk dielectric and optimising the geometry of the supermolecule within the polarisable continuum.

A supermolecule approach with a solvent molecule embedded in the cavity has been touched upon by Szafran⁵⁷. This study, on the tautomerisation of pyridones, found that the inclusion of one hydroxide ion in the cavity provided better correlation with experimental results than the polarisable continuum alone. Recent work on metal ion solvation by Furuki⁵⁸ included several water molecules inside the cavity, and obtained close correlation with experimental results, however neither of these studies optimised the geometry of the complex within the cavity.

2.9. Computational details

All semi-empirical calculations, including the COSMO investigation have been performed using the MOPAC 6⁵⁹ and MOPAC 93⁶⁰ programs on Sparc workstations.

All ab initio calculations have been performed using the Gaussian 90⁶¹, Gaussian 92⁶² and Gaussian 94⁶³ programs on Sparc workstations and Fujitsu VP2200 supercomputers located at ANSTO, Lucas Heights and ANUSF, Canberra. The core has been frozen for all Møller-Plesset calculations, apart from those in Chapter 3, which were performed before analytical frozen-core gradients became available.

2.10. Conclusions

The range of molecular orbital calculations currently being performed on different chemical systems is staggering, there seem to be as many basis sets, levels of theory and methods of electron correlation as there are chemical problems. There is also a divergent pathway of very small molecules being studied at extremely high

levels of theory, and extremely large chemical systems such as nucleic acids being investigated with small basis sets and Hartree-Fock theory. Another tendency of theoretical studies is to expand the level of theory to meet the currently available computational resources.

In this study, a number of molecules are to be studied, ranging from two to twenty non-hydrogen atoms. Since all these molecules are to be compared with each other, it would be convenient to have a consistent level of theory applicable to, and able to give reliable structural and energetic information about every molecule in this set. From Chapter 1, it is clear that this study will encompass open- and closed-shell systems, organic molecules containing nitrogen, and transition states in which bonds are partly formed. Electron correlation is going to be an important part of comparison between these differing types of electronic states, since it is generally agreed that MP2 accounts for a great deal of the correlation energy, there will be an attempt to obtain an MP2 energy for each molecule and transition structure in this study. Higher levels of electron correlation will be investigated where it is deemed necessary or desirable.

The electrostatic effects of solvation will be investigated using the SCRF method at the MP2 level of theory. The supermolecule and COSMO approaches to solvation will be investigated, with an aim to extending the results to our correlated energies. In the case of molecules which are too large to perform geometry optimisations at the MP2 level, single point MP2 calculations will be performed using an appropriate basis set. The reliability of these single point energies will be discussed.

At this point it is worth mentioning the density functional theory (DFT) and its application to organic chemistry. The development of DFT has paralleled this study, and it is probably now worth investigating the differences between the energies and structures of molecules in this study optimised with the recent improved correlated DFT methods, however at the commencement of this study, the DFT methods available would be considered undesirable and unreliable. Still now there is a question

over the relative energies of transition structures calculated using DFT, and hence it is not used in this study.

Chapter 3. The Stevens [1,2] rearrangement

3.1. Introduction

There has only been one theoretical study of the mechanism of the Stevens rearrangement of alkylammonium ylides. Semi-empirical calculations using the MINDO/3 Hamiltonian by Dewar and Ramsden in 1975¹⁹ suggested that the concerted pericyclic mechanism involved only a small activation barrier compared to the high energy gain from the exothermic reaction. In this, and following chapters, an attempt to gain understanding of the factors controlling the mechanism of the Stevens rearrangement will be made. It is expected that, starting with a simple ylide rearrangement, then gradually adding bulky aryl and alkyl groups and electron withdrawing functionality to the skeleton, we can obtain some insight into what factors affect the reaction mechanism. This initial study deals with the structures and energies of species involved in radical and concerted mechanisms of the hypothetical gas-phase rearrangement of the simplest possible alkylammonium ylide, methylammonium methylene **2** to ethylamine **1** (section 3.2) and of the carbonyl analogue methylammonium formylmethylene **6** to 2-aminopropanal **5** (section 3.3) using initially the semi-empirical MNDO theory and then extending it to more rigorous ab initio methods.

Optimised structures for species involved in the methylammonium methylene system are displayed in Figure 3.1 and for the methylammonium formylmethylene system in Figure 3.2. Optimised bond lengths (in Å) and angles (in degrees) of the molecules and radicals for each basis set and level of theory are shown in Tables 3.1 through 3.10. Relative energies of the species are given in Tables 3.11 and 3.12, and schematic energy profiles based on these results are displayed in Figures 3.3 and 3.4.

3.2. The Stevens rearrangement of methylammonium methylyde (2)

3.2.1. Ethylamine (1)

Both theoretical^{64,65} and experimental⁶⁶⁻⁶⁹ studies on ethylamine **1** have shown it to be of C_s symmetry, with a large CCN angle due to the hyperconjugative effect recently reported⁷⁰. In order to make a useful comparison between this amine and other species in this report, we have carried out our own calculations on this molecule; the optimised geometry is presented in Table 3.1, and is in agreement with previous calculations and diffraction data. It is noted that this molecule was handled well by MNDO, and that the molecular geometry did not change noticeably with basis set, or with electron correlation.

3.2.2. Methylammonium methylyde (2)

Two local minima were located on the potential surface for this ylide, one of C_s symmetry **2a**, and one of C_1 symmetry **2b** corresponding to rotation of the C_A-N bond. At post-SCF levels of theory, it is predicted that the C_s structure is of lower energy by 2 kJ mol⁻¹. Structural parameters and energies for this C_s geometry are given in Table 3.2, and the C_1 geometry in Table 3.3.

Previous studies on the smaller ylide $^-CH_2N^+H_3$ ⁷¹ indicated an expected C-N bond length of 1.559 Å. We predict the methylated species to have a similar bond length of 1.531 Å at our best level of theory, and the CNC angle to be close to 120°. The C-N bond distance seems to be rather reliant upon basis set at the lower levels of theory, however calculations on the ylide with basis sets larger than 6-31G(d) (including addition of further primitive Gaussians and extra polarisation functions) did not significantly alter the C-N distance. Incorporation of electron correlation shows the two C-N bonds to begin to average out. The ylide lies above the amine in energy by 300 kJ mol⁻¹; this is comparable to the energy difference for the rearrangement of

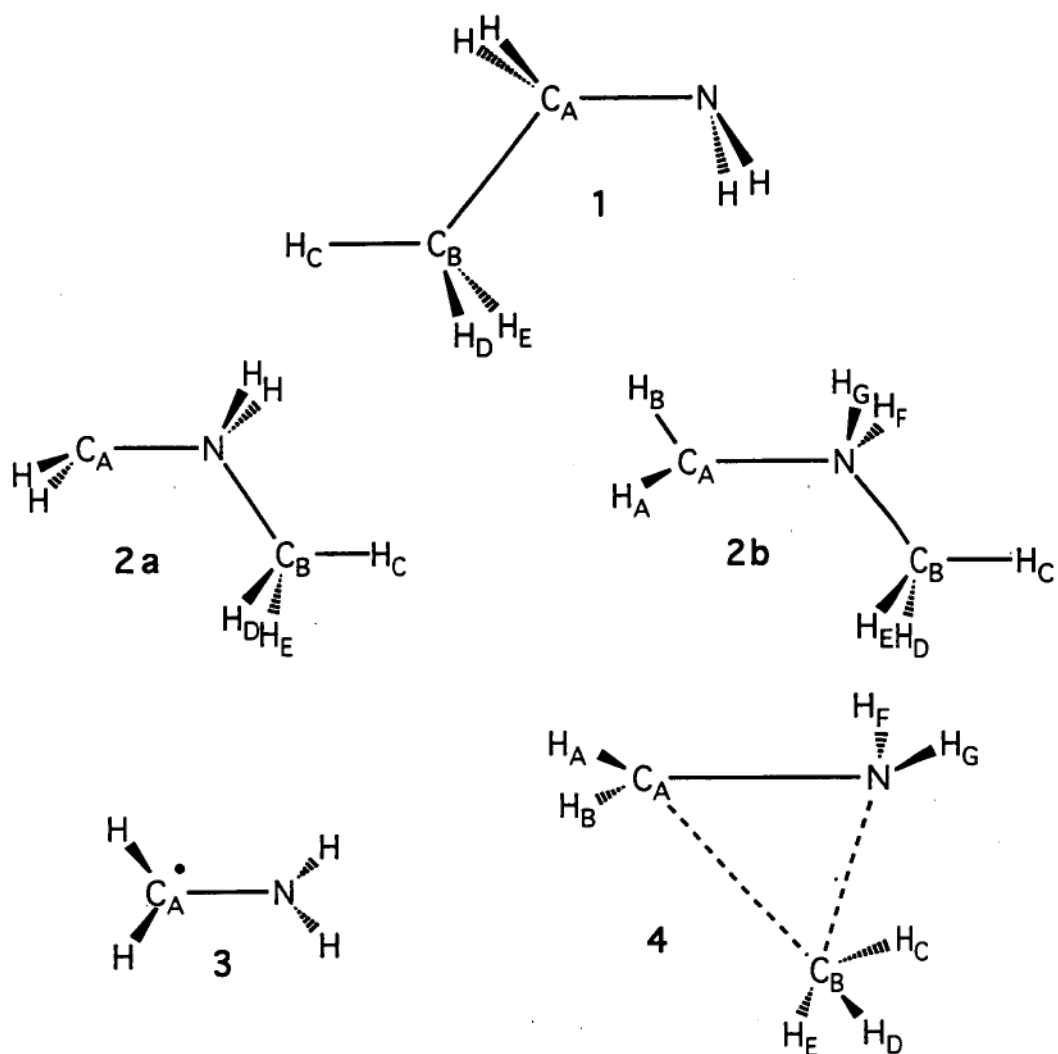


Figure 3.1. Species involved in the Stevens rearrangement of methylammonium methylyde

Table 3.1. Structural parameters and energies for ethylamine C_s symmetry 1

	MNDO	RHF/3-21G	RHF/6-31G(d)	MP2/6-31G(d)
NC _A	1.467	1.472	1.454	1.465
C _A C _B	1.537	1.543	1.529	1.526
C _A H	1.119	1.083	1.085	1.095
C _B H _C	1.109	1.085	1.086	1.095
C _B H _{DE}	1.109	1.085	1.087	1.095
NH	1.008	1.005	1.003	1.019
C _B C _A N	117.0	114.4	115.5	115.5
C _B C _A H	110.3	109.7	109.6	109.8
C _A C _B H _C	109.9	111.1	111.2	111.5
C _A C _B H _{DE}	112.1	110.4	111.0	110.7
C _A NH	108.9	113.4	110.6	109.2
NC _A C _B H _{DE}	60.65	59.81	59.93	59.80
HC _A C _B H _{DE}	57.85	58.71	58.12	58.34
C _B C _A NH	58.08	63.95	59.08	57.64
E/a.u.	-20.6905	-133.504147	-134.247608	-134.688245 ^a
E ₀ /a.u.		-133.4054	-134.1480	-134.5927

	RHF/ 6-311G(d)	MP2/ 6-311G(d)	RHF/ 6-311G(2d)	RHF/ 6-311+G(d)
NC _A	1.455	1.462	1.522	1.528
C _A C _B	1.528	1.528	1.455	1.454
C _A H	1.085	1.094	1.084	1.087
C _B H _C	1.087	1.094	1.085	1.087
C _B H _{DE}	1.087	1.094	1.084	1.085
NH	1.000	1.013	1.001	0.999
C _B C _A N	115.5	115.6	115.6	115.6
C _B C _A H	109.7	109.7	111.3	111.1
C _A C _B H _C	111.3	111.6	111.2	111.2
C _A C _B H _{DE}	111.1	110.7	109.7	109.7
C _A NH	110.7	109.6	109.7	111.3
NC _A C _B H _{DE}	59.92	59.77	59.92	59.99
HC _A C _B H _{DE}	58.09	58.26	57.97	58.10
C _B C _A NH	59.18	58.46	57.68	59.89
E/a.u.	-134.27608	-134.785247	-134.278140	-134.279202
E ₀ /a.u.	-134.1770		-134.1794	

Table 3.1. (cont.)

	MP2/ 6-311+G(d)	RHF/ 6-311G(2df)	Expt ^b	RHF/ 3-21G(N*) ^c
NC _A	1.528	1.524	1.470	1.471
C _A C _B	1.461	1.453	1.531	1.543
C _A H	1.094	1.085		1.084
C _B H _C	1.093	1.086		1.085
C _B H _{DE}	1.093	1.085		1.085
NH	1.013	1.000		1.014
C _B C _A N	115.7	115.4	115.0	114.9
C _B C _A H	111.2	111.3		109.5
C _A C _B H _C	110.9	111.0		111.1
C _A C _B H _{DE}	109.7	109.6		110.4
C _A NH	110.8	110.6		108.2
HNH	59.91	59.90		
HC _A H	58.24	58.09		
H _D C _B H _E	59.75	58.95		
E/a.u.	-134.791346	-134.284116		-134.78525

^a Higher level energies from this wavefunction: MP3 E=-134.706598 a.u., MP4 E=-134.724620 a.u., CCSD E=-134.714846 a.u.

^b Experimental results from Hamada⁶⁹

^c Previous theoretical results from Batista⁶⁵

Table 3.2. Structural parameters and energies for methylammonium methylene C_s symmetry **2a**.

	MNDO	RHF/ 3-21G	RHF/ 6-31G(d)	MP2/ 6-31G(d)	RHF/ 6-311G(d)
NC _A	1.415	1.655	1.576	1.537	1.566
NC _B	1.535	1.499	1.474	1.494	1.473
C _A H	1.077	1.100	1.095	1.102	1.095
C _B H _C	1.111	1.084	1.086	1.095	1.086
C _B H _{DE}	1.108	1.079	1.080	1.089	1.079
NH	1.025	1.008	1.004	1.022	1.000
CNC	118.3	117.6	120.0	120.3	119.8
NC _A H	118.6	99.81	101.4	102.3	102.1
NC _B H _C	109.9	111.4	111.6	112.1	111.3
NC _B H _{DE}	109.4	107.7	108.2	107.2	108.4
C _B NH	106.3	111.4	109.9	109.2	109.8
C _A NC _B H _D	59.96	58.83	58.99	58.56	59.06
C _B NC _A H	85.04	54.00	54.10	54.70	54.33
H _C C _B NH	56.56	59.00	57.62	57.11	57.63
E/a.u.	-20.5683	-133.390436	-134.125641	-134.564997 ^a	-134.161327
E ₀ /a.u.		-133.2927	-134.0260	-134.4695	-134.0625

	MP2/ 6-311G(d)	RHF/ 6-311G(2d)	MP2/ 6-311G(2d)	RHF/ 6-311G(2d,p)
NC _A	1.531	1.470	1.486	1.472
NC _B	1.492	1.559	1.528	1.558
C _A H	1.101	1.083	1.092	1.086
C _B H _C	1.095	1.077	1.086	1.080
C _B H _{DE}	1.088	1.093	1.100	1.094
NH	1.016	1.001	1.018	1.002
CNC	120.0	119.8	120.1	119.6
NC _A H	103.0	111.4	111.9	111.3
NC _B H _C	111.7	108.5	107.8	108.3
NC _B H _{DE}	107.4	102.1	103.1	102.4
C _B NH	109.1	109.8	109.5	109.8
HNH	58.57	59.04	58.58	59.03
HC _A H	55.08	54.06	54.33	54.57
H _D C _B H _E	57.42	57.43	57.07	57.69
E/a.u.	-134.671188	-134.163261	-134.705674	-134.177850

Table 3.2. (cont.)

	MP2/ 6-311G(2d,p)	RHF/ 6-311+G(d)	MP2/ 6-311+G(d)	RHF/ 6-311G(2df)
NC _A	1.489	1.475	1.494	1.471
NC _B	1.529	1.557	1.521	1.558
C _A H	1.093	1.085	1.095	1.085
C _B H _C	1.087	1.080	1.088	1.078
C _B H _{DE}	1.100	1.093	1.098	1.093
NH	1.018	1.000	1.017	1.002
CNC	119.9	120.2	120.6	119.6
NC _A H	111.7	111.1	111.3	111.4
NC _B H _C	107.5	108.5	107.7	108.3
NC _B H _{DE}	102.7	102.9	104.4	102.3
C _B NH	109.3	109.6	108.9	109.9
HNH	58.61	59.10	58.74	59.03
HC _A H	54.58	55.21	56.63	54.50
H _D C _B H _E	57.24	57.49	57.29	57.65
E/a.u.	-134.758375	-134.165877	-134.679753	-134.700310

^a Higher-level energies from this wavefunction: MP3 E=-134.583579 a.u., MP4 E=-134.603307 a.u., CCSD E=-134.592963 a.u.

Table 3.3. Structural parameters and energies for methylammonium methylene C_1 symmetry **2b**.

	RHF/3-21G	RHF/6-31G(d)	MP2/6-31G(d)
NC _B	1.497	1.470	1.481
NC _A	1.655	1.577	1.537
C _B H _C	1.082	1.084	1.093
C _B H _D	1.079	1.080	1.089
C _B H _E	1.076	1.078	1.087
C _A H _A	1.010	1.094	1.101
C _A H _B	1.010	1.095	1.101
NH _F	1.012	1.010	1.036
NH _G	1.008	1.003	1.021
CNC	107.8	110.6	110.1
NC _B H _C	111.2	111.1	111.1
NC _B H _D	107.9	108.3	107.6
NC _B H _E	106.3	107.3	106.1
NC _A H _A	100.1	101.5	102.7
NC _A H _B	99.9	101.5	102.6
C _B NH _F	110.7	109.1	107.7
C _B NH _G	109.8	108.7	108.1
C _A NC _B H _C	188.5	185.6	186.3
C _A NC _B H _D	67.4	64.9	65.6
C _A NC _B H _E	-49.5	-52.5	-51.0
C _B NC _A H _A	181.3	179.6	178.2
C _B NC _A H _B	-70.7	-72.3	-72.4
H _C C _B NH _F	61.1	56.5	55.4
H _C C _B NH _G	-58.8	-58.9	-58.3
E/a.u.	-133.390606	-134.125685	-134.564403
E ₀ /a.u.	-133.292927	-134.026841	-134.469891

$^{-}\text{CH}_2\text{N}^+\text{H}_3$ to CH_3NH_2 found previously⁶⁷. As in that study, we find the effect of going from 6-31G(d) to 6-311G(d) is to lower the relative energy by about 20 kJ mol⁻¹.

It is worth noting the performance of MNDO in describing this molecule. There seem to be two major flaws in the predicted MNDO geometry: the N–C bond lengths are quite different to those predicted using ab initio methods; and the $\text{NC}_\text{A}\text{H}$ angle is 118.6°, whereas our ab initio results suggest a much smaller angle of 103.0°. The relative energies are comparable with ab initio energies, but it could be concluded that MNDO does not handle the ylide geometry particularly well.

3.3.3. Aminomethyl radical (3)

The aminomethyl radical has been the subject of several studies (mostly at low levels of theory), due to its importance in the captodative effect⁷² and for the study of carbenium ions^{64,73}. Predicted geometries and energies for the radical **3** are set out in Table 3.4. Our calculations use quite different basis sets, yet give bond lengths and angles consistent with those previously reported by Peeters, Leroy and Matagne⁷³, who claimed a C–N distance of 1.394 Å at UHF/6-31G, comparable to our UHF/6-31G(d) value of 1.403 Å. It is worth noting that the C–N bond distance in the radical is predicted to be considerably shorter than that of the amine and ylide species. The equilibrium geometry of the molecule changes little with basis set or with inclusion of correlation effects, yet the bond angles predicted by MNDO are quite different to those calculated using ab initio techniques. As is expected with open-shell systems, the addition of electron correlation has a marked effect on the relative energy; SCF methods indicate the radical lies about 260 kJ mol⁻¹ above the amine, yet at MP2 and higher orders of electron correlation this is much increased to 370-390 kJ mol⁻¹.

Table 3.4. Structural parameters and energies for aminomethyl radical 3.

	MNDO	ROHF/ 3-21G	UHF/ 3-21G	ROHF/ 6-31G(d)	UHF/ 6-31G(d)
CN	1.391	1.406	1.404	1.403	1.402
CH	1.084	1.074	1.073	1.076	1.076
NH	1.004	1.000	1.000	0.999	0.999
HCN	119.9	115.8	116.4	115.2	115.7
CNH	112.9	118.1	118.2	113.3	113.5
HCH	119.5	117.0	33.96	116.2	46.10
HNH	108.3	114.8	146.3	109.4	125.8
E/a.u.	-14.3764	-94.060065	-94.063047	-94.582835	-94.586733
E ₀ /a.u.		-94.0072		-94.5288	

	UMP2/ 6-31G(d)	ROHF/ 6-311G(d)	UHF/ 6-311G(d)	UMP2/ 6-311G(d)
CN	1.401	1.401	1.401	1.398
CH	1.083	1.076	1.076	1.082
NH	1.014	0.996	0.996	1.008
HCN	115.4	115.7	115.7	115.6
CNH	113.5	113.5	113.4	114.0
HCH	117.2	116.1	45.97	117.4
HNH	109.8	109.6	126.2	110.9
E/a.u.	-94.868593 ^a	-94.605253	-94.609318	-94.937256
E ₀ /a.u.	-94.8168	-94.5515		

	UHF/ 6-311G(2d)	UHF/ 6-311+G(d)	MP2/ 6-311+G(d)	UHF/ 6-311G(2df)
CN	1.400	1.400	1.396	1.399
CH	1.074	1.076	1.082	1.074
NH	0.998	0.996	1.008	0.996
HCN	115.9	115.9	116.0	115.6
CNH	112.4	114.1	114.9	113.5
HCH	47.72	44.64	41.90	44.71
HNH	122.3	127.9	131.4	126.6
E/a.u.	-94.610783	-94.612905	-94.943992	-94.611715

^a Higher-level energies calculated from this wavefunction: UMP3 E=-94.809540 a.u., UMP4 E=-94.866452 a.u., CCSD E=-94.887629 a.u.

3.2.4. Concerted Transition structure for 2a → 1 (4)

With the use of the eigenvector following routine of Baker, maximising the contribution to the eigenvector from the CNC angle, the transition geometry for this rearrangement was located, **4**. Structural parameters and energies of this transition structure are displayed in Table 3.5. As a second check, energy minimisations were carried out starting from this structure with the CNC angle increased and decreased by three degrees. Increasing the angle and optimising returned the ylide geometry, decreasing the angle returned the amine geometry. The CNC angle for the transition structure is predicted to be 75° , with bond lengths along the axes of the 3-membered ring calculated to be 1.493 Å, 1.817 Å and 2.042 Å at MP2/6-311G(d). The C_A-N bond in the transition geometry is shown to be close to the average of the corresponding bond in the ylide and amine. Increasing the size of the basis set has some effect upon the optimised geometry up to 6-31G(d), but little thereafter. Electron correlation shortens the bonds about the heterocycle.

Electron correlation has a considerable effect on the relative energy of the transition structure; at the higher SCF levels **4** is predicted to lie 590 kJ mol^{-1} above the amine, yet incorporation of correlation energy reduces this significantly to 540 kJ mol^{-1} . The necessity for a moderate basis set with polarisation functions is evidenced by the large differences in relative energy between the calculations for 3-21G and 6-31G(d) basis sets. MNDO describes this species particularly poorly, both in terms of its geometry and its relative energy.

Table 3.5. Structural parameters and energies of concerted transition geometry 4.

	MNDO	RHF/ 3-21G	RHF/ 6-31G(d)	MP2/ 6-31G(d)	RHF/ 6-311G(d)
NC _A	1.462	1.559	1.504	1.493	1.502
NC _B	1.585	1.883	1.870	1.806	1.892
CC	1.901	2.059	2.059	2.044	2.076
C _A H _A	1.092	1.090	1.092	1.100	1.092
C _A H _B	1.092	1.084	1.084	1.088	1.085
C _B H _C	1.137	1.083	1.083	1.104	1.080
C _B H _D	1.112	1.071	1.071	1.086	1.070
C _B H _E	1.112	1.070	1.071	1.086	1.070
NH _F	1.020	1.015	1.015	1.046	1.010
NH _G	1.020	1.006	1.000	1.016	1.000
CNC	77.09	72.81	74.32	75.94	74.45
NC _A H _A	116.7	110.8	111.7	113.1	111.7
NC _A H _B	116.7	105.9	106.7	107.7	106.8
NC _B H _C	98.4	91.09	91.63	93.90	90.93
NC _B H _D	117.3	122.6	119.3	120.9	119.2
NC _B H _E	117.3	106.0	108.2	111.0	107.3
C _B NH _F	120.5	135.7	139.3	139.8	139.8
C _B NH _G	120.5	102.1	100.2	96.17	99.59
C _A NC _B H _C	180.0	163.2	165.6	165.2	164.6
C _A NC _B H _D	69.65	47.41	50.33	50.79	48.90
C _A NC _B H _E	290.4	276.8	279.3	278.2	278.8
C _B NC _A H _A	110.7	146.2	150.2	153.3	151.4
C _B NC _A H _B	249.3	265.2	268.3	274.1	269.2
H _C C _B NH _F	68.62	48.55	47.90	40.97	47.32
H _C C _B NH _G	291.4	272.1	274.8	275.1	293.9
E/a.u.	-20.5332	-133.293915	-134.020934	-134.479046 ^a	-134.053084
E ₀ /a.u.		-133.1997	-133.9266	-134.3886	-133.9588

Table 3.5. (cont.)

	MP2/ 6-311G(d)	RHF/ 6-311G(2d)	RHF/ 6-311+G(d)	MP2/ 6-311+G(d)	RHF/ 6-311G(2df)
NC _A	1.493	1.899	1.905	1.883	1.843
NC _B	1.817	1.496	1.500	1.493	1.496
CC	2.042	2.087	2.092	2.060	2.079
C _A H _A	1.100	1.076	1.078	1.099	1.078
C _A H _B	1.088	1.067	1.070	1.085	1.068
C _B H _C	1.101	1.067	1.070	1.085	1.069
C _B H _D	1.085	1.090	1.091	1.099	1.090
C _B H _E	1.085	1.083	1.084	1.087	1.083
NH _F	1.036	1.011	1.010	1.036	1.011
NH _G	1.010	1.000	0.996	1.010	0.997
CNC	75.46	74.82	74.77	75.77	74.67
NC _A H _A	113.2	90.75	90.54	93.10	90.74
NC _A H _B	107.9	118.7	118.6	121.4	119.0
NC _B H _C	93.50	107.1	106.9	109.7	106.9
NC _B H _D	122.2	111.9	112.1	113.6	112.1
NC _B H _E	109.8	106.8	107.2	108.4	107.1
C _B NH _F	139.4	141.3	139.7	139.3	140.6
C _B NH _G	95.73	99.09	99.51	95.58	98.73
C _A NC _B H _C	163.7	164.5	164.3	163.7	164.2
C _A NC _B H _D	48.78	48.59	48.42	48.58	48.39
C _A NC _B H _E	276.5	278.9	278.8	277.0	278.6
C _B NC _A H _A	153.6	152.4	151.6	153.6	151.7
C _B NC _A H _B	274.4	270.1	270.3	275.7	270.2
H _C C _B NH _F	41.03	46.94	46.95	41.27	46.33
H _C C _B NH _G	274.1	273.5	273.8	274.8	273.7
E/a.u.	-134.581724	-134.053496	-134.057167	-134.588877	-134.061414
E ₀ /a.u.		-133.95957			

^a Higher-level energies calculated from this wavefunction: MP3 E=-134.492854 a.u., MP4 E=-134.518954 a.u., CCSD E=-134.505270 a.u.

3.3. The Stevens rearrangement of methylammonium formylmethylide (6)

3.3.1. 2-aminopropanal (5)

The 2-aminopropanal molecule has not yet been reported in isolation, although its presence has been shown in a flame oxidation experiment⁷⁴. It is an intermediate which undergoes a rapid Claisen condensation⁷⁵ with any available substrate, including itself. It has not been the subject of any previous theoretical calculations. Our predicted structure **5** is for the *S* optical isomer of 2-aminopropanal, and is set out in detail in Table 3.6. There are no surprises in the geometry; it is overall similar to **1**. MNDO seems to overestimate the bond distances but is reasonably good at predicting the geometry of the molecule.

3.3.2. Methylammonium formylmethylide (6)

Calculations on the ylide **6**, displayed in Table 3.7 show the two N–C bond lengths to be remarkably close, most likely due to some charge delocalisation to the carbonyl group. The eigenvector associated with the highest occupied molecular orbital shows a considerable contribution from the oxygen p orbital perpendicular to the near-planar O=C–C–N backbone (dihedral angle of 1°). This would also account for the slightly shortened C–C bond. The N–C_B bond length is considerably shorter than in **2**, and the CNC angle is not close to 120°. Increasing the size of the basis set seems to shorten most of the bonds between the heavy atoms, but electron correlation has little effect upon this equilibrium geometry. MNDO predicts a NC_AC_C angle considerably different to that from ab initio, and is hence a poor method for describing the ylide. **6** is predicted to lie about 170 kJ mol⁻¹ in energy above the amine, with electron correlation lowering this energy difference by 20-30 kJ mol⁻¹. MNDO gives a somewhat higher value. From these results it can be seen that ylide **6** is, relatively,

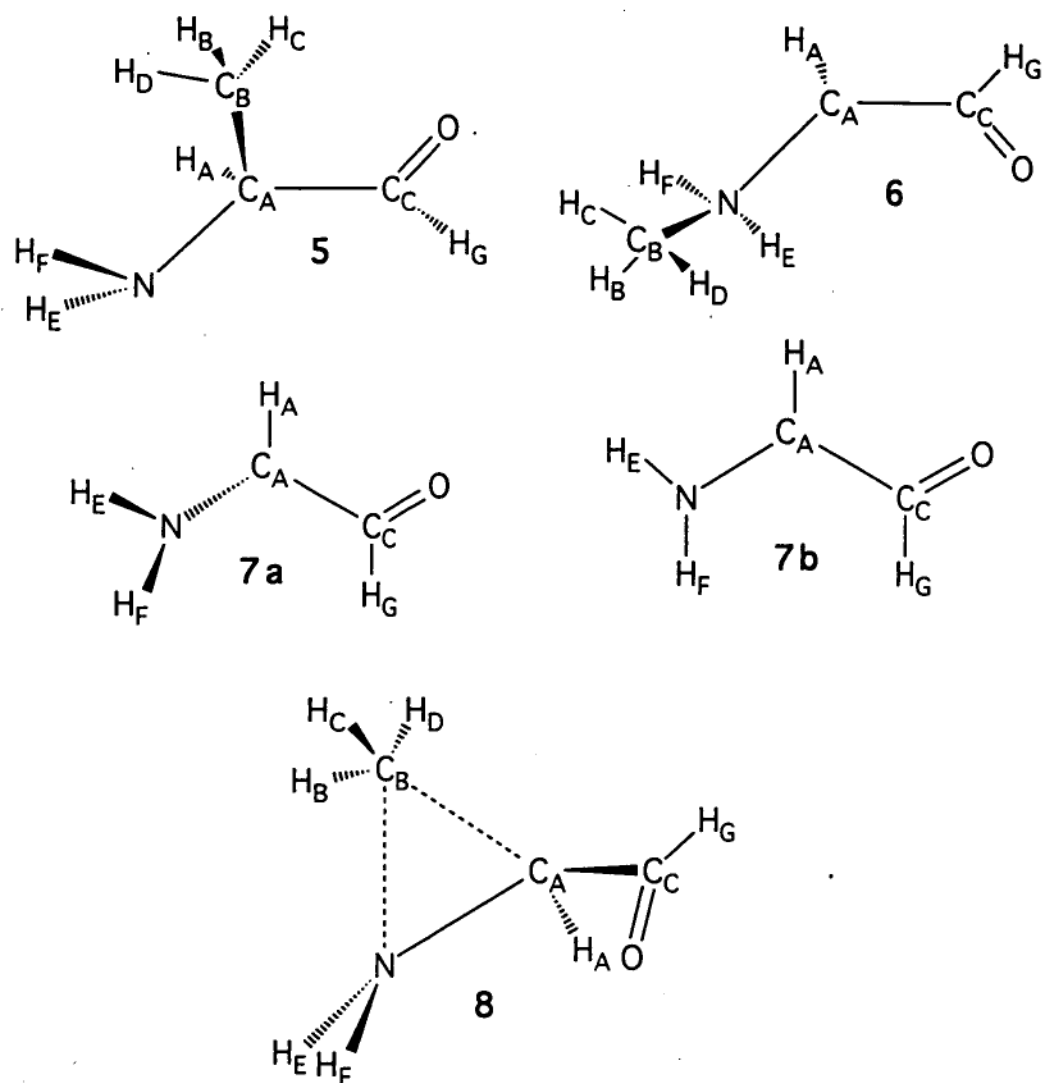


Figure 3.2. Species involved in the Stevens rearrangement of methylammonium formylmethylide

Table 3.6. Structural parameters and energies for 2-aminopropanal 5.

	MNDO	RHF/ 3-21G	RHF/ 6-31G(d)	MP2 ^a / 6-31G(d)	RHF/ 6-311G(d)
NC _A	1.471	1.469	1.456	1.465	1.456
C _A C _B	1.545	1.533	1.526	1.522	1.525
C _A C _C	1.543	1.516	1.519	1.516	1.519
C _C O	1.219	1.208	1.188	1.223	1.182
C _A H _A	1.124	1.087	1.089	1.100	1.089
C _B H _B	1.110	1.084	1.086	1.093	1.085
C _B H _C	1.109	1.082	1.083	1.092	1.083
C _B H _D	1.108	1.084	1.085	1.094	1.085
NH _E	1.009	1.003	1.001	1.018	0.998
NH _F	1.009	1.005	1.003	1.020	1.000
C _C H _G	1.110	1.085	1.093	1.108	1.095
NC _A CC	107.5	106.8	107.5	106.9	107.6
C _A CCO	124.9	124.5	124.6	124.3	124.9
C _C C _A C _B	113.0	111.1	112.3	111.8	112.5
C _C C _A H _A	106.5	106.4	104.9	105.3	104.7
C _A C _B H _B	110.8	110.6	110.2	110.4	110.3
C _A C _B H _C	110.4	110.5	111.2	111.1	111.4
C _A C _B H _D	112.8	110.0	110.7	110.1	110.8
C _A NH _E	109.5	114.5	111.0	109.8	111.1
C _A NH _F	111.1	113.6	110.9	109.3	111.0
C _A C _C H _G	113.6	112.9	114.0	114.1	113.9
OC _C C _A N	293.1	216.4	220.0	219.7	220.4
C _B C _A CCO	62.53	343.4	348.5	348.1	349.1
H _A C _A CCO	179.2	102.6	107.0	107.0	107.5
H _B C _B C _A CC	173.6	176.4	177.2	177.2	177.0
H _C C _B C _A CC	55.00	55.48	56.7	56.3	56.63
H _D C _B C _A CC	294.4	296.4	297.0	297.1	296.9
H _E NC _A CC	193.4	204.1	196.6	193.1	198.1
H _F NC _A CC	77.47	74.88	77.72	77.08	78.08
H _G CC _A N	113.2	36.46	40.34	39.42	40.71
E/a.u.	-37.2109	-245.592332	-246.972848	-247.718297	-247.029416
E ₀ /a.u.		-245.4833	-246.8628		

^a Higher-level energies calculated from this wavefunction: MP3 E=-247.725860 a.u., MP4 E=-247.764620 a.u.

Table 3.7. Structural parameters and energies for methylammonium formylmethylide **6**.

	MNDO	RHF/ 3-21G	RHF/ 6-31G(d)	MP2 ^a / 6-31G(d)	RHF/ 6-311G(d)
NC _A	1.447	1.502	1.471	1.461	1.473
NC _B	1.517	1.499	1.477	1.481	1.476
C _A C _C	1.419	1.360	1.370	1.377	1.372
C _C O	1.242	1.281	1.244	1.288	1.237
C _A H _A	1.083	1.062	1.068	1.078	1.068
C _B H _B	1.112	1.082	1.083	1.092	1.083
C _B H _C	1.110	1.079	1.080	1.090	1.080
C _B H _D	1.109	1.077	1.078	1.089	1.078
NH _E	1.027	1.064	1.025	1.103	1.017
NH _F	1.026	1.010	1.007	1.024	1.007
C _C H _G	1.113	1.081	1.091	1.097	1.092
C _A NC _B	115.8	115.0	116.3	116.1	116.3
NC _A C _C	121.9	107.7	110.7	107.5	111.2
C _A C _C O	126.2	121.0	123.4	120.5	123.7
NC _A H _A	114.8	119.5	118.2	120.6	118.0
NC _B H _B	109.3	109.9	110.0	109.9	109.9
NC _B H _C	109.7	109.1	109.0	109.6	109.1
NC _B H _D	109.8	107.2	107.8	107.0	107.8
C _A NH _E	110.4	95.5	99.7	94.4	100.5
C _A NH _F	108.4	112.8	112.5	113.8	112.3
C _A C _C H _G	113.7	118.2	116.5	119.7	116.3
C _C C _A NC _B	96.35	113.9	114.5	112.0	113.5
OC _C C _A N	359.2	0.63	0.46	1.30	0.29
H _B C _B NC _A	178.2	183.5	182.3	184.2	183.5
H _C C _B NC _A	58.54	63.50	61.75	63.01	62.87
H _D C _B NC _A	298.2	303.7	302.9	304.1	303.9
H _E NC _A C _C	333.1	357.5	356.1	356.2	355.1
H _F NC _A C _C	217.7	242.9	242.6	242.4	241.4
H _A C _A NC _B	276.9	294.5	294.7	293.9	294.1
H _G C _C C _A N	179.0	180.5	180.4	181.0	180.1
E/a.u.	-37.1387	-245.541831	-246.909120	-247.665409	-246.967162
E ₀ /a.u.		-245.4312	-246.7974		

^a Higher-level energies calculated from this wavefunction: MP3 E=-247.668225 a.u., MP4 E=-247.709752 a.u.

much more stable than ylide **2** and the simple ylide $\text{CH}_2\text{N}^+\text{H}_3$, which is consistent with the charge delocalisation mentioned above.

3.3.3. Aminoformylmethyl radical (**7**)

Several studies of the aminoformyl methyl radical have been carried out in reference to the captodative and anomeric effect and this work has recently been reviewed⁷⁶. The only reported molecular geometry, calculated by Pasto⁷² has indicated a planar structure of C_s symmetry **7b**; however, our calculations show that when a basis set incorporating polarisation functions is used, as well as in the semi-empirical calculation, the equilibrium geometry involves the amine group being out of the plane, and of C_1 symmetry **7a**. No minimum on the potential surface could be found for **7a** at either ROHF/3-21G or UHF/3-21G, nor could a minimum be located for **7b** at MNDO. Optimised structures and energies for **7a** are given in Table 3.8, and for **7b** in Table 3.9. Frequency calculations at ROHF/6-31G(d) on **7b** produce one imaginary frequency of $422i\text{ cm}^{-1}$, corresponding to the N atom moving into the plane and the two amine hydrogens moving out of the plane. Similar calculations on **7a** predict this frequency to lie at 561 cm^{-1} . At ROHF/6-31G(d), we predict an energy of -207.321593 a.u. for **7b** and -207.322496 a.u. for **7a**. At all our levels of theory, **7a** is lower in energy than **7b**, hence we predict **7a** to be the correct equilibrium geometry of this radical species.

The C–N bond in the radical is predicted to be about 0.1 \AA shorter than that in the amine or the ylide, and there are some small changes in the geometry with inclusion of electron correlation. SCF methods indicate that the radicals lie roughly 200 kJ mol^{-1} above the amine **5**, and (as with the ethylamine system) this energy difference is increased to over 300 kJ mol^{-1} with electron correlation.

Table 3.8. Structural parameters and energies for aminoformylmethyl radical C_1 symmetry **7a**.

	MNDO	ROHF/ 6-31G(d)	UHF/ 6-31G(d)	UMP2 ^a / 6-31G(d)	UHF/ 6-311G(d)
C _{AN}	1.384	1.370	1.375	1.355	1.375
C _{CC_A}	1.469	1.432	1.406	1.429	1.407
O _{CC}	1.225	1.202	1.232	1.214	1.226
C _{AH_A}	1.091	1.072	1.073	1.083	1.073
NH _E	1.004	0.996	0.996	1.011	0.993
NH _F	1.004	0.997	0.997	1.009	0.994
C _{CH_G}	1.112	1.097	1.090	1.118	1.092
C _{CC_{AN}}	122.0	122.1	123.3	121.8	123.5
O _{CC_{CA}}	122.8	124.1	122.6	125.1	122.9
H _{AC_{AC_C}}	120.4	119.7	119.3	120.0	119.1
C _{ANH_E}	115.9	117.1	116.5	119.6	116.4
C _{ANH_F}	113.8	117.5	116.9	120.4	117.5
C _{AC_{CH_G}}	116.7	115.3	117.6	113.4	116.9
O _{CC_{CAN}}	178.1	182.6	182.9	182.1	183.2
H _{AC_{AC_{CO}}}	5.2	356.6	358.2	359.0	358.3
H _{ENC_{AC_C}}	160.8	198.7	202.4	192.1	202.3
H _{FNC_{AC_C}}	32.4	338.4	339.6	348.6	339.5
H _{GCC_{CAN}}	357.9	3.18	3.35	2.50	3.55
E/a.u.	-30.9100	-207.322496	-207.334462	-207.910016	-207.383497
E ₀ /a.u.		-207.2569			

^a Higher-level energies calculated from this wavefunction: UMP3 E=-207.916210 a.u., UMP4 E=-207.945238 a.u.

Table 3.9. Structural parameters and energies for aminoformylmethyl radical C_s symmetry **7b**.

	ROHF/ 3-21G	UHF/ 3-21G	ROHF/ 6-31G(d)	UHF/ 6-31G(d)	UMP2/ 6-31G(d)
$C_A N$	1.362	1.367	1.359	1.361	1.352
$C_C C_A$	1.417	1.380	1.428	1.405	1.428
$O C_C$	1.228	1.290	1.204	1.232	1.215
$C_A H_A$	1.069	1.071	1.071	1.073	1.082
$N H_E$	0.997	0.996	0.994	0.991	1.007
$N H_F$	0.995	0.994	0.991	0.993	1.010
$C_C H_G$	1.089	1.099	1.097	1.091	1.119
$C_C C_A N$	122.5	124.4	122.3	123.4	121.8
$O C_C C_A$	124.4	122.0	124.2	122.7	125.1
$H_A C_A C_C$	119.4	118.7	119.8	119.4	120.1
$C_A N H_E$	121.4	121.3	121.2	121.2	120.6
$C_A N H_F$	121.2	121.0	121.3	121.6	120.9
$C_A C_C H_G$	114.5	118.3	115.3	117.4	113.4
$E/a.u.$	-206.181711	-206.181711	-207.321593	-207.333305	-207.909923
$E_0/a.u.$	-206.0973		-207.2569		

3.3.4. Concerted transition geometry for 6 → 5 (8)

The concerted transition structure for this rearrangement, **8**, was located using eigenvector following, and the reaction path was verified by optimising along the reaction coordinate (motion of the C-N-C angle) back to the ylide and amine structures. Since there are two isomeric pathways for this reaction, there is also a mirror image of this transition structure of equal energy, which would lead to the formation of the other optical isomer of 2-aminopropanal. Structural parameters and energies are given in Table 3.8. The CNC angle is predicted to be 72° , with bond lengths at MP2/6-31G(d) of 1.494 Å (N-C_A), 1.817 Å (N-C_B) and 1.947 Å (C-C) around the small heterocycle. The N-C_A bond changes very little in going from the ylide to the transition structure to the amine. We predict the transition structure to lie about 480 kJ mol⁻¹ above the amine in energy. Incorporation of electron correlation energy lowers this figure to about 420 kJ mol⁻¹.

The cyclic section of the transition structure is remarkably similar in shape to the corresponding section of the transition structure **4**. Addition of the carbonyl group to the molecule seems to have little effect on the overall geometry of the heterocycle. The highest occupied molecular orbital corresponds to an antibonding interaction between N-C_B, with some participation from the oxygen p orbital. This is consistent with a formally symmetry-forbidden concerted rearrangement.

There is no significant effect on the geometry by increasing the basis set, however MNDO treats this species particularly poorly, significantly underestimating the bond lengths between the heavy atoms, and predicting bond angles up to 12° different from ab initio methods. Incorporation of electron correlation in the optimisation shortens the bond lengths along the cyclic part of the molecule, but has little effect on the rest of the structure.

Table 3.10. Structural parameters and energies for concerted transition geometry 8.

	MNDO	RHF/ 3-21G	RHF/ 6-31G(d)	MP2 ^a / 6-31G(d)	RHF/ 6-311G(d)
NC _A	1.460	1.529	1.494	1.494	1.493
NC _B	1.660	1.923	1.913	1.817	1.934
C _A C _B	1.848	2.041	2.052	1.947	2.073
C _A C _C	1.468	1.392	1.399	1.404	1.398
OC _C	1.229	1.258	1.225	1.264	1.221
C _A H _A	1.099	1.068	1.074	1.083	1.075
C _B H _B	1.129	1.075	1.076	1.097	1.074
C _B H _C	1.112	1.076	1.074	1.095	1.073
C _B H _D	1.109	1.079	1.072	1.087	1.070
NH _E	1.016	1.012	1.007	1.036	1.003
NH _F	1.017	1.005	1.002	1.021	0.998
C _C H _G	1.112	1.086	1.094	1.103	1.095
C _A NC _B	72.32	71.47	72.92	71.30	73.18
C _C C _A N	122.5	111.3	113.6	110.7	114.0
OC _C C _A	126.1	123.0	123.7	120.8	124.2
NC _A H _A	114.6	116.8	116.0	117.1	116.0
NC _B H _B	94.51	89.82	90.02	93.13	89.35
NC _B H _C	119.8	128.6	125.9	131.4	125.0
NC _A H _D	116.7	95.53	97.92	99.82	97.50
C _A NH _E	115.2	107.7	109.1	104.7	110.1
C _A NH _F	113.4	114.9	113.5	115.7	113.1
C _A C _C H _G	113.2	115.9	115.8	118.1	115.6
C _C C _A NC _B	112.9	98.10	100.1	106.7	97.50
OC _C C _A N	356.6	348.0	348.5	351.2	348.3
H _B C _B NC _A	175.2	156.8	158.9	156.3	159.3
H _C C _B NC _A	66.39	38.60	41.64	38.85	41.86
H _D C _B NC _A	284.5	270.9	272.9	268.3	273.7
H _E NC _A C _C	356.0	347.3	344.7	354.2	347.3
H _F NC _A C _C	232.4	218.7	220.0	227.0	214.9
H _A C _A NC _B	257.6	250.3	249.9	257.7	257.6
H _G C _C C _A N	178.8	172.2	172.8	175.8	172.4
E/a.u.	-37.0782	-245.424053	-246.788030	-247.558490	-246.846074
E ₀ /a.u.		-245.3176	-246.6816		

^a Higher-level energies calculated using this wavefunction: MP3 E=-247.555919 a.u., MP4 E=-247.604848 a.u.

3.4. Energy profile of the prototype Stevens rearrangement

The relative energies of the species involved in the rearrangement of methylammonium methylide are displayed in Table 3.11, and those for the methylammonium formylmethylide system in Table 3.12. From these tables, energy profiles of the reactions are shown in Figures 3.3 and 3.4. The total radical energy is the sum of the energies of the predicted radical species and a free methyl radical.

At the Hartree-Fock level of theory, methylammonium methylide is predicted to dissociate to the radical products, the only barrier to that reaction being the energy required for the homolytic cleavage of the C–N bond, which is expected to be negligible. Incorporation of correlation energy had a marked effect on the shape of the reaction profile, there is an appreciable endothermicity towards the formation of the radicals; however in the gas phase, this free radical process is still predicted to be significantly favoured over a concerted 1,2-shift via structure 4.

For methylammonium formylmethylide, it is predicted that there is a substantial activation barrier for this reaction, about 200 kJ mol^{-1} , whether the mechanism is via a pair of radical intermediates or a concerted transition structure. The biradical mechanism is certainly favoured, however the two pathways are considerably closer in energy than is the case for the smaller ylide.

MNDO calculations predict the radical intermediates to have a total energy lower than the ylide for both rearrangements; however MNDO is known to overestimate the stability of open-shell systems. Due to the fragmentation into two separate entities, there is also a considerable stabilisation of the radical pathway when zero-point vibrational energy is taken into account. Increasing the basis set has little effect on the overall profile of either reaction pathway; in the methylammonium formylmethylide rearrangement, the relative energies are all raised with basis set by a similar amount. Incorporation of electron correlation has a marked effect on the energies of the transition structures and radical species; as expected, the radicals are raised in energy and the transition structures are lowered. Further electron correlation

has some effect upon the methylammonium methylene rearrangement; MP3 predicts a decrease in activation energy. However, for both systems MP4 energies are remarkably close to MP2 energies, and CCSD calculations only show a slight difference in the relative energies of the radical species - indicating that higher-order electron correlation is not important in further studies of these rearrangements.

3.5. Conclusions

We have found equilibrium structures for all the species involved in each possible pathway of the two reactions studied. Concerted transition structures for the pericyclic mechanisms have also been located, and the geometries reveal that some amount of bonding is retained in these formally symmetry-forbidden processes.

The two reactions studied are both predicted to proceed via the radical-pair mechanism in the gas phase, however the introduction of an electron-withdrawing carbonyl group is seen to stabilise the concerted transition structure with respect to the radical intermediates. Further work on the Stevens rearrangement system may shed light as to the effect of bulky alkyl and aryl groups (which exist in the systems that have been experimentally studied) on the relative energies of the intermediate species. It can be seen that semi-empirical methods are not reliable for describing the cyclic transition structure, yet optimisation at this level can be a time-saving device in obtaining a useful initial geometry for ab initio calculations.

Table 3.11. Relative energies^a (in kJ mol⁻¹ relative to **1**) for species involved in the Stevens rearrangement of methylammonium methyllide (**2a** → **1**).

	Ylide 2a	Transition structure 4	Radical Intermediates ^b
MNDO	320	412	244
RHF/3-21G	299(296) ^c	552(540)	275(235)
UHF/3-21G			259(219)
RHF/6-31G(d)	320(320)	595(581)	289(247)
UHF/6-31G(d)			267(225)
MP2/6-31G(d)	324(324)	549(568)	385(350)
MP3/6-31G(d) ^d	323	561	369
MP4/6-31G(d) ^d	319	540	388
CCSD/6-31G(d) ^d	320	550	363
RHF/6-311G(d)	301(300)	585(572)	284(246)
UHF/6-311G(d)			262(224)
MP2/6-311G(d)	299	534	381
RHF/6-311+G(d)	298	583	281
UHF/6-311+G(d)			259
MP2/6-311+G(d)	293	532	377
RHF/6-311G(2d)	302(301)	590(577)	263(224)
UHF/6-311G(2df)	302	585	257
MP2/6-311G(2df) ^e	299	529	385

^a Based on total energies given in Tables 3.1-3.5 unless otherwise noted.

^b Includes energy of **3** and planar methyl radical (see Appendix A) at a consistent level of theory

^c Values in parentheses include correction for zero-point vibrational energy

^d Based on geometries optimised at MP2/6-311G(d)

^e Based on geometry optimised at RHF/6-311G(2df)

Table 3.12: Relative energies^a (in kJ mol⁻¹ relative to **5**) for species involved in the Stevens rearrangement of methylammonium formylmethylide (**6** → **5**).

	Ylide 6	Transition structure 8	Radical intermediates ^b
MNDO	187	348	209
RHF/3-21G	132(137) ^c	442(435)	187(152) ^d
UHF/3-21G			179(144) ^d
RHF/6-31G(d)	167(172)	485(476)	251(214)
UHF/6-31G(d)			208(170)
MP2/6-31G(d)	139	420	355
MP36-31G(d) ^e	151	446	327
MP46-31G(d) ^e	144	419	354
UHF/6-311G(d)	163	481	207

^a Based on total energies in Tables 3.6-3.10 unless otherwise noted

^b Includes energy of **7a** and planar methyl radical (see Appendix A) at a consistent level of theory

^c Values in parentheses include correction for zero-point vibrational energy

^d Includes energy of **7b**, rather than **7a**

^e Based on geometries optimised at MP2/6-31G(d)

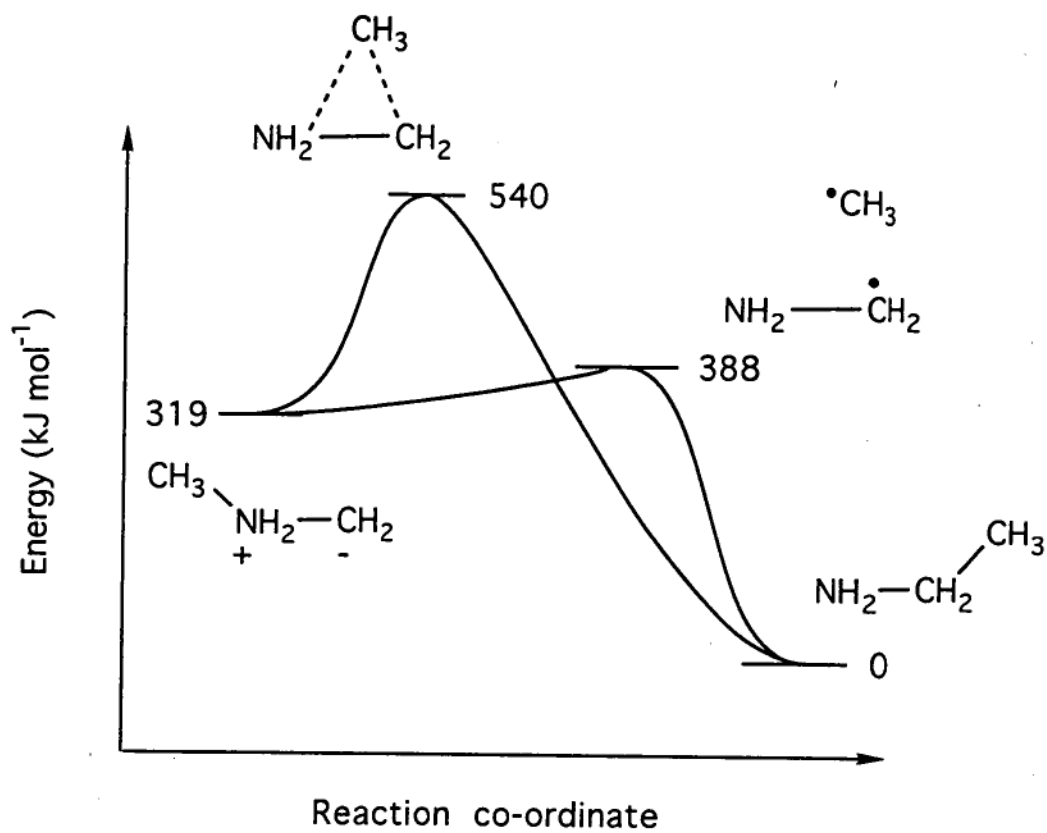


Figure 3.3. Energy diagram for the Stevens rearrangement of methylammonium methylene **2a**

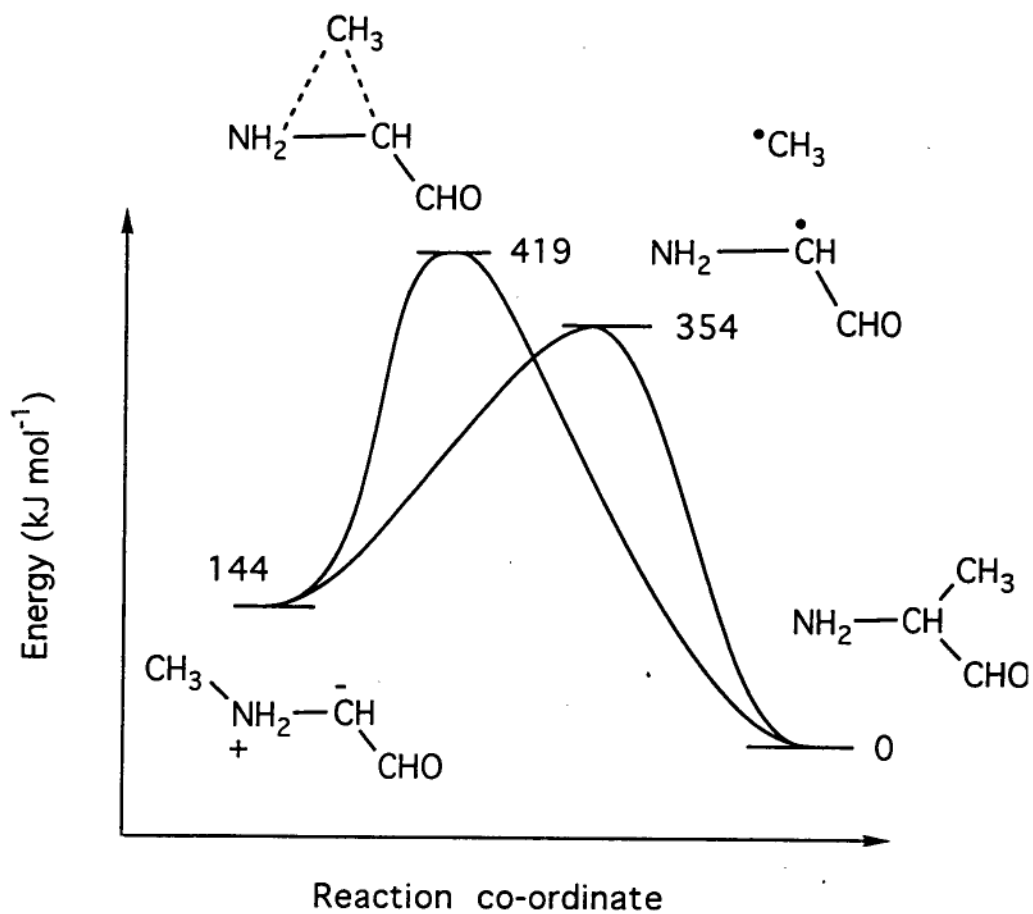


Figure 3.4. Energy diagram for the Stevens rearrangement of methylammonium formylmethylyde **6**

Chapter 4. Effects of substitution on the Stevens rearrangement

4.1. Introduction

In the previous chapter, two prototype Stevens rearrangements were investigated using ab initio and semi-empirical methods. This study pursues further the effects of steric and electronic factors on the relative energies of species involved in the rearrangement of alkylammonium ylides. Three ylides have been chosen for study at ab initio levels in order to discern these effects: trimethylammonium methylide **3y**, dimethylammonium formylmethylide **5y** and trimethylammonium formylmethylide **6y**. **3y** has recently been reported as a possible intermediate in the thermal degradation of the tetramethylammonium cation in molecular sieves⁷⁷. The Stevens rearrangement product of this ylide is N,N-dimethylethylamine **3a**. **5y** and **6y** rearrange to 2-(methylamino)propanal **5a** and 2-(dimethylamino)propanal **6a** respectively, and incorporate a carbonyl group on the carbanion and a differing amount of steric hindrance of a slightly electron-donating character about the nitrogen atom.

Semi-empirical calculations provide a means of optimising molecular geometries in a much shorter time period than for a complete ab initio optimisation, and are thus useful for comparing different combinations of molecules. Although energies from semi-empirical calculations for the systems considered here may not always be reliable, comparison of a series of related systems can provide information with regard to trends in endothermicity due to steric and electronic effects.

This chapter reports a comprehensive study of the geometries and relative energies of twelve Stevens rearrangement systems, shown in Figure 4.1 and Figure 4.2 calculated using semi-empirical methods. Starting from the simplest possible rearrangement (methylammonium ylide **1y** to methylamine **1a**), functional groups are added, progressing through the systems 2-6 studied at the ab initio level, until we

have the original reaction reported by Stevens⁹ in 1928 of phenylacylbenzylidimethylammonium ylide **9y** to 2-(dimethylamino)-3-phenylpropiophenone **9a**. Some molecules related to these species have been studied at the MINDO/3 level by Dewar and Ramsden¹⁹; comparisons between their results and our calculations will be made.

Geometries and energy trends across the twelve systems will be compared, along with the idea of using a bromine atom to mimic the steric effects of a phenyl group. In this study we have performed calculations with explicit (C₆H₅) and model (Br) phenyl groups to determine what magnitude of error might be introduced into larger systems by using this model. Incorporating an entire C₆H₅ moiety into a geometry optimisation can increase computational time significantly, particularly in the case of ab initio calculations which are expected to follow this work, however the replacement of a hydrogen by a halogen does not increase the number of structural parameters to be optimised.

In an effort to generalise our results to experimentally observable systems such as **7**, **8** and **9**, ab initio calculations will be compared with semi-empirical calculations using the MNDO, AM1 and PM3 hamiltonians. The reliability of single-point MP2/6-31G(d) calculations on geometries optimised at the semi-empirical PM3 level will be investigated as a possible method of obtaining reliable ab initio relative energies for systems too large to optimise fully at an ab initio level.

Bond lengths (in Å) and angles (in degrees) for species optimised at ab initio levels are listed in Tables 4.1-4.9, with the relative energies given in Tables 4.10-4.12. Important structural parameters for the twelve systems studied at the semi-empirical level are presented in Tables 4.13-4.15, with relative energies presented in Table 4.16.

Relative energies of Stevens rearrangement pathways calculated at ab initio and semi-empirical levels are graphed against complexity of ylide in Figures 4.3-4.5. Figure 4.6 compares the energies of species fully-optimised MP2/6-31G(d) with energies calculated at MP2/6-31G(d) at the optimised PM3 geometry.

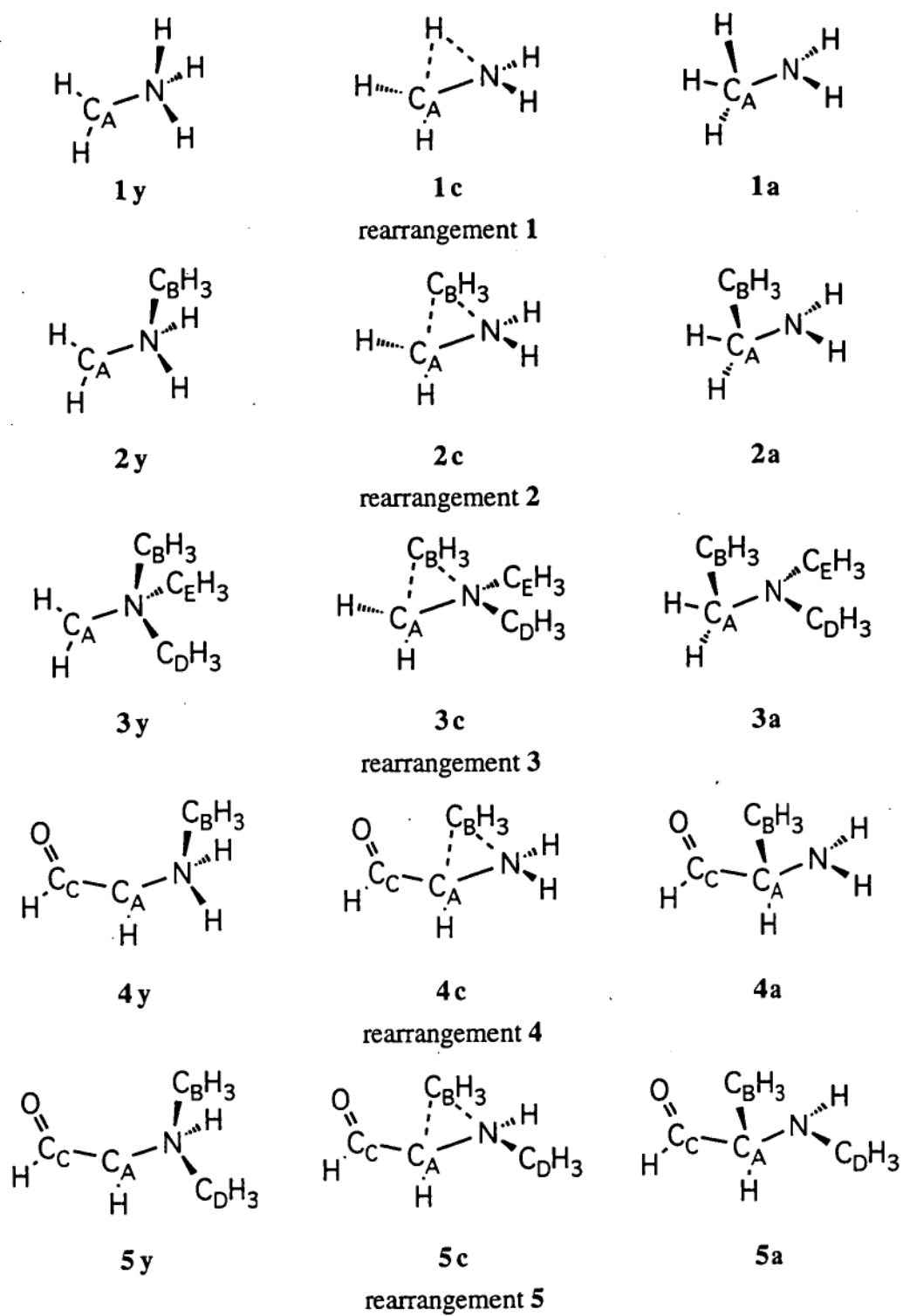


Figure 4.1. Structures of ylides, concerted transition geometries and amines studied theoretically.

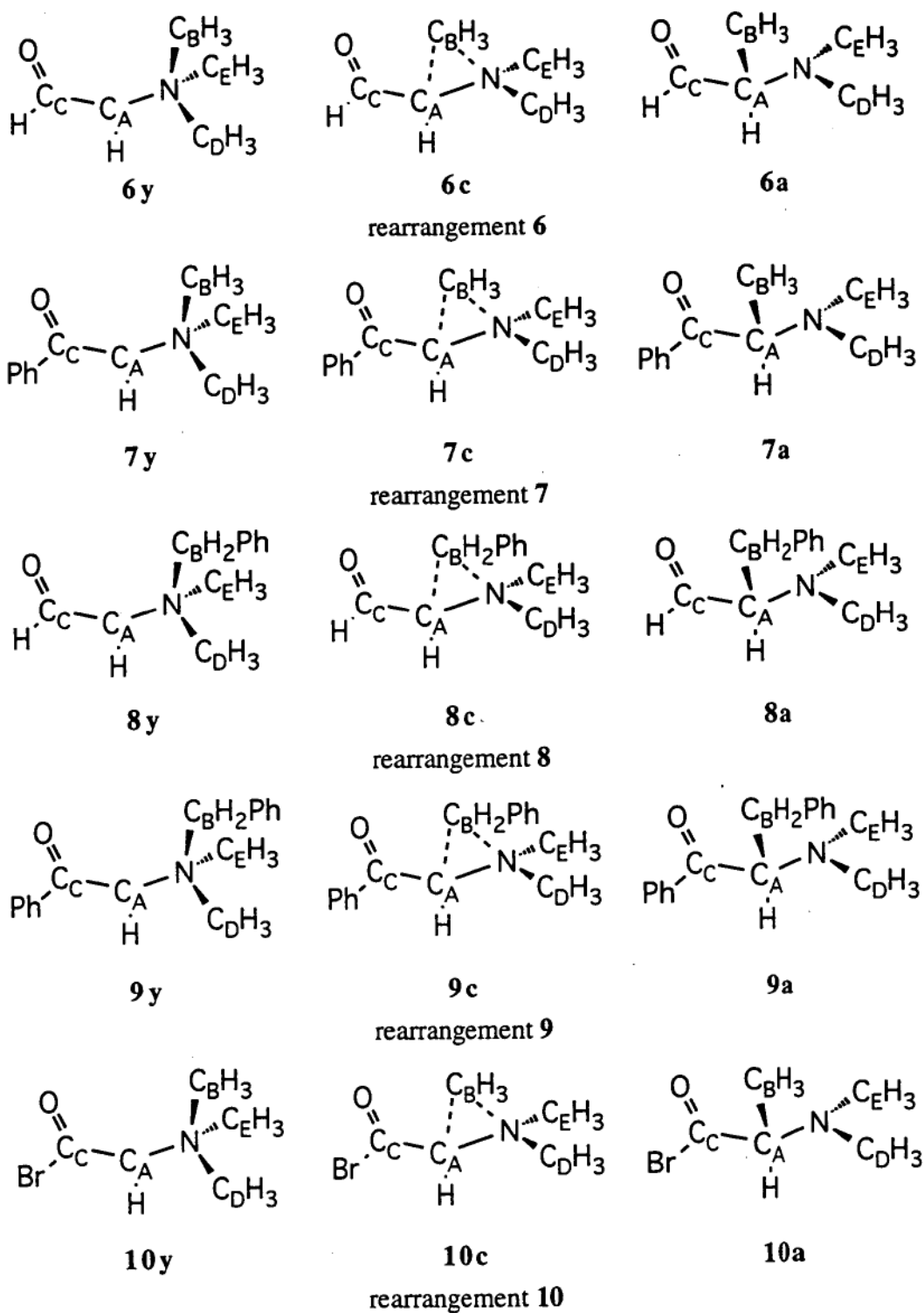


Figure 4.1. (cont) Structures of ylides, concerted transition geometries and amines studied theoretically.

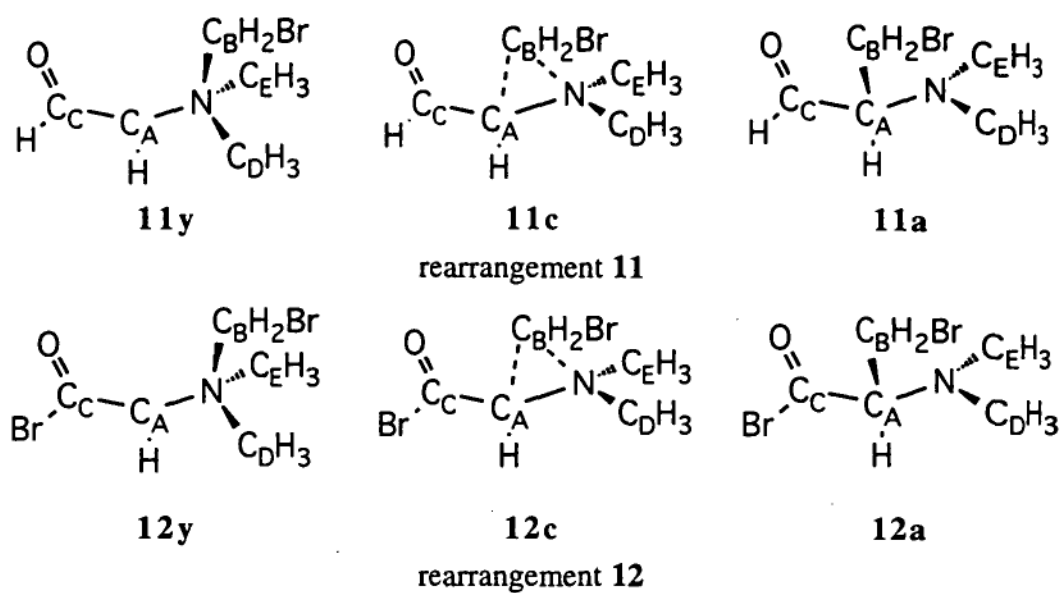


Figure 4.1. (cont.) Structures of ylides, concerted transition geometries and amines studied theoretically.

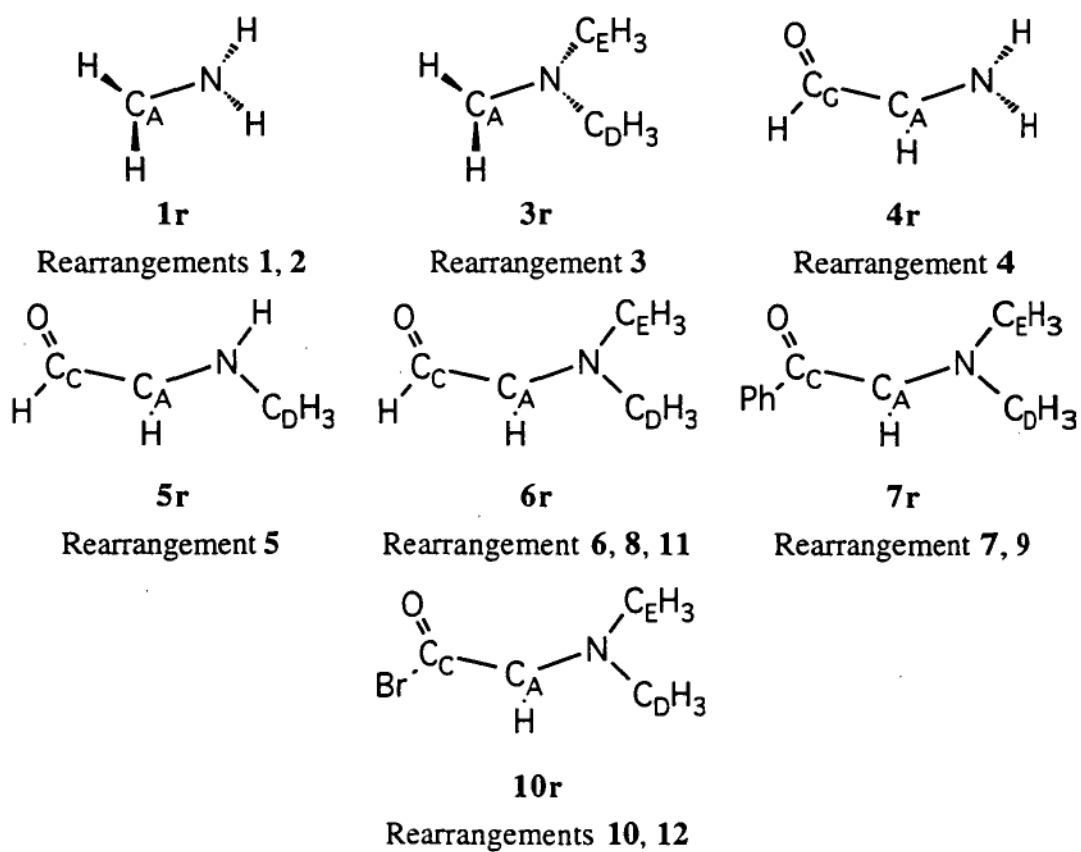


Figure 4.2. Amine radicals studied as Stevens rearrangement intermediates

4.2. Ab initio studies of substitution

4.2.1. Effect on amine geometries

Although the three amines reported in this study are the predicted end products of the ylide rearrangements, two of them are not expected to be stable and will undergo spontaneous Claisen condensation reactions with any available substrate, including themselves. Hence there is no available spectroscopic or crystallographic information with which to compare our theoretical data. Amine **3a**, however is well characterised by experiment^{78,79} and theory^{80,81}. Our calculations are necessary in order to compare energies between molecules and are comparable to previous RHF/3-21G(N*) calculations by de Carvalho and Teixeira-Dias⁸¹ (Table 4.1). The structures bear no surprises, all of the bond angles and distances are reasonable for organic amines. Our calculated structure for amine **6a** is in agreement with recent theoretical calculations by Frenking⁸² (Table 4.3).

The most notable difference between the structure of **3a** and the two carbonyl-containing amines **5a** and **6a** is the orientation of the nitrogen lone pair. In **3a**, the lone pair is *gauche* to C_B along the NC_A bond, whereas calculations on **5a** and **6a** predict the lone pair to be *trans* to C_B. This would indicate that a concerted pathway for the rearrangement is most likely to be accompanied by a nitrogen inversion or rotation about the NC_A bond.

Table 4.1. Structural parameters and energies for N,N-dimethylethylamine 3a

	RHF/3-21G(N*) ^a	RHF/3-21G	RHF/6-31G(d)	MP2/6-31G(d)
C _A N	1.467	1.471	1.453	1.462
C _B C _A	1.539	1.536	1.526	1.523
C _D N	1.462	1.466	1.447	1.457
C _E N	1.462	1.466	1.447	1.457
H _A C _A		1.093	1.096	1.109
H _B C _A		1.083	1.085	1.096
H _C C _B		1.085	1.086	1.094
H _D C _B		1.083	1.085	1.093
H _E C _B		1.083	1.084	1.092
H _F C _D		1.083	1.084	1.093
H _G C _D		1.093	1.095	1.106
H _H C _D		1.080	1.082	1.091
H _I C _E		1.083	1.084	1.094
H _J C _E		1.083	1.084	1.095
H _K C _E		1.093	1.095	1.106
C _B C _A N	112.3	112.2	113.5	113.0
C _D N _C _A	111.4	114.0	113.3	111.6
C _E N _C _A	110.0	112.8	111.5	109.9
H _A C _A N		111.5	113.3	111.2
H _B C _A N		107.2	107.3	107.0
H _C C _B C _A		110.1	109.9	110.0
H _D C _B C _A		109.2	110.3	109.8
H _E C _B C _A		111.9	112.5	112.3
H _F C _D N		109.1	109.5	109.0
H _G C _D N		112.6	112.8	112.6
H _H C _D N		110.3	110.7	110.5
H _I C _E N		109.3	109.8	109.4
H _J C _E N		109.5	109.9	109.5
H _K C _E N		112.9	113.1	112.9
C _D N _C _A C _B		67.34	67.64	66.87
C _E N _C _A C _B		196.5	193.7	188.8
H _A C _A N _C _E		72.67	69.39	64.64
H _B C _A N _C _E		315.4	313.2	308.5
H _C C _B C _A N		170.6	171.9	170.8
H _D C _B C _A N		50.94	52.39	51.31
H _E C _B C _A N		290.5	291.3	290.4
H _F C _D N _C _A		183.3	181.2	178.2
H _G C _D N _C _A		62.99	60.94	57.99
H _H C _D N _C _A		301.7	259.5	296.5
H _I C _E N _C _A		173.8	175.9	177.7
H _J C _E N _C _A		55.39	57.44	59.14
H _K C _E N _C _A		294.4	296.6	298.3
E/ a.u.		-211.129549	-212.303906	-212.995424 ^b

^a Theoretical results from de Carvalho⁸¹

^b Higher-level energies calculated from this wavefunction: MP3 E=-213.043379 a.u., MP4 E=-213.076243 a.u.

Table 4.2. Structural parameters and energies for 2-(methylamino) propanal **5a**

	RHF/3-21G	RHF/6-31G(d)	MP2/6-31G(d)
C _A N	1.465	1.453	1.463
C _B C _A	1.534	1.528	1.524
C _C C _A	1.516	1.520	1.519
OCC	1.208	1.188	1.224
C _D N	1.468	1.450	1.462
H _A C _A	1.087	1.090	1.102
H _B C _B	1.083	1.084	1.093
H _C C _B	1.082	1.083	1.092
H _D C _B	1.084	1.085	1.094
H _E N	1.005	1.002	1.021
H _F C _C	1.085	1.093	1.108
H _G C _D	1.082	1.083	1.093
H _H C _D	1.083	1.084	1.094
H _I C _D	1.089	1.090	1.100
C _B C _A C _C	111.0	112.0	111.7
C _C C _A N	106.8	107.3	106.8
OCC _A	124.6	124.7	124.4
C _D NC _A	116.6	115.9	114.1
H _A C _A C _C	106.5	105.0	105.5
H _B C _B C _A	111.0	110.8	111.0
H _C C _B C _A	110.3	110.9	110.7
H _D C _B C _A	110.0	110.6	110.0
H _E NC _A	112.2	110.0	108.5
H _F C _C C _A	112.9	113.9	114.0
H _G C _D N	108.9	109.0	108.7
H _H C _D N	108.9	109.0	108.6
H _I C _D N	114.1	114.5	114.9
OCC _A N	216.9	221.5	221.5
C _B C _A C _C O	343.9	350.0	350.0
H _A C _A C _C O	103.2	108.4	109.0
H _B C _B C _A C _C	176.7	177.0	177.4
H _C C _B C _A C _C	55.91	56.61	56.54
H _D C _B C _A C _C	297.1	297.4	297.8
C _D NC _A C _A	203.0	201.7	197.6
H _E NC _A C _C	70.96	76.12	75.68
H _F C _C C _A N	36.96	41.69	40.96
H _G C _D NC _A	176.9	179.3	180.3
H _H C _D NC _A	59.39	61.90	63.09
H _I C _D NC _A	298.2	300.5	301.8
E/a.u.	-284.403852	-285.999565	286.854997 ^a

^a Higher-level energies calculated from this wavefunction: MP3 E=-286.891894 a.u.,
MP4 E=-286.938033 a.u.

Table 4.3. Structural parameters and energies for 2-(dimethylamino)propanal **6a**

	RHF/3-21G	RHF/6-31G(d)	MP2/6-31G(d)
C _A N	1.466	1.455	1.465
C _C C _A	1.516	1.520	1.519
OCC	1.208	1.188	1.224
C _B C _A	1.535	1.530	1.526
H _A C _A	1.088	1.089	1.102
H _B C _B	1.083	1.085	1.093
H _C C _B	1.082	1.083	1.092
H _D C _B	1.082	1.083	1.092
C _D N	1.464	1.447	1.456
C _E N	1.467	1.449	1.459
H _E C _C	1.086	1.094	1.109
H _F C _D	1.083	1.084	1.094
H _G C _D	1.083	1.084	1.093
H _H C _D	1.090	1.092	1.103
H _I C _E	1.083	1.084	1.094
H _J C _E	1.089	1.091	1.102
H _K C _E	1.083	1.084	1.094
C _C C _A N	107.1	108.1	107.1
OCC _A	124.7	124.8	124.5
C _B C _A CC	111.1	111.9	111.7
H _A C _A CC	105.9	104.1	105.0
H _B C _B C _A	110.9	110.8	111.0
H _C C _B C _A	109.6	110.0	109.8
H _D C _B C _A	110.9	111.7	111.1
C _D NC _A	115.3	114.5	113.1
C _E NC _A	115.1	114.7	112.9
H _E C _C C _A	112.9	113.9	113.9
H _F C _D N	109.0	109.3	108.8
H _G C _D N	109.6	110.0	109.4
H _H C _D N	113.2	113.7	113.8
H _I C _E N	109.0	109.2	108.7
H _J C _E N	113.1	113.5	113.6
H _K C _E N	109.9	110.4	110.0
OCC _A N	216.8	217.1	219.5
C _B C _A CCO	345.6	347.8	349.7
H _A C _A CCO	103.6	104.7	107.5
H _B C _B C _A N	179.2	179.0	179.8
H _C C _B C _A N	59.07	59.24	59.76
H _D C _B C _A N	300.4	300.1	301.2
C _D NC _A CC	204.7	204.5	199.5
C _E NC _A CC	70.07	72.80	72.50
H _E C _C C _A N	37.43	38.28	39.71
H _F C _D NC _B	168.8	170.4	172.3
H _G C _D NC _B	50.67	52.28	54.28
H _H C _D NC _B	289.3	290.7	292.6
H _I C _E NC _B	194.5	193.7	191.3
H _J C _E NC _B	73.97	73.19	70.96
H _K C _E NC _B	312.7	311.8	309.4
E/a.u.	-323.217074	-325.026585	-326.016228

4.2.2. Effect on ylide geometries

An early MINDO/3 investigation of **3y**¹⁹ indicated the ylide was of C_s symmetry, two of the methyl groups on the ammonium being related by symmetry. We predict a considerably larger $C_A N C_B$ angle of 115.8° at MP2/6-31G(d) compared to 105.1° at MINDO/3 (Table 4.4), however the rest of the geometry is in good agreement. We predict **5y** and **6y** to be of C_s symmetry as well (Tables 4.5 and 4.6). This element of symmetry, relatively uncommon in medium-sized organic molecules, is due to the nitrogen atom bearing four substituents, two of which are the same, and the fact that the remaining skeleton of the molecule comprises carbanions and carbonyl carbons which lend themselves to planar, delocalised structures. We have investigated other (C_1) conformations of the ylides, but the C_s conformations are the lowest in energy at all levels of theory. This is in contrast to the corresponding situation with amines, in which the lowest energy structure is often a *gauche* C_1 conformer⁸⁰.

The $C_A N$ bond in **3y** is considerably longer than in either **5y** or **6y**; this can be attributed to delocalisation and an effective increase in the charge separation between the onium and carbanion. C_A bears a charge of -0.347 in **3y**, however the interaction of the carbonyl group lowers this to -0.112 in **5y** and -0.136 in **6y** calculated at MP2/6-31G(d). This delocalisation also leads to short $C_A C_C$ bond distances in **5y** and **6y**.

Frequency calculations at the RHF/6-31G(d) level predict that the most intense absorptions in the infrared spectrum of the ylides would occur at 2823 cm^{-1} and 2783 cm^{-1} for **3y**, 1607 cm^{-1} and 2554 cm^{-1} for **5y** and 1623 cm^{-1} and 2815 cm^{-1} for **6y** (the ab initio values have been scaled by 0.9).

Figure 4.4. Structural parameters and energies for trimethylammonium methylyde $3y$

	MINDO/3 ^a	RHF/3-21G	RHF/6-31G(d)	MP2/6-31G(d)
C _A N	1.471	1.626	1.574	1.539
C _B N	1.479	1.493	1.477	1.493
H _C C _B		1.085	1.086	1.097
H _A C _A		1.100	1.095	1.104
C _D N	1.499	1.493	1.474	1.484
H _D C _B		1.079	1.080	1.090
H _F C _D		1.084	1.085	1.094
H _G C _D		1.076	1.077	1.088
H _H C _D		1.079	1.080	1.090
C _B NC _A	105.1	114.3	114.7	115.8
H _C C _B N		111.0	111.4	111.8
H _A C _A N		100.9	101.8	102.3
C _D NC _B		110.5	109.6	109.0
H _D C _B N		108.3	108.6	107.6
H _F C _D N		110.2	110.5	110.4
H _G C _D N		107.3	108.0	106.9
H _H C _D N		108.4	108.7	108.0
H _A C _A NC _B		305.7	305.9	305.5
C _D NC _B H _C		60.73	59.87	59.30
H _D C _B NC _A		59.23	59.21	58.85
H _F C _D NC _A		174.1	175.5	174.5
H _G C _D NC _A		52.32	53.80	52.32
H _H C _D NC _A		294.6	295.8	295.0
E/a.u.		-211.022840	-212.187806	-212.883085 ^b

^a Theoretical results from Dewar¹⁹

^b Higher-level energies calculated from this wavefunction: MP3 E=-212.929812 a.u., MP4 E=-212.965181 a.u.

Table 4.5. Structural parameters and energies for dimethylammonium formylmethylyde **5y**

	RHF/3-21G	RHF/6-31G(d)	MP2/6-31G(d)
C _A N	1.498	1.472	1.463
C _B N	1.494	1.477	1.482
C _C C _A	1.360	1.360	1.379
OCC	1.281	1.244	1.287
C _A H _A	1.063	1.069	1.080
C _B H _B	1.082	1.083	1.093
C _B H _C	1.078	1.078	1.089
C _B H _D	1.080	1.081	1.092
NH _E	1.055	1.023	1.091
C _C H _F	1.082	1.091	1.099
C _B NC _A	113.5	113.9	114.1
C _C C _A N	108.3	111.3	108.1
OCC _A	121.3	123.5	120.9
C _C C _A H _A	132.7	130.9	132.0
NC _B H _B	109.9	110.2	110.0
NC _B H _C	107.8	108.1	107.5
NC _B H _D	108.7	108.9	109.1
C _A NH _E	95.64	98.79	94.60
C _A C _C H _F	118.0	116.5	119.4
C _B NC _A CC	245.1	245.2	245.8
H _B C _B NC _A	174.5	174.9	173.7
H _C C _B NC _A	53.99	54.25	53.39
H _D C _B NC _A	295.0	295.3	294.3
E/a.u.	-284.358206	-285.941175	-286.809709 ^a

^a Higher-level energies calculated from this wavefunction: MP3 E=-286.839847 a.u., MP4 E=-286.887980 a.u.

Table 4.6. Structural parameters and energies for trimethylammonium formylmethylide **6y**

	RHF/3-21G	RHF/6-31G(d)	MP2/6-31G(d)
C _B N	1.495	1.478	1.486
C _A N	1.507	1.490	1.481
C _C C _A	1.361	1.371	1.383
OC _C	1.270	1.238	1.272
H _B C _B	1.081	1.082	1.092
H _C C _B	1.079	1.080	1.090
C _D N	1.514	1.493	1.502
H _A C _A	1.064	1.068	1.080
H _E C _C	1.089	1.097	1.110
H _F C _D	1.082	1.084	1.094
H _G C _D	1.078	1.079	1.089
H _H C _D	1.077	1.076	1.090
C _A NC _B	109.6	108.8	109.3
C _C C _A N	117.2	119.2	117.8
OC _C C _A	127.4	128.0	127.3
H _B C _B N	109.2	109.6	109.3
H _C C _B N	108.5	108.9	108.3
C _D NC _A	109.3	110.5	110.1
H _A C _A N	115.3	115.0	115.8
H _E C _C C _A	113.1	112.7	113.3
H _F C _D N	109.4	109.5	109.4
H _G C _D N	107.5	107.9	107.2
H _H C _D N	105.8	107.6	106.1
H _C C _B NC _A	59.69	59.68	59.59
C _D NC _A C _C	59.47	60.37	59.99
H _G C _D NC _B	60.06	60.00	59.80
H _H C _D NC _B	301.9	301.3	301.6
E/a.u.	-323.169776	-324.962957	-325.964502

4.2.3. Effect on radical intermediates

The radical pathway for the Stevens rearrangement of the three ylides presented here involves the planar methyl radical and an amine radical formed by the dissociation of this methyl radical from the ylide. Structures **3r**, **5r** and **6r** are optimised geometries for the radicals formed by removal of a methyl radical from ylides **3y**, **5y** and **6y**. Radicals **3r** and **6r** are of C_s symmetry, as may be expected from the ylide structures, however the three different nitrogen substituents on **5r** lead to a slight deviation from planarity of the molecular skeleton. All three radicals are predicted to have very short $C_A N$ distances. ROHF and UHF calculations predict very similar structures for the radicals, UHF energies being slightly lower, as is expected. The UHF wavefunctions for the three radicals show a slight degree of spin contamination ($\langle s^2 \rangle = 0.7602$ for **3r**, 0.8287 for **5r**, 0.8320 for **6r**). Comparisons of the spin-projected energies (PUHF and PUMP2) and single-point calculations on the optimised UMP2/6-31G(d) geometry using restricted open-shell MP2 (ROMP2) theory show little difference in relative energies of the radicals (see Tables 4.7-4.9).

The chemistry of radical **3r** has been known for some time, and there have been several studies of its structure in relation to carbon-centred α -amine radicals^{83,84}. Our geometry for this radical is in good agreement with theoretical and experimental results reported by Shaffer and co-workers⁸⁴ (Table 4.7).

Table 4.7. Structural parameters and energies for trimethylaminomethyl radical **3r**

	ROHF/3-21G	UHF/3-21G	ROHF/6-31G(d)
C _A N	1.402	1.401	1.394
C _D N	1.460	1.460	1.446
H _A C _A	1.074	1.074	1.076
H _F C _D	1.083	1.083	1.084
H _G C _D	1.090	1.089	1.092
H _H C _D	1.083	1.082	1.083
C _D NC _A	117.7	117.8	115.3
H _A C _A N	116.0	116.5	115.5
H _F C _D N	109.5	109.5	109.7
H _G C _D N	112.5	112.5	112.8
H _H C _D N	109.5	109.4	109.7
H _A C _A NC _D	35.69	33.88	41.85
H _F C _D NC _A	198.3	199.1	192.1
H _G C _D NC _A	77.59	78.35	71.36
H _H C _D NC _A	316.9	317.7	310.6
E/ a.u.	-171.686014	-171.689062	-172.640912

Table 4.7. (cont.)

	UHF/6-31G(d) ^a	UMP2/6-31G(d) ^b	UMP2/6-31+G(d) ^c
C _A N	1.393	1.391	1.384
C _D N	1.445	1.453	1.454
H _A C _A	1.076	1.085	
H _F C _D	1.084	1.093	
H _G C _D	1.091	1.101	
H _H C _D	1.083	1.092	
C _D NC _A	115.5	115.7	
H _A C _A N	116.0	115.5	
H _F C _D N	109.7	109.3	
H _G C _D N	112.8	112.4	
H _H C _D N	109.7	109.2	
H _A C _A NC _D	40.20	40.61	
H _F C _D NC _A	193.0	193.7	
H _G C _D NC _A	72.25	72.86	
H _H C _D NC _A	311.5	312.3	
E/ a.u.	-172.644972	-173.181133	

^a PUHF energy -172.647250 a.u.

^b Higher-level energies calculated from this wavefunction: PUMP2 E=-173.182220 a.u., ROMP2 E=-173.181438 a.u., UMP3 E=-173.218787 a.u., UMP4 E=-173.244696 a.u.

^c Previous theoretical results from Shaffer⁸⁴

Table 4.8. Structural parameters and energies for methylaminoformylmethyl radical
5r

	ROHF/ 3-21G	UHF/ 3-21G	ROHF/ 6-31G(d)	UHF/ ^a 6-31G(d)	UMP2/ ^b 6-31G(d)
C _A N	1.350	1.359	1.349	1.356	1.338
C _C C _A	1.415	1.385	1.428	1.411	1.431
O _C C	1.235	1.287	1.209	1.229	1.228
C _D N	1.456	1.071	1.442	1.443	1.446
H _A C _A	1.069	1.556	1.073	1.079	1.084
H _E N	1.001	0.999	0.998	0.997	1.021
H _F C _C	1.082	1.076	1.091	1.087	1.108
H _G C _D	1.086	1.086	1.088	1.088	1.096
H _H C _D	1.081	1.082	1.082	1.082	1.091
H _I C _D	1.083	1.083	1.083	1.083	1.091
C _C C _A N	118.3	121.6	119.4	121.3	115.6
O _C C _C A	122.8	122.0	123.2	122.8	122.3
C _D NC _A	124.5	120.7	123.0	122.0	125.8
H _A C _A C _C	122.3	123.9	121.9	121.1	124.7
H _E NC _A	115.1	116.0	114.3	114.1	112.3
H _F C _C C _A	115.5	117.8	115.8	116.8	115.5
H _G C _D N	102.0	112.4	112.7	112.9	111.6
H _H C _D N	109.3	109.4	109.3	109.3	109.6
H _I C _D N	109.9	109.7	109.7	109.6	109.1
O _C C _C A _N	0.9081	1.316	3.230	3.834	1.606
H _A C _A C _C O	180.0	180.3	180.1	180.7	180.0
C _D NC _A C _C	184.9	187.4	196.5	200.4	188.0
H _E NC _A C _C	358.4	359.0	351.2	350.3	356.5
H _F C _C C _A N	180.9	181.4	182.9	183.6	181.5
H _G C _D NC _A	80.56	83.93	75.09	73.98	91.26
H _H C _D NC _A	201.0	204.7	195.9	195.0	212.0
H _I C _D NC _A	319.7	323.1	314.2	313.0	330.9
E/a.u.	-244.981156	-244.997324	-246.358046	-246.367676	-247.064645

^a PUHF energy is -246.372798 a.u.

^b Higher-level energies calculated from this wavefunction: PUMP2 E=-247.071865 a.u., ROMP2 E=-247.073076 a.u., UMP3 E=-247.093544 a.u., UMP4 E=-247.130788 a.u.

Table 4.9. Structural parameters and energies for dimethylaminoformylmethyl radical **6r**

	ROHF/ 3-21G	UHF/ 3-21G	ROHF/ 6-31G(d)	UHF/ ^a 6-31G(d)	UMP2/ ^b 6-31G(d)
C _A N	1.350	1.357	1.349	1.353	1.346
C _C C _A	1.414	1.388	1.429	1.412	1.431
O _C C	1.239	1.285	1.210	1.229	1.228
C _D N	1.468	1.464	1.450	1.449	1.461
C _E N	1.461	1.460	1.444	1.444	1.453
H _A C _A	1.070	1.072	1.073	1.074	1.085
H _E C _C	1.085	1.078	1.093	1.089	1.112
H _F C _D	1.085	1.086	1.087	1.087	1.095
H _G C _D	1.074	1.074	1.074	1.074	1.088
H _I C _E	1.085	1.085	1.086	1.087	1.095
H _K C _E	1.081	1.081	1.081	1.081	1.090
C _A N _C _D	123.4	123.6	124.6	124.6	123.8
C _C C _A N	127.6	129.4	128.3	129.3	126.7
O _C C _C _A	128.2	127.1	128.2	127.7	128.6
C _E N _C _A	121.0	120.9	120.3	120.3	120.8
H _A C _A N	115.7	114.7	115.3	114.7	115.5
H _E C _C _C _A	111.9	114.4	112.0	113.1	110.8
H _F C _D N	109.8	110.0	109.9	100.0	109.2
H _G C _D N	108.6	109.0	109.9	110.1	108.2
H _I C _E N	110.3	110.5	110.7	100.7	110.0
H _K C _E N	110.1	110.2	110.5	110.5	109.8
E/a.u.	-283.793429	-283.809293	-285.380916	-285.390718	-286.222357

^a PUHF energy is -285.397933 a.u.

^b PUMP2 energy is -286.229984 a.u., ROMP2 energy is -286.231412 a.u.

4.2.4. Effect on concerted transition geometries

Concerted transition geometries were located, and characterized by frequency calculations, for all three ylide rearrangements. **3c** is the transition geometry for (**3y**→**3a**), **5c** is the transition geometry for (**5y**→**5a**) and **6c** is the transition geometry for (**6y**→**6a**). In all cases there is a considerable retention of bonding between the migratory methyl group and both the nitrogen atom and C_A. The C_ANC_B angle, the parameter most explicitly defining the rearrangement, has a magnitude at MP2/6-31G(d) of 73.8° for **3c**, 71.2° for **5c** and 71.1° for **6c**. This remarkable similarity of angle indicates that the transition geometry is not heavily dependant upon the substituents at either end of the molecule.

Incorporation of correlation energy increases the orbital overlap about the small heterocycle and hence shortens the bond distances from the Hartree-Fock values.

There is still some degree of delocalisation evident in **5c** and **6c**, the OC_CC_AN backbone being bent by only 10° in **5c** and 18° in **6c** at MP2/6-31G(d). Following the transition structures for **5c** and **6c** "downhill" by decreasing the C_ANC_B angle leads to the respective amines in a different configuration to **5a** or **6a**, the methyl group being gauche to the lone pair on the nitrogen. To complete the rearrangement requires either a nitrogen inversion or rotation about the NC_A bond, both of which are expected to have low activation energies.

Table 4.10. Structural parameters and energies for concerted transition geometry **3c**

	RHF/3-21G	RHF/6-31G(d)	MP2/6-31G(d) ^a
C _{BN}	1.862	1.849	1.801
C _{AN}	1.556	1.512	1.510
H _A C _A	1.085	1.085	1.092
H _C C _B	1.087	1.089	1.110
H _D C _B	1.073	1.074	1.089
H _E C _B	1.072	1.072	1.088
C _{DN}	1.465	1.445	1.454
C _{EN}	1.470	1.451	1.466
H _B C _A	1.091	1.094	1.106
H _F C _D	1.081	1.082	1.091
H _G C _D	1.084	1.086	1.095
H _H C _D	1.088	1.090	1.100
H _I C _E	1.084	1.086	1.095
H _J C _E	1.082	1.083	1.092
H _K C _E	1.090	1.091	1.102
C _{AN} C _B	72.52	72.88	73.81
H _A C _{AN}	106.7	107.1	107.3
H _C C _{BN}	90.92	91.3	92.99
H _D C _{BN}	124.9	123.7	123.7
H _E C _{BN}	106.1	107.7	111.5
C _{DN} C _A	111.7	111.7	110.7
C _{EN} C _A	116.2	116.7	117.0
H _B C _{AN}	109.3	109.8	110.3
H _F C _{DN}	109.0	109.5	108.5
H _G C _{DN}	110.4	110.7	110.5
H _H C _{DN}	110.5	110.6	109.6
H _I C _{EN}	110.9	111.3	111.7
H _J C _{EN}	109.2	109.6	108.8
H _K C _{EN}	109.7	109.8	107.9
H _A C _{AN} C _B	99.05	97.51	93.50
H _C C _{BN} C _A	171.4	174.4	178.9
H _D C _{BN} C _A	55.69	59.46	64.99
H _E C _{BN} C _A	283.5	286.4	290.0
C _{DN} C _A H _A	204.0	210.9	196.3
C _{EN} C _A H _A	335.2	332.8	325.9
H _B C _{AN} C _B	218.2	215.1	212.3
H _F C _{DN} C _B	31.85	33.31	35.35
H _G C _{DN} C _B	271.5	272.8	274.3
H _H C _{DN} C _B	150.6	152.0	153.5
H _I C _{EN} C _B	177.9	178.7	182.1
H _J C _{EN} C _B	57.86	58.65	61.28
H _K C _{EN} C _B	299.0	299.9	303.5
E/ a.u.	-210.925440	212.085325	-212.799898

^a Higher-level energies calculated from this wavefunction: MP3 E=-212.840576 a.u., MP4 E=-212.883150 a.u.

Table 4.11. Structural parameters and energies for concerted transition geometry **5c**

	RHF/3-21G	RHF/6-31G(d)	MP2/6-31G(d) ^a
C _B N	1.911	1.894	1.820
C _A N	1.520	1.487	1.489
C _C C _A	1.393	1.401	1.408
O _C C	1.250	1.225	1.265
H _B C _B	1.076	1.078	1.097
H _C C _B	1.077	1.076	1.097
H _D C _B	1.072	1.072	1.088
C _D N	1.465	1.446	1.454
H _E N	1.013	1.006	1.037
H _A C _A	1.068	1.073	1.084
H _F C _C	1.086	1.094	1.104
H _G C _D	1.084	1.085	1.094
H _H C _D	1.082	1.083	1.092
H _I C _D	1.088	1.089	1.099
C _A N _C _B	71.40	72.46	71.17
C _C C _A N	111.7	114.0	111.3
O _C C _A	122.9	123.6	120.9
H _B C _B N	90.06	90.54	93.11
H _C C _B N	129.6	128.2	132.8
H _D C _B N	96.03	98.05	99.50
C _D N _C _A	116.0	115.9	116.3
H _E N _C _A	106.0	106.6	102.9
H _A C _A N	116.5	115.7	116.3
H _F C _C C _A	116.0	116.0	118.2
H _G C _D N	109.3	109.7	109.1
H _H C _D N	109.8	110.1	110.0
H _I C _D N	111.2	111.2	110.2
C _C C _A N _C _B	100.1	103.8	109.4
O _C C _A N	348.2	348.4	350.2
H _B C _B N _C _A	154.8	155.0	152.3
H _C C _B N _C _A	36.55	37.60	34.50
H _D C _B N _C _A	268.8	268.8	264.4
C _D N _C _A C _C	223.4	227.5	232.9
H _E N _C _A C _C	352.8	354.6	359.3
H _A C _A N _C _B	253.4	255.0	260.5
H _F C _C C _A N	172.2	172.7	175.0
H _G C _D N _C _B	20.53	22.58	19.46
H _H C _D N _C _B	261.5	263.5	260.2
H _I C _D N _C _B	140.1	142.0	138.5
E/a.u.	-284.239562	-285.820857	-286.704986

^a Higher-level energies calculated from this wavefunction: MP3 E=-286.729935 a.u., MP4 E=-286.787613 a.u.

Table 4.12. Structural parameters and energies for concerted transition geometry 6c

	RHF/3-21G	RHF/6-31G(d)	MP2/6-31G(d)
C _B N	1.973	1.974	1.874
C _A N	1.507	1.479	1.488
C _C C _A	1.395	1.405	1.414
O _C C	1.251	1.224	1.258
H _B C _B	1.073	1.074	1.096
H _C C _B	1.075	1.073	1.094
H _D C _B	1.072	1.071	1.088
C _D N	1.465	1.447	1.454
C _E N	1.474	1.457	1.463
H _A C _A	1.073	1.078	1.090
H _E C _C	1.089	1.096	1.110
H _F C _D	1.083	1.083	1.092
H _G C _D	1.083	1.084	1.110
H _H C _D	1.089	1.090	1.092
H _I C _E	1.083	1.084	1.093
H _J C _E	1.077	1.078	1.091
H _K C _E	1.090	1.091	1.102
C _A N _C _B	71.31	72.75	71.08
C _C C _A N	120.2	121.5	121.1
O _C C _C _A	127.4	128.0	126.9
H _B C _B N	87.41	87.70	90.95
H _C C _B N	125.1	122.3	127.1
H _D C _B N	98.2	100.7	103.2
C _D N _C _A	112.3	111.5	111.9
C _E N _C _A	114.0	114.8	114.3
H _A C _A N	114.4	114.4	114.4
H _E C _C _C _A	112.7	112.6	113.0
H _F C _D N	109.9	110.3	109.6
H _G C _D N	109.4	110.0	109.4
H _H C _D N	111.0	111.2	110.3
H _I C _E N	109.7	109.8	109.6
H _J C _E N	108.2	109.5	108.4
H _K C _E N	108.2	109.7	108.3
C _C C _A N _C _B	85.33	84.97	88.65
O _C C _C _A N	341.0	342.3	341.9
H _B C _B N _C _A	163.2	165.4	165.3
H _C C _B N _C _A	47.30	50.15	50.56
H _D C _B N _C _A	277.9	280.0	277.8
C _D N _C _A C _C	190.9	189.0	192.8
C _E N _C _A C _C	321.3	317.8	323.0
H _A C _A N _C _B	238.6	235.9	241.1
H _E C _C _C _A N	166.4	167.4	167.5
H _F C _D N _C _B	24.66	27.15	26.57
H _G C _D N _C _B	264.9	267.2	266.7
H _H C _D N _C _B	144.6	146.8	146.3
H _I C _E N _C _B	175.2	178.9	178.2
H _J C _E N _C _B	54.09	58.11	56.26
H _K C _E N _C _B	295.6	299.1	298.8
E/a.u.	-323.055436	-324.848798	-325.866403

4.2.5. Effect on the reaction profile

The three rearrangements are all predicted to proceed via dissociation to a pair of radicals and recombination to the respective amine. In no case is the concerted pathway competitive. The activation barriers towards the formation of the radicals are 94 kJ mol⁻¹ for **3y**, 191 kJ mol⁻¹ for **5y** at MP4/6-31G(d), and 181 kJ mol⁻¹ for **6y** at MP2/6-31G(d) (for **3y** and **5y** the MP2 and MP4 values are fairly similar).

In comparing the three ylides, ylide **3y** is predicted to be the least thermodynamically stable with respect to the corresponding amine. This leads to a lower activation energy for the rearrangement of this system, as the radical pairs are predicted to be only slightly higher in energy. Ylide **5y** is seen to be considerably more stable, and the concerted transition geometry is also considerably lower in energy due to the delocalisation across the carbanion, yet it is still not a competing factor in the rearrangement.

Ylide **6y** produces remarkably similar relative energies to **5y**. This could be an indication that further steric effects on the nitrogen atom are of little importance in determining the reaction pathway.

The importance of electron correlation in these relative energy calculations must be stressed. Hartree-Fock energies tend to overestimate the stabilities of the radical species and lead to a considerably smaller (or in the case of **3y**, negative) energy barrier to the formation of radicals. The need to incorporate correlation, unfortunately restricts the size of molecules that can be reliably studied at an ab initio level. Higher levels of correlation such as MP3 and MP4 have very little effect on the relative energies of species.

Zero-point vibrational energies have been calculated, but they have little effect on the overall reaction pathway. As would be expected, they favour the radical pairs slightly.

Table 4.13. Relative energies (in kJ mol⁻¹ with respect to **3a**) for Stevens rearrangement of trimethylammonium methylide **3y**

	ylide 3y	transition geometry 3c	radical pair ^a
RHF/3-21G	280	536	273
UHF/3-21G			257
RHF/6-31G(d)	305	574	284
UHF/6-31G(d)			259 ^b
MP2/6-31G(d)	295	513	382 ^c
ROMP2/6-31G(d) ^d			382
MP3/6-31G(d) ^d	298	532	366
MP4/6-31G(d) ^d	292	507	386

^a Based on the energy of **3r** and a planar methyl radical (Appendix A)

^b PUHF value is 249 kJ mol⁻¹

^c PUMP2 value is 372 kJ mol⁻¹

^d Based on structures optimised at MP2/6-31G(d)

Table 4.14. Relative energies (in kJ mol⁻¹ with respect to **5a**) for Stevens rearrangement of dimethylammonium formylmethylide **5y**

	ylide 5y	transition geometry 5c	radical pair ^a
RHF/3-21G	120	431	219
UHF/3-21G			168
RHF/6-31G(d)	153	469	228
UHF/6-31G(d)			191 ^b
MP2/6-31G(d)	119	394	319 ^c
ROMP2/6-31G(d) ^d			305
MP3/6-31G(d) ^d	137	425	297
MP4/6-31G(d) ^d	131	395	322

^a Based on the energy of **5r** and a planar methyl radical

^b PUHF value is 170 kJ mol⁻¹

^c PUMP2 value is 295 kJ mol⁻¹

^d Based on structures optimised at MP2/6-31G(d)

Table 4.15. Relative energies (in kJ mol⁻¹ with respect to **6a**) for Stevens rearrangement of trimethylammonium formylmethylide **6y**

	ylide 6y	transition geometry 6c	radical pair ^a
RHF/3-21G	124	424	221
UHF/3-21G			171
RHF/6-31G(d)	167	467	239
UHF/6-31G(d)			202 ^b
MP2/6-31G(d)	136	393	329 ^c
ROMP2/6-31G(d) ^d			305

^a Based on the energy of **6r** and a planar methyl radical

^b PUHF value is 175 kJ mol⁻¹

^c PUMP2 value is 303 kJ mol⁻¹

^d Based on structures optimised at MP2/6-31G(d)

4.3. Semi-empirical studies of more complex ylides

4.3.1. Geometries of species predicted by semi-empirical theory

Important bond distances and angles for all species involved in rearrangements **1-12** are set out in Table 4.16 (MNDO structures), Table 4.17 (AM1 structures) and Table 4.18 (PM3 structures). The geometries of all the species studied change relatively little as the functionality on the central atoms is increased. Certainly the lowest energy conformations about N and C_A remain the same in all cases.

The amines all have a rather simple structure, with no quirks of geometry. The ylides, where possible, exhibit C_s symmetry dependent upon the groups around the nitrogen atom (ie, in systems **1, 2, 3, 6** and **10**). The OC_CC_AN backbone is close to planar in all ylides. All the radicals incorporating the carbonyl group tend to be planar except for the methyl or hydrogen amine substituents. The transition geometries are close to the ylides in nature, substituents on the atoms around the small heterocycle arranging themselves above and below the cyclic plane.

Table 4.16. MNDO optimised parameters for species involved in rearrangements 1-12

	1a	2a	3a	4a	5a	6a
NC _A	1.460	1.467	1.473	1.456	1.472	1.476
C _A C _C				1.526	1.546	1.548
NC _D			1.463			1.467
NC _E			1.463		1.463	1.467
C _C O				1.188	1.219	1.220
C _A H				1.085	1.123	1.126
C _A C _B		1.537	1.538	1.519	1.545	1.546
C _C C _A N				107.5	106.1	106.9
C _A NC _D			116.7			116.3
C _A NC _E			116.9		118.4	119.2
OC _C C _A				124.6	125.1	125.6
HC _A N				106.4	108.4	108.1
NC _A C _B		117.0	111.5	115.8	116.1	116.2

	7a	8a	9a	10a	11a	12a
NC _A	1.474	1.476	1.477	1.468	1.474	1.469
C _A C _C	1.560	1.548	1.560	1.549	1.550	1.551
NC _D	1.467	1.467	1.467	1.467	1.468	1.468
NC _E	1.470	1.467	1.467	1.466	1.467	1.467
C _C O	1.224	1.219	1.224	1.206	1.219	1.208
C _A H	1.125	1.123	1.123	1.123	1.125	1.123
C _A C _B	1.547	1.561	1.563	1.548	1.548	1.550
C _C C _A N	107.7	106.8	107.0	107.3	107.2	106.7
C _A NC _D	115.9	116.0	116.1	116.3	116.2	116.4
C _A NC _E	120.0	120.2	120.4	121.0	120.1	121.0
OC _C C _A	122.6	126.0	122.8	128.0	125.6	127.1
HC _A N	107.9	107.6	107.5	108.6	107.9	108.6
NC _A C _B	116.5	115.9	115.2	117.3	115.3	115.6

Table 4.16. (cont.)

	1y	2y	3y	4y	5y	6y
NC _A	1.403	1.415	1.438	1.447	1.458	1.470
NC _B		1.535	1.528	1.517	1.523	1.536
C _A C _C				1.419	1.418	1.417
NC _D			1.553			1.531
NC _E			1.528		1.523	1.536
C _C O				1.242	1.242	1.241
C _A H				1.083	1.083	1.085
C _A NC _B		118.3	109.2	115.8	111.9	111.0
C _C C _A N				121.9	122.0	126.0
C _A NC _D			111.5			108.0
C _A NC _E			109.2		111.9	111.0
OC _C C _A				126.2	126.5	128.6
HC _A N				114.8	115.3	114.8

	7y	8y	9y	10y	11y	12y
NC _A	1.472	1.474	1.475	1.476	1.471	1.477
NC _B	1.536	1.555	1.556	1.536	1.532	1.532
C _A C _C	1.423	1.417	1.423	1.405	1.420	1.408
NC _D	1.532	1.531	1.532	1.534	1.535	1.538
NC _E	1.536	1.534	1.535	1.536	1.539	1.539
C _C O	1.245	1.241	1.245	1.225	1.240	1.225
C _A H	1.085	1.086	1.086	1.085	1.086	1.086
C _A NC _B	111.2	108.3	108.4	111.1	107.2	107.4
C _C C _A N	125.5	126.6	126.1	124.6	126.5	125.1
C _A NC _D	107.8	106.9	106.1	107.6	107.4	107.0
C _A NC _E	111.2	110.6	110.9	111.1	111.7	111.9
OC _C C _A	126.4	128.9	126.6	132.2	128.5	131.9
HC _A N	114.3	114.6	114.1	114.7	114.7	114.4

Table 4.16. (cont.)

	1r	3r	4r	5r	6r	7r	10r
NC _A	1.391	1.393	1.376	1.378	1.382	1.383	1.381
C _A C _C			1.406	1.462	1.462	1.471	1.455
NC _D		1.464			1.469	1.468	1.472
NC _E		1.464		1.462	1.470	1.469	1.471
C _C O			1.232	1.226	1.227	1.231	1.214
C _A H			1.073	1.094	1.094	1.093	1.093
C _C C _A N			123.3	127.5	127.9	126.6	125.7
C _A NC _D		118.5			118.1	118.0	117.9
C _A NC _E		118.5		126.7	123.4	123.7	123.8
OC _C C _A			122.6	127.1	127.8	124.8	130.1
HC _A N			117.2	115.5	116.6	116.4	117.1

	1c	2c	3c	4c	5c	6c
NC _A	1.480	1.462	1.483	1.529	1.468	1.481
NC _B	1.149 ^a	1.585	1.528	1.913	1.662	1.662
C _A C _C				1.399	1.466	1.462
NC _D			1.553			1.506
NC _E			1.528		1.491	1.504
C _C O				1.225	1.230	1.229
C _A H				1.074	1.098	1.100
C _A C _B	1.491 ^a	1.901		2.069	1.860	1.870
C _A NC _B	67.76 ^a	77.09	78.80	72.92	72.60	72.75
C _C C _A N				113.6	122.3	127.7
C _A NC _D			115.0			113.4
C _A NC _E			115.0		118.9	120.0
OC _C C _A				123.7	126.4	128.9
HC _A N				116.0	115.4	113.5
NC _A C _B	45.49 ^a	54.36	52.97	62.13	58.53	58.09

^a In rearrangement 1, C_B is the hydrogen atom migrating from N to C_A

Table 4.16. (cont.)

	7c	8c	9c	10c	11c	12c
NC _A	1.483	1.478	1.479	1.481	1.493	1.495
NC _B	1.662	1.722	1.722	1.687	1.539	1.559
C _A C _C	1.471	1.460	1.469	1.453	1.469	1.468
NC _D	1.506	1.507	1.507	1.505	1.520	1.519
NC _E	1.504	1.504	1.505	1.503	1.520	1.517
C _C O	1.233	1.230	1.234	1.215	1.226	1.213
C _A H	1.100	1.100	1.100	1.099	1.099	1.101
C _A C _B	1.870	1.900	1.901	1.868	1.822	1.870
C _A NC _B	72.71	72.39	72.39	71.94	73.87	71.24
C _C C _A N	127.2	128.3	127.8	126.1	127.3	125.8
C _A NC _D	113.3	112.0	111.8	113.3	113.7	113.9
C _A NC _E	120.3	118.3	118.9	120.1	120.1	120.7
OC _C C _A	126.2	129.1	126.3	131.8	128.4	130.8
HC _A N	112.8	113.6	112.9	113.5	113.4	113.4
NC _A C _B	58.07	59.76	59.73	59.15	54.22	56.05

Table 4.17. AM1 optimised structures for species involved in rearrangements 1-12

	1a	2a	3a	4a	5a	6a
NC _A	1.432	1.441	1.452	1.449	1.453	1.463
C _A C _C				1.523	1.524	1.526
NC _D			1.444			1.446
NC _E			1.444		1.437	1.445
C _C O				1.230	1.229	1.231
C _A H				1.134	1.133	1.135
C _A C _B		1.522	1.521	1.532	1.531	1.528
C _C C _A N				113.0	112.1	111.4
C _A NC _D			114.0			113.0
C _A NC _E			114.0		114.9	114.0
OC _C C _A				123.8	124.1	121.3
HC _A N				105.7	105.9	106.7
NC _A C _B		116.8	117.4	115.9	116.7	116.2

	7a	8a	9a	10a	11a	12a
NC _A	1.463	1.462	1.463	1.460	1.461	1.460
C _A C _C	1.535	1.529	1.536	1.534	1.531	1.538
NC _D	1.447	1.446	1.446	1.446	1.447	1.446
NC _E	1.446	1.446	1.446	1.445	1.446	1.445
C _C O	1.234	1.229	1.234	1.222	1.228	1.224
C _A H	1.133	1.133	1.132	1.133	1.133	1.133
C _A C _B	1.529	1.541	1.542	1.530	1.532	1.534
C _C C _A N	110.8	110.3	109.6	109.9	110.2	109.2
C _A NC _D	112.7	113.0	112.9	112.9	113.0	113.1
C _A NC _E	114.4	114.2	114.3	114.6	114.3	114.6
OC _C C _A	122.1	123.5	121.5	124.0	123.1	122.9
HC _A N	106.6	107.0	107.0	107.3	106.8	107.4
NC _A C _B	116.2	115.8	115.4	116.6	115.2	115.3

	1y	2y	3y	4y	5y	6y
NC _A	1.387	1.394	1.404	1.432	1.439	1.449
NC _B		1.401	1.5053	1.479	1.485	1.496
C _A C _C				1.407	1.406	1.403
NC _D			1.491			1.489
NC _E			1.505		1.485	1.496
C _C O				1.258	1.258	1.258
C _A H				1.089	1.088	1.090
C _A NC _B		116.9	111.2	113.5	111.8	110.2
C _C C _A N				119.4	119.5	122.0
C _A NC _D			111.0			110.1
C _A NC _E			111.4		111.8	110.2
OC _C C _A				124.0	124.2	126.1
HC _A N				116.1	116.0	115.5

Table 4.17. (cont.)

	7y	8y	9y	10y	11y	12y
NC _A	1.449	1.450	1.450	1.453	1.452	1.456
NC _B	1.496	1.513	1.513	1.495	1.498	1.498
C _A C _C	1.408	1.402	1.408	1.396	1.405	1.398
NC _D	1.490	1.489	1.489	1.491	1.490	1.492
NC _E	1.496	1.494	1.494	1.495	1.495	1.495
C _C O	1.263	1.259	1.264	1.248	1.257	1.247
C _A H	1.091	1.091	1.091	1.092	1.091	1.092
C _A NC _B	110.3	108.8	109.0	110.3	107.3	107.6
C _C C _A N	121.7	122.4	122.0	121.3	122.2	121.5
C _A NC _D	109.8	109.8	109.6	109.6	109.7	109.1
C _A NC _E	110.4	110.0	110.2	110.3	110.0	110.1
OC _C C _A	124.5	126.2	124.6	127.8	125.9	127.5
HC _A N	115.4	115.4	115.3	115.3	115.4	115.3

	1r	3r	4r	5r	6r	7r	10r
NC _A	1.354	1.385	1.352	1.354	1.360	1.361	1.381
C _A C _C			1.450	1.444	1.444	1.448	1.455
NC _D		1.441			1.440	1.440	1.472
NC _E		1.441		1.432	1.440	1.440	1.471
C _C O			1.239	1.241	1.241	1.246	1.214
C _A H			1.101	1.102	1.102	1.102	1.093
C _C C _A N			123.6	126.2	125.8	125.3	125.7
C _A NC _D		118.7			119.6	119.1	117.9
C _A NC _E		118.4		123.6	121.2	121.2	123.8
OC _C C _A			121.7	125.5	125.7	124.2	130.1
HC _A N			117.8	116.0	116.6	116.7	117.1

Table 4.17. (cont.)

	1c	2c	3c	4c	5c	6c
NC _A	1.456	1.440	1.447	1.444	1.447	1.452
NC _B	1.155 ^a	1.610	1.620	1.699	1.710	1.757
C _A C _C				1.451	1.450	1.441
NC _D			1.466			1.461
NC _E			1.466		1.451	1.458
C _C O				1.242	1.243	1.223
C _A H				1.103	1.103	1.107
C _A C _B	1.468	1.838	1.865	1.835	1.853	1.884
C _A NC _B	67.26	73.90	74.66	70.93	71.32	71.17
C _C C _A N				120.4	120.3	123.8
C _A NC _D			115.0			113.4
C _A NC _E			115.0		116.3	116.9
OC _C C _A				124.0	124.1	127.8
HC _A N				115.9	115.9	114.3
NC _A C _B	46.55 ^a	57.28	56.89	61.03	60.95	61.96

^a In rearrangement 1, C_B is the hydrogen atom migrating from N to C_A

	7c	8c	9c	10c	11c	12c
NC _A	1.453	1.452	1.453	1.454	1.452	1.455
NC _B	1.723	1.821	1.824	1.564	1.717	1.587
C _A C _C	1.452	1.439	1.447	1.451	1.447	1.450
NC _D	1.462	1.460	1.461	1.471	1.461	1.470
NC _E	1.459	1.459	1.459	1.469	1.459	1.466
C _C O	1.247	1.224	1.250	1.240	1.241	1.234
C _A H	1.105	1.103	1.103	1.105	1.106	1.108
C _A C _B	1.866	2.000	2.010	1.846	1.857	1.831
C _A NC _B	71.40	74.36	74.69	75.34	71.20	73.85
C _C C _A N	124.3	125.2	124.2	124.5	124.9	123.3
C _A NC _D	113.2	112.9	112.7	113.8	113.5	113.6
C _A NC _E	116.9	115.8	116.2	117.6	116.7	117.9
OC _C C _A	124.6	126.9	124.3	126.0	126.7	126.3
HC _A N	114.3	114.4	114.0	115.0	114.5	114.9
NC _A C _B	61.06	61.25	61.08	55.05	61.05	61.06

Table 4.18. PM3 optimised structures for species involved in rearrangements 1-12

	1a	2a	3a	4a	5a	6a
NC _A	1.468	1.474	1.487	1.485	1.489	1.499
C _A C _C				1.528	1.529	1.527
NC _D			1.479			1.480
NC _E			1.480		1.473	1.480
C _C O				1.208	1.208	1.210
C _A H				1.118	1.118	1.120
C _A C _B		1.518	1.518	1.522	1.524	1.523
C _C C _A N				107.5	108.8	108.7
C _A NC _D			113.9			113.0
C _A NC _E			113.9		114.3	114.4
OC _C C _A				123.5	123.6	122.6
HC _A N				106.3	106.4	105.9
NC _A C _B		117.0	116.1	113.9	114.8	114.9

	7a	8a	9a	10a	11a	12a
NC _A	1.499	1.499	1.499	1.496	1.501	1.499
C _A C _C	1.537	1.528	1.537	1.507	1.532	1.515
NC _D	1.481	1.480	1.482	1.481	1.480	1.480
NC _E	1.480	1.480	1.480	1.480	1.480	1.480
C _C O	1.219	1.208	1.214	1.181	1.207	1.187
C _A H	1.121	1.121	1.122	1.122	1.121	1.123
C _A C _B	1.523	1.537	1.536	1.525	1.512	1.515
C _C C _A N	108.2	106.8	108.2	100.0	106.6	107.2
C _A NC _D	112.4	113.0	112.4	112.3	113.1	112.6
C _A NC _E	115.0	114.0	115.3	115.2	114.1	114.9
OC _C C _A	123.2	124.4	123.2	136.1	124.0	132.0
HC _A N	106.3	106.2	106.3	106.8	106.0	107.1
NC _A C _B	115.2	114.7	114.8	115.6	114.6	114.8

Table 4.18. (cont.)

	1y	2y	3y	4y	5y	6y
NC _A	1.363	1.365	1.379	1.409	1.417	1.429
NC _B		1.546	1.543	1.516	1.518	1.523
C _A C _C				1.420	1.418	1.416
NC _D			1.516			1.521
NC _E			1.543		1.518	1.523
C _C O				1.233	1.234	1.234
C _A H				1.091	1.091	1.093
C _A NC _B		116.5	112.4	114.3	112.2	112.2
C _C C _A N				120.8	120.9	123.9
C _A NC _D			101.7			109.7
C _A NC _E			112.5		112.2	112.2
OC _C C _A				123.4	123.6	125.7
HC _A N				119.1	118.4	117.9

	7y	8y	9y	10y	11y	12y
NC _A	1.430	1.432	1.433	1.438	1.430	1.439
NC _B	1.523	1.545	1.544	1.522	1.520	1.519
C _A C _C	1.419	1.415	1.419	1.391	1.419	1.394
NC _D	1.521	1.519	1.519	1.518	1.519	1.517
NC _E	1.523	1.520	1.519	1.522	1.520	1.519
C _C O	1.240	1.235	1.241	1.206	1.233	1.206
C _A H	1.094	1.093	1.095	1.097	1.094	1.097
C _A NC _B	112.3	110.2	110.3	111.7	109.0	108.8
C _C C _A N	123.5	124.2	123.9	123.2	124.2	123.5
C _A NC _D	109.5	109.3	109.0	109.5	109.5	109.3
C _A NC _E	112.3	111.8	111.9	111.7	112.6	112.1
OC _C C _A	124.8	125.9	125.0	135.8	125.5	135.3
HC _A N	118.1	117.8	118.0	118.3	117.8	118.2

Table 4.18. (cont.)

	1r	3r	4r	5r	6r	7r	10r
NC _A	1.376	1.386	1.373	1.373	1.378	1.378	1.381
C _A C _C			1.456	1.448	1.447	1.451	1.455
NC _D		1.478			1.478	1.479	1.472
NC _E		1.478		1.468	1.474	1.474	1.471
C _C O			1.215	1.218	1.219	1.224	1.214
C _A H			1.096	1.096	1.097	1.097	1.093
C _C C _A N			121.2	126.6	126.7	126.3	125.7
C _A NC _D		117.2			117.7	117.4	117.9
C _A NC _E		117.0		123.6	122.4	122.6	123.8
OC _C C _A			122.2	125.7	126.1	125.5	130.1
HC _A N			118.4	115.7	116.0	116.3	117.1

	1c	2c	3c	4c	5c	6c
NC _A	1.488	1.466	1.474	1.474	1.477	1.485
NC _B	1.190 ^a	1.711	1.716	1.792	1.798	1.802
C _A C _C				1.449	1.448	1.446
NC _D			1.495			1.494
NC _E			1.495		1.483	1.488
C _C O				1.223	1.223	1.222
C _A H				1.098	1.098	1.100
C _A C _B	1.443	1.955	1.952	1.938	1.952	1.958
C _A NC _B	64.10	75.48	76.23	72.08	72.43	72.41
C _C C _A N				119.9	120.0	125.8
C _A NC _D			114.6			112.5
C _A NC _E			114.6		115.5	118.4
OC _C C _A				124.0	124.2	127.2
HC _A N				116.4	116.2	114.2
NC _A C _B	47.87 ^a	54.36	57.42	61.59	61.43	61.31

^a In rearrangement 1, C_B is the hydrogen atom migrating from N to C_A

Table 4.18. (cont.)

	7c	8c	9c	10c	11c	12c
NC _A	1.485	1.484	1.484	1.486	1.472	1.482
NC _B	1.800	1.863	1.858	1.830	1.524	1.569
C _A C _C	1.451	1.443	1.448	1.422	1.454	1.438
NC _D	1.494	1.495	1.495	1.492	1.508	1.503
NC _E	1.488	1.489	1.489	1.487	1.503	1.498
C _C O	1.228	1.223	1.229	1.196	1.219	1.199
C _A H	1.101	1.100	1.101	1.102	1.102	1.106
C _A C _B	1.960	1.992	1.998	1.966	1.922	1.482
C _A NC _B	72.55	72.05	72.42	71.86	79.75	75.75
C _C C _A N	125.4	126.0	125.7	124.0	125.7	123.9
C _A NC _D	112.4	111.7	111.5	112.7	113.4	113.5
C _A NC _E	118.8	117.7	118.2	117.7	119.7	119.1
OC _C C _A	125.9	127.2	126.0	137.1	125.5	133.2
HC _A N	114.2	113.9	113.4	115.0	116.2	116.5
NC _A C _B	61.19	62.82	62.49	62.24	51.31	54.2

The first four structures represent a very simple skeleton for a Stevens rearrangement system. There are considerable changes in bond lengths and angles as this skeleton is built up. Dewar and Ramsden's¹⁹ MINDO/3 study on rearrangement **3** predicted bond lengths generally a little shorter than our MNDO calculations, but the geometries are essentially the same. Our predicted C_ANC_B angle in the transition geometry is 78.8° (MNDO); MINDO/3 gives 80.0°, so our transition geometries are comparable.

Once the skeleton is established, rearrangements **5** and **6** involve adding one and two methyl groups to the nitrogen atom. Replacing one of the amine hydrogens with a methyl group increases most of the bond lengths, but has little effect on bond angles. The second methyl group has virtually no effect on the geometry. Replacing one hydrogen with a methyl group on the ylide brings the molecule into C_s symmetry (the methyl group in the conformation predicted to undergo the rearrangement is one of the two out of the σ plane) and brings about a decrease in the C_ANC_B angle. The addition of the final methyl group sees an increase in the C_CC_AN and OC_CC_A angles

due to the steric effects of the methyl group upon the carbonyl group. The first methyl group added to the radical has a similar effect on these two parameters. Replacing one of the hydrogens on the transition geometry with a methyl group has a marked effect on the bond lengths around the heterocycle, shortening them considerably, as well as the effect on the $C_C C_A N$ and $O_C C_C C_A$ angles mentioned previously. It seems that the major factor in the geometry of these systems is the initial replacement of one hydrogen with a methyl group; the second such substitution has little effect on the molecular geometry.

Rearrangements **7-9** involve phenyl substituents as observed in ylides used in synthesis. MNDO predicts the plane of the ring to be almost perpendicular to the $C_C O$ bond, however AM1 and PM3 provide a more realistic picture of the expected delocalisation. The most obvious difference between rearrangements **6** and **7** is the consistent decrease in the $O_C C_C C_A$ angle. Apart from the shortening of this angle, there is very little difference between the structures of the four species involved in each rearrangement. Dewar and Ramsden¹⁹ have carried out calculations on the ylide **7y**; our calculations are in good agreement with their MINDO/3 geometries.

Rearrangement **8**, with the phenyl group on C_B , exhibits similar behaviour as **6** with regards to the amine. $N C_B$ is longer than the corresponding bond length in the ylide, but it is in the transition geometry where some significant geometric differences arise. The $N C_B$ bond is much longer in **8** than in **6**, most likely due to the need to accommodate the phenyl group at the $C_A N C_B$ angle which remains remarkably consistent throughout all our reaction systems. A corollary of this is the long $C_A C_B$ distance for the bond being formed.

The substitution of phenyl groups at both positions leads to Stevens' original rearrangement of phenylacylbenzyltrimethylammonium ylide (rearrangement **9**). The effect is quite interesting; there is a push-pull interaction between the two "halves" of the molecule, the amine end and the carbonyl end. Those parameters associated with the nitrogen atom are similar to those predicted for **8**, those involving C_C resemble **7**. Since the heterocycle of **9** resembles that of **7**, the carbonyl group seems to be the

directing force in determining the transition geometry. These results for system **9** contrast the case of adding methyl groups to N, in which only one substitution had to be made for the important geometry changes to become apparent.

4.3.2. The use of a halogen to approximate the steric effect of a phenyl group

Replacing the phenyl group in **7** with a bromine atom (with a view to mimicking the steric effects of this phenyl group) leads to system **10**. In all four structures, this substitution shortens the $C_C O$ bond and increases the $O_C C_C C_A$ angle, but has little effect on the rest of the molecule.

Replacing the phenyl group on C_B in **6** with a bromine atom gives rearrangement **11**. There is not as consistent an effect in operation here. The amine geometry is virtually identical to **8**, with a slightly smaller $C_A C_B$ bond distance. In the ylide, the $N C_B$ bond is shorter, this is also in evidence in the transition geometry.

Rearrangement **12** has bromine atoms in both positions. There are many changes between the geometries of **12** and **9**, most noticeably in the carbonyl region. $C_C O$ is much smaller, and the corresponding angle $C_A C_C O$ has opened considerably. The heterocycle of the concerted transition geometry also changes noticeably, $N C_B$ is shorter and the $C_A N C_B$ angle much wider. Overall, the geometry changes are too great for the bromine atom to be considered a reasonable steric approximation of a phenyl group in geometry optimisation.

4.3.3. Relative energies of species

The energies of intermediate steps in the two pathways of the Stevens rearrangement are given in Table 4.19. At MNDO, the dissociative pathway is generally found to have no energy barrier, however MNDO is known to overestimate stability of radicals. AM1 and PM3, in general, indicate some barrier to the formation of radicals. The concerted transition geometry is energetically unfavourable, with an

energy barrier calculated for rearrangement **9** of 133 kJ mol⁻¹ at MNDO, 187 kJ mol⁻¹ at AM1 and 206 kJ mol⁻¹ at PM3. The first system involves the migration of a hydrogen atom, and is predicted to rearrange via a concerted transition structure due to the very high energy of the hydrogen radical.

Previous MINDO/3 calculations¹⁹ on **3** indicate an activation barrier towards the concerted transition geometry of 17 kJ mol⁻¹. Our calculations indicate 50 kJ mol⁻¹ at MNDO, but at AM1 and PM3, the barrier is more than 100 kJ mol⁻¹. Similarly, the radicals were reported to be favoured over the ylide by 42 kJ mol⁻¹, our calculations give a value of 207-136 kJ mol⁻¹, depending on the method used. Predictions of relative energies by semi-empirical methods are dependent on the parameterisation method used, however the system presented in rearrangement **3** is still very simple, and the large changes in relative energy as the molecule is "built up" from this point show that it is not an adequate system to comment on experimentally studied reactions.

Some trends in relative energy are apparent. Increasing the steric bulk around N leads to a stabilisation of the ylide and a destabilisation of the transition structure, and hence there is an overall increase in the barrier towards the concerted reaction. Larger groups on the nitrogen atom may increase this energy gap, and (at this level of theory) these results certainly rule out any possibility of a concerted rearrangement.

The effects on relative energies of adding bromine and phenyl groups to **6** are interesting for their inconsistency. The radicals show similar behaviour: bromine atoms on either C_C or C_B lower the energy, having a bromine on both atoms lowers the energy further, and phenyl groups show reasonably similar trends. However, while adding bromine atoms to the transition geometry lowers the energy, adding phenyl groups causes the relative energy to increase (at MNDO), or stay roughly the same (at AM1 and PM3). This can be attributed to the significant geometry changes that were noted between the bromo- and phenyl-substituted transition geometries. The ylides remain fairly consistent: substitution at C_C lowers the energy slightly, substitution at C_B raises the energy significantly, and the effect of both substitutions is

between these (in the bromine case a slight lowering of energy, in the phenyl case a slight raising of energy).

The HOMO-LUMO gaps in the ylides and transition geometries are predicted to be quite large, in the order of 8 eV. Due to the inherent inaccuracies in calculating orbital separations at MNDO, little can be drawn from this, however it was deemed sufficiently large to not warrant a multiconfiguration treatment.

Table 4.19. Relative energies of species (in kJ mol⁻¹ with respect to appropriate amine)

	ylide			radical pathway			concerted pathway		
	MNDO	AM1	PM3	MNDO	AM1	PM3	MNDO	AM1	PM3
1	274	230	166	384	315	332	330	314	312
2	320	277	210	244	260	267	412	433	398
3	394	320	256	237	265	275	444	443	411
4	187	140	100	209	225	230	348	368	329
5	217	155	120	197	221	237	353	371	334
6	260	175	149	196	218	239	377	383	355
7	259	174	146	195	219	237	378	383	352
8	284	175	143	184	192	212	412	382	350
9	266	174	143	165	193	213	396	381	349
10	239	155	152	193	242	244	368	372	336
11	280	179	149	180	183	242	327	368	308
12	246	160	124	165	205	241	327	365	308

4.3.4. Comparison with ab initio predictions

Figures 4.3-4.5 contain comparisons of the semi-empirical energies with MP2/6-31G(d) optimised energies where these have been calculated. It can be seen from these graphs that for the most part, the semi-empirical energies do not compare favourably with the optimised MP2/6-31G(d) energies. It is found that the geometries at MNDO differ considerably to those optimised using ab initio theory (MNDO underestimates the delocalisation seen at MP2/6-31G(d)), although the AM1 and PM3 geometries are somewhat better.

It is well known that the stability of open-shell systems is overestimated by semi-empirical methods. This is evident in Figure 4.4, however the trends in relative energy at the semi-empirical level are not too different to the trends at MP2/6-31G(d). The ylide and concerted transition structure semi-empirical energies match the trends at *ab initio* a little more closely. In all cases, the evidence is that the radical pair pathway is lower in energy than the concerted transition geometry.

Extending the model to the experimentally observable Stevens rearrangements 7, 8 and 9 gives information on the effect of further steric hindrance around the migratory group and the carbonyl. There seems to be very little change in energy from the prototype rearrangements 5 and 6 to the experimental rearrangements 7-9, apart from the radical pairs, which have become predictably lower in energy (since one would expect a highly-substituted radical to be more stable than smaller radicals).

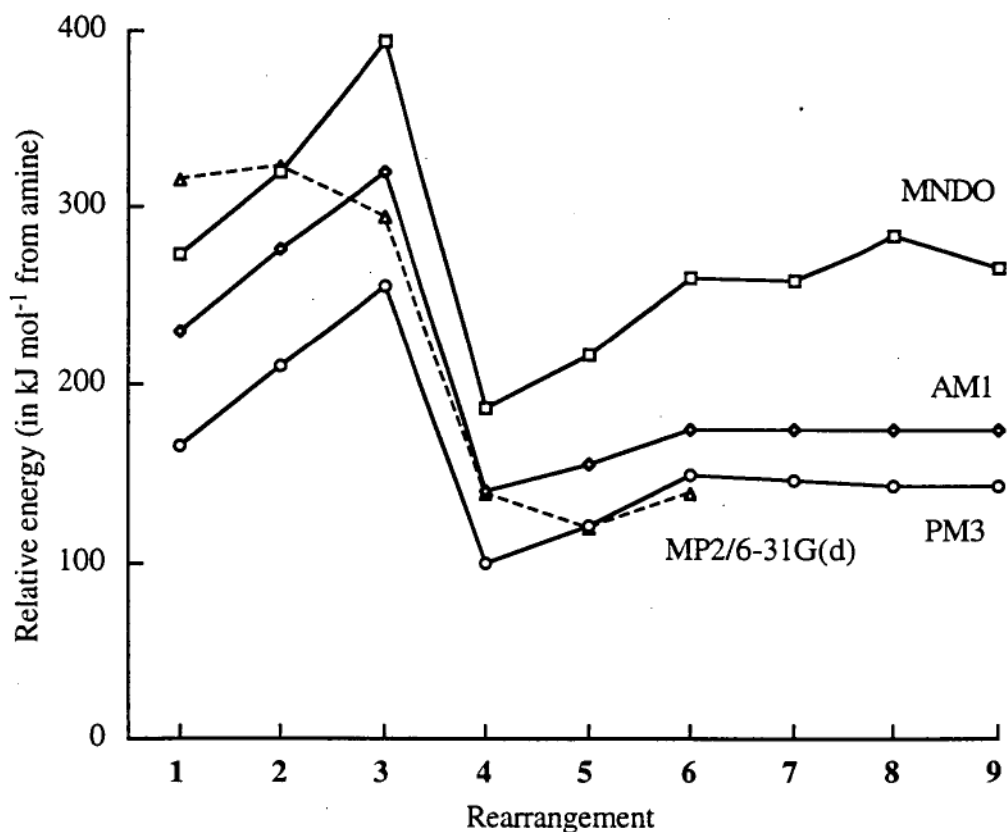


Figure 4.3. Comparison of relative energies of ylides 1y-9y calculated at semi-empirical and *ab initio* levels

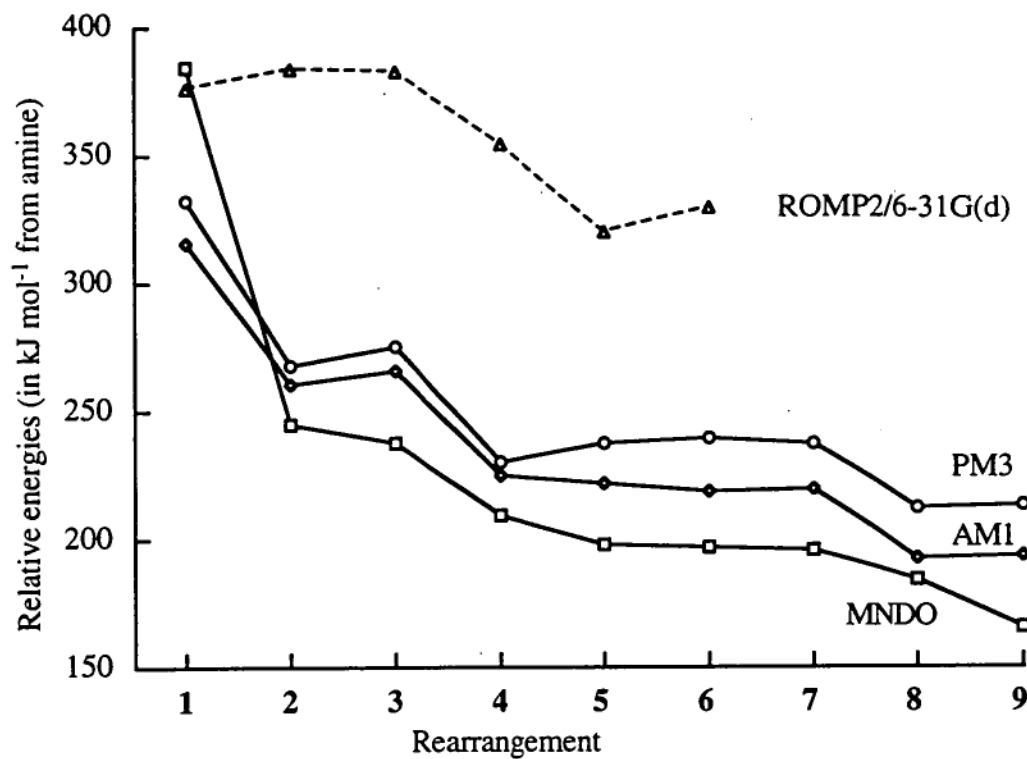


Figure 4.4. Comparison of relative energies of radical intermediates (1r-9r, plus a hydrogen, methyl or benzyl radical, as appropriate) calculated at semi-empirical and ab initio levels

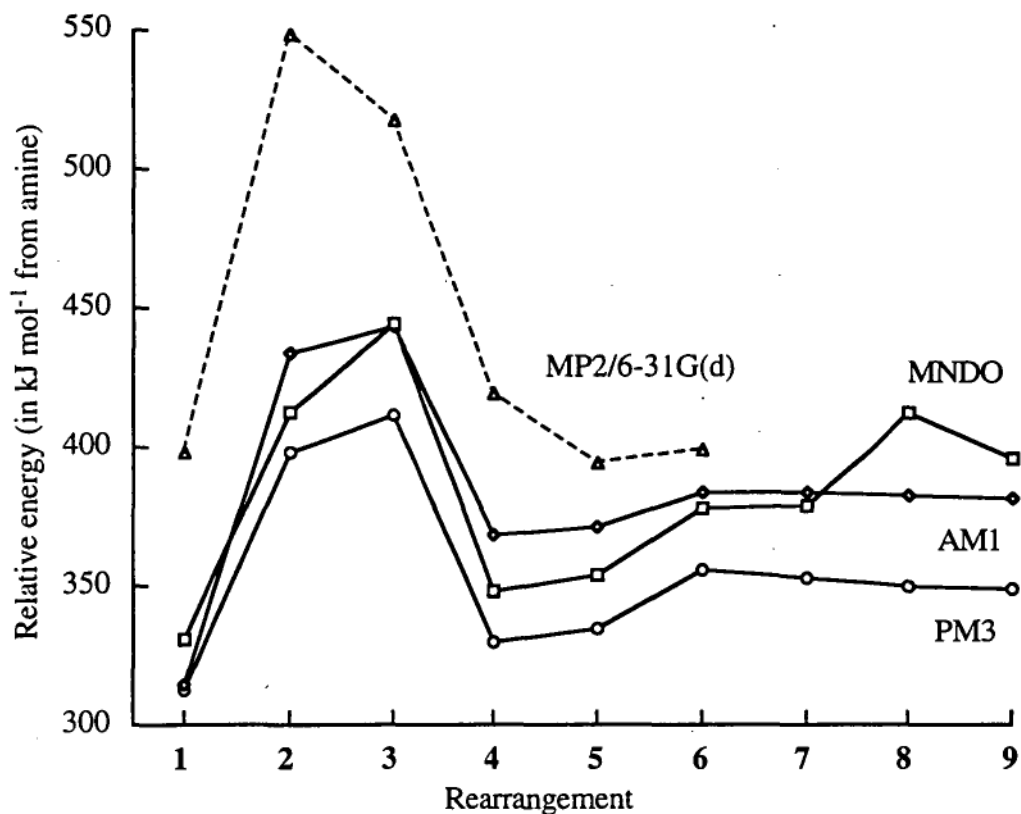


Figure 4.5. Comparison of relative energies of concerted transition geometries 1c-9c calculated at semi-empirical and ab initio levels

4.4. Single-point MP2/6-31G(d) calculations on optimised semi-empirical geometries

Semi-empirical calculations do not take into account explicitly electron correlation, which we have seen in the course of this study to be an important factor in the determination of relative energies, particularly in the case of the radical intermediates. Since the PM3 optimised geometries for 1-6 are relatively close to those predicted at MP2/6-31G(d), we have tested the performance of single-point MP2/6-31G(d) calculations at the optimised PM3 geometries. Further energy minimisation at MP2/6-31G(d) is unrealistic, as the largest of these systems 9 involves 38 atoms, 108 parameters and 323 basis functions. Due to the high degree of spin contamination in UHF wavefunctions of large conjugated radicals⁸⁵, and the fact

that the half-electron method used in the semi-empirical calculation is analogous to the ROHF method in ab initio, restricted open-shell MP2 (ROMP2) single-point calculations have been performed on the radical species.

A comparison of these single point MP2/6-31G(d)//PM3 energies with the optimised MP2/6-31G(d) energies is shown in Figure 4.6. The single-point energies compare very favourably with trends seen in optimised energies, and indeed for the larger of the rearrangements (6 in particular) there is little difference at all in the relative energy. Indeed in some cases where the semi-empirical optimised energy predicted a trend opposite to the ab initio (for example, in Figure 4a, where the relative energy of ylide 5 is higher than ylide 4 at all semi-empirical levels, yet lower at MP2/6-31G(d)), the single-point energies follow the optimised energy trends well.

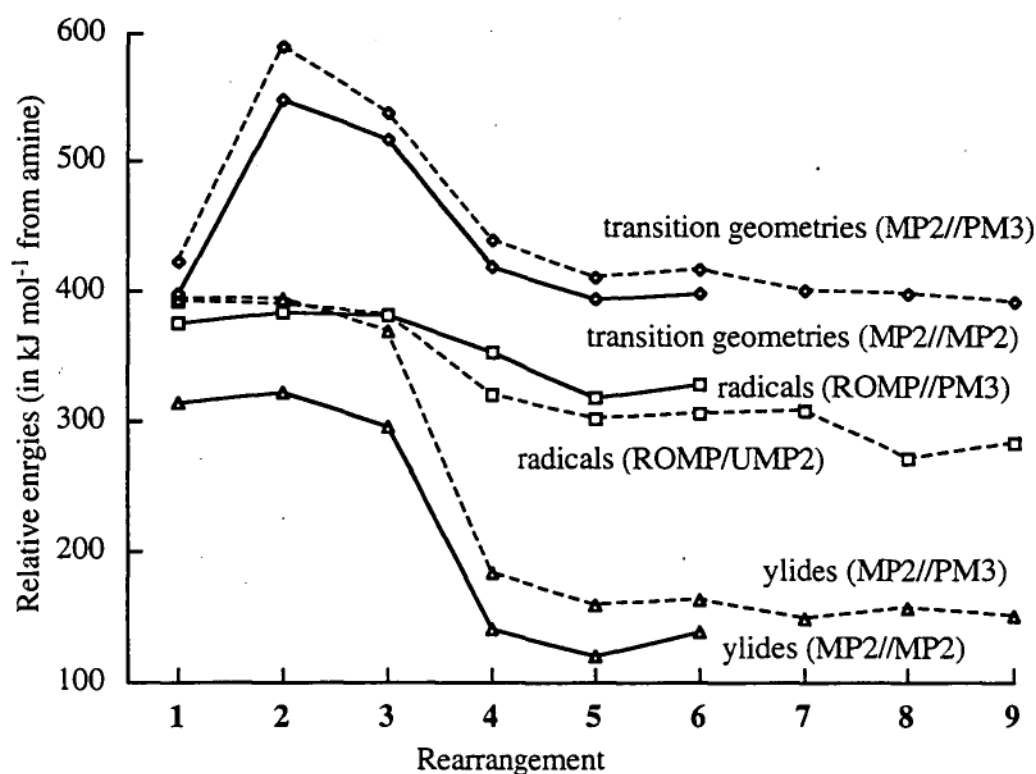


Figure 4.6. Comparison of single-point (using PM3 optimised geometry) and optimised MP2/6-31G(d) energies

4.5. Conclusions

We have completely optimised structures and calculated relative energies at three semi-empirical levels for an experimentally-observed Stevens rearrangement. In calculating the energy differences between the radical pathway and the pericyclic mechanism, we have seen that the important geometry parameters change little as the steric nature of functional groups close to the moving group is varied. The use of a bromine atom to mimic the steric effects of a phenyl group is found not to be a reasonable assumption for the rearrangements, and if higher-level calculations are to be performed on these systems, a complete aromatic system is going to have to be incorporated in the geometry optimisation.

The structures and relative energies of three ylides and their rearrangement intermediates and products have been calculated at an ab initio level of theory high enough for us to make reliable predictions about the chemical nature of these systems. The Stevens rearrangement of all three ylides is predicted to proceed via a dissociation to two radical species, involving a small energy barrier, and recombination to the alkylamine.

The PM3 and AM1 Hamiltonians have been shown to provide structures and relative energies comparable with ab initio calculations, however the MNDO method is insufficient for studying these systems, as it does not incorporate the delocalisation seen at the ab initio level, and overestimates the stability of radical species.

Single-point MP2 calculations on PM3 optimised geometries provide quite reasonable energies for comparison with ab initio values, and allow us to make reliable predictions for the (large) experimentally observable systems.

Chapter 5. Evaluation of alternative pathways in the Stevens rearrangement.

5.1. Introduction.

As mentioned in Chapter 1, the ion-pair mechanism for the Stevens rearrangement was originally proposed by T.S. Stevens⁹. In principle, heterolytic fragmentation of the ylides would lead to two ionic intermediates which could then recombine to give the amine product of the Stevens rearrangement.

The ylides which undergo the Stevens rearrangement are typically generated using a organolithium base, leaving free lithium cations in solution. It has been suggested that the interaction of a lithium cation may catalyse the Stevens rearrangement⁸⁶, but no suggested catalysed mechanisms have been proposed.

In order to examine these effects, calculations have been performed on ion-pair and lithiated pathways of the Stevens rearrangement of methylammonium methylide and methylammonium formylmethylide, the two ylides initially studied in Chapter 3. Comparisons of the ion-pair and lithiated transition structures with the original pathways will be done using these smaller ylides, in order to determine whether further calculations are required on the larger systems.

Optimised energies for the ion-pair pathways of methylammonium methylide and methylammonium formylmethylide are given in Table 5.1, and for larger ylides in Table 5.2. Optimised structural parameters and energies for ion pair species are presented in Tables 5.3-5.6. Relative energies for the Stevens rearrangement of lithiated methylammonium methylide are presented in Table 5.7, and for lithiated methylammonium formylmethylide in Table 5.8. The structures of species involved in lithiated rearrangements are given in Tables 5.9-5.23, and a diagram of them in Figure 5.2.

5.2. The ion-pair pathway

There are two possible sets of dissociation intermediates: a carbanion and cationic amine, or a carbocation and anionic amine, as shown in Figure 5.1. Calculations on these two possible sets of intermediates for methylammonium methylene and methylammonium formylmethylene, at ab initio levels up to MP2/6-31G(d), show that the former set gives lower relative energies (Table 5.1). However both pathways are extremely high in energy, and could not be considered as the actual mechanism for the rearrangement.

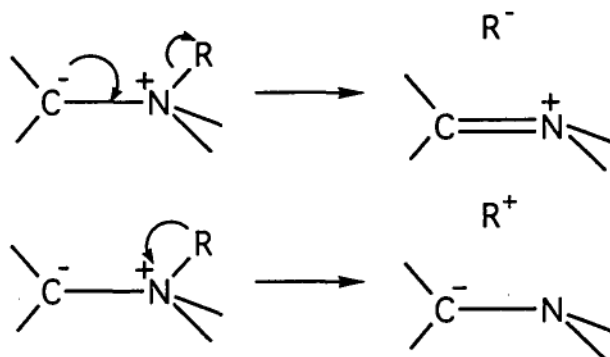


Figure 5.1. The two possible heterolytic dissociation pathways of ammonium ylides

Table 5.1. Optimised relative energies (in kJ mol⁻¹ with respect to amine) for ion-pair mechanisms

	PM3	RHF/3-21G	RHF/6-31G(d)	MP2/6-31G(d)
CH ₃ ⁻ + CH ₂ NH ₂ ⁺	1043	803	1047	1084
CH ₃ ⁺ + CH ₂ NH ₂ ⁻	1294	1176	1408	1497
CH ₃ ⁻ + CHOCHNH ₂ ⁺	1052	1119	1092	1127
CH ₃ ⁺ + CHOCHNH ₂ ⁻	1065	1176	1154	1226

In experimentally observable Stevens rearrangement systems, the ions would be considerably larger, and calculations have been performed on the ionic fragments formed from dissociation of the four largest experimentally-observed ylides from Chapter 4. The relative energies at both PM3 and single point MP2/6-31G(d) calculations on the PM3 optimised geometry are presented in Table 5.2. It can be seen that the ion pairs are very high in energy. Although the energies are slightly lower than the PM3 energies for the smaller rearrangements, the relative energies are not low enough for the ion-pair pathway to warrant significant attention. Recall that rearrangement via dissociation to two radicals were predicted to have activation energies of 200-250 kJ mol⁻¹ for these systems in Chapter 4.

Table 5.2. PM3 optimised relative energies (in kJ mol⁻¹ with respect to amine) for ion-pair mechanisms of experimentally-observable rearrangements

	PM3	MP2/6-31G(d)//PM3
CH ₃ ⁻ + (CHO)HC-N(CH ₃) ₂ ⁻	1020	1118
CH ₃ ⁺ + (CHO)HC-N(CH ₃) ₂ ⁻	1060	1205
CH ₃ ⁻ + (PhCO)HC-N(CH ₃) ₂ ⁺	996	1275
CH ₃ ⁺ + (PhCO)HC-N(CH ₃) ₂ ⁻	1048	1417
CH ₂ Ph ⁻ + (CHO)HC-N(CH ₃) ₂ ⁺	760	873
CH ₂ Ph ⁺ + (CHO)HC-N(CH ₃) ₂ ⁻	816	893
CH ₂ Ph ⁻ + (PhCO)HC-N(CH ₃) ₂ ⁺	740	1004
CH ₂ Ph ⁺ + (PhCO)HC-N(CH ₃) ₂ ⁻	807	1066

Table 5.3. Structural parameters and energies for CH₂NH₂⁺ (C_{2v})

	PM3	RHF/ 3-21G	RHF/ 6-31G(d)	MP2/ 6-31G(d)
CN	1.294	1.268	1.264	1.283
CH	1.097	1.072	1.075	1.085
NH	0.990	1.010	1.006	1.023
NCH	122.5	122.2	121.9	121.7
CNH	121.8	120.2	119.8	119.5
E/a.u.	-334.44903 ^a	-93.862400	-94.383177	-94.659580

^a Energy in eV

Table 5.4. Structural parameters, energies and a_0 values for CH_2NH_2^- (C_s)

	PM3	RHF/ 3-21G	RHF/ 6-31G(d)	MP2/ 6-31G(d)
CN	1.452	1.615	1.567	1.583
CH	1.095	1.122	1.117	1.123
NH	1.006	1.021	1.010	1.027
NCH	106.3	100.6	101.3	100.4
CNH	109.7	104.8	104.2	102.5
cis-HCNH	64.8	74.2	75.75	77.45
trans-HCNH	111.9	108.5	105.8	103.5
E/a.u.	-340.74002 ^a	-93.948710	-94.480582	-94.780121

^a Energy in eV**Table 5.5.** Structural parameters and energies for $\text{C}_2\text{H}_4\text{NO}^+$ (C_s)

	PM3	RHF/3-21G	RHF/6-31G(d)	MP2/6-31G(d)
C_{AN}	1.298	1.267	1.266	1.287
C_{CC_A}	1.529	1.510	1.518	1.509
OC_C	1.195	1.200	1.176	1.218
$H_{A C_A}$	1.110	1.074	1.077	1.089
H_{EN}	0.989	1.011	1.006	1.025
H_{FN}	0.990	1.012	1.007	1.025
H_{GC_C}	1.103	1.077	1.087	1.103
$C_{CC_{AN}}$	122.5	122.7	122.6	122.0
OC_{CC_A}	118.6	117.6	117.1	117.7
$H_{A C_A C_C}$	117.0	117.0	117.8	118.6
H_{ENC_A}	121.9	122.2	121.9	121.9
H_{FNC_A}	121.3	122.6	122.3	121.9
H_{GCC_A}	117.5	117.2	117.9	117.9
E/a.u.	-746.23524 ^a	-205.929169	-207.091473	-207.665844

^a Energy in eV

Table 5.6. Structural parameters and energies for $C_2H_4NO^-$

	PM3	RHF/3-21G	RHF/6-31G(d)	MP2/6-31G(d)
C_{AN}	1.437	1.463	1.454	1.461
C_{CC_A}	1.384	1.362	1.365	1.382
OC_C	1.256	1.269	1.250	1.276
H_{AC_A}	1.089	1.075	1.079	1.089
H_{EN}	1.004	1.009	1.041	1.022
H_{FN}	1.004	1.009	1.041	1.022
H_{GC_C}	1.112	1.117	1.119	1.137
$C_{CC_{AN}}$	123.3	123.0	123.7	123.4
OC_{CC_A}	126.9	131.7	131.1	131.1
$H_{AC_{AC_C}}$	122.7	120.9	120.9	121.1
$H_{EN_{CA}}$	109.0	114.2	111.7	110.1
$H_{FN_{CA}}$	109.0	114.2	111.7	110.1
$H_{GC_{CC_A}}$	117.1	110.2	111.8	111.0
$OC_{CC_{AN}}$	180.0	180.0	180.0	180.0
$H_{AC_{AC_{CO}}}$	0.000	0.024	0.002	0.001
$H_{EN_{CA_{CC}}}$	302.1	296.6	300.8	302.7
$H_{FN_{CA_{CC}}}$	57.71	63.36	59.25	57.26
$H_{GC_{CC_{AN}}}$	0.004	359.9	0.000	0.000
E/a.u.	-755.00229 ^a	-206.135276	-207.302743	-207.905493

^a Energy in eV

5.3. Interaction of lithium ions

5.3.1. Lithium ion interaction with methylammonium methyllide

The co-ordination of a lithium cation to methylammonium methyllide is energetically favourable: the ion formed with a lithium attached to the anionic carbon of the ylide is 208 kJ mol^{-1} lower in energy than the ylide and a lithium cation at MP2/6-31G(d). The rearrangement of this species to the lithiated amine (in which the lithium resides on the nitrogen lone pair) can take place by any of five possible mechanisms (Table 5.7). The fully concerted transition involving both the methyl group and the lithium cation migrating at the same time is predicted to be very high in energy. Analogues of the ion-pair mechanism are also high in energy (the lithium cation resides on the former negative ion in each case). Two analogues of the radical mechanism are also possible: the lithium may be removed in a concerted fashion with the methyl group, or the methyl radical may be formed along with a lithiated amine radical. It is this pathway which is the lowest in energy. A comparison of the lithiated relative energies with the original pathways reported in Chapter 3 shows that the barrier to the formation of the intermediates is raised by the incorporation of the lithium cation, and that the magnitude of the enthalpy of the rearrangement is lowered. The prediction is that lithium cations present in the system do not catalyse the Stevens rearrangement of methylammonium methyllide.

Table 5.7. Relative energies (in kJ mol⁻¹ relative to amine-Li⁺) of pathways for the methylammonium methylide-Li⁺ system (optimised UHF relative energies in parentheses)

	RHF/ 3-21G	RHF/ 6-31G(d)	MP2/ 6-31G(d)	MP2/6-31G(d) unlithiated
amine-Li ⁺	0	0	0	0
ylide-Li ⁺	189	188	189	323
concerted TS-Li ⁺	620	643	616	549
CH ₃ [•] + CH ₂ NH ₂ Li ^{•+}	306 (289)	313 (292)	409 ^a	383
CH ₃ Li ^{•+} + CH ₂ NH ₂ [•]	446 (432)	451 (435)	624 ^a	
CH ₃ Li + CH ₂ NH ₂ ⁺	438	414	438	1084
CH ₃ ⁺ + CH ₂ NH ₂ Li	762	752	836	1497

5.3.2. Interaction of a lithium ion with methylammonium formylmethylide

The presence of the carbonyl group on methylammonium formylmethylide makes it an interesting study of the effect of lithium interaction. The lithium ion has a possibility of co-ordinating to the oxygen lone pair, the nitrogen lone pair, or the formally anionic carbon, depending on the species. Structures which are energy minima for this rearrangement are shown in Figure 5.2, and their relative energies are given in Table 5.8. Optimised geometries for these structures are given in Tables 5.9-5.23.

The lowest energy structure for the lithiated amine involves a bridging Li co-ordinated to both the oxygen and nitrogen **1c**. The lowest energy structure for the ylide involves a lithium cation co-ordinated solely to the oxygen **1b**, and a very short carbon-carbon bond length indicative of a double bond. This ylide would be expected to rearrange to an amine with the lithium co-ordinated to the oxygen **1d**. The transition structure between **1d** and **1c** is only 10 kJ mol⁻¹ higher in energy than **1d**, and hence this would not impose any further significant barrier to the rearrangement.

The energies of the concerted transition geometry **1g** and the lithiated radicals **1e** and **1f** (there is no minimum corresponding to **1e** at MP2/6-31G(d)) indicate that the radical pathway is favoured for the rearrangement of **1b**. However, as with the smaller system, the activation energy is higher than for the unlithiated pathway (which was studied in Chapter 3) and the magnitude of the enthalpy of the rearrangement is lower. Hence it is predicted that the lithium cations which are present from the formation of the ylide in solution do not play a part in the Stevens rearrangement.

Table 5.8. Optimised relative energies (in kJ mol⁻¹ relative to **1c**) of pathways for the methylammonium formylmethylide-Li⁺ system (see Figure 5.2 for structures, optimised UHF relative energies in parentheses).

	RHF/3-21G	RHF/6-31G(d)	MP2/6-31G(d)	MP2/6-31G(d) unlithiated
1a	265	240	222	
1b	91	119	107	139
1c	0	0	0	0
1d	89	75	92	
TS 1d-1c	99	86	101	
1e + CH ₃ [•]	248 (295)	254 (288)	–	
1f + CH ₃ [•]	241 (263)	244 (270)	350 ^a	354
1g	416	446	410	419

^a UMP2 optimised energy

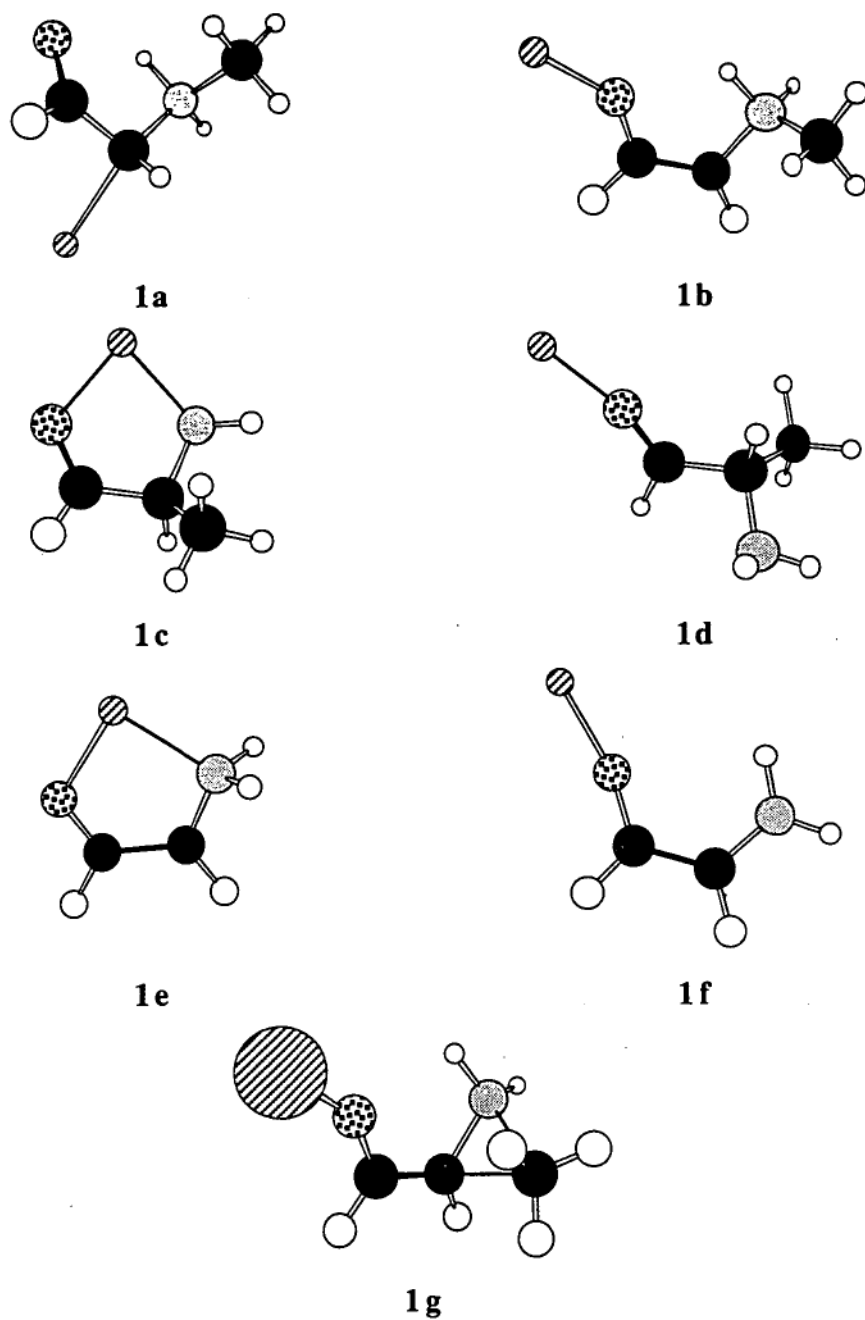


Figure 5.2. Species considered in the rearrangement of lithiated methylammonium formylmethylyde

5.4. Conclusions

Using all the theoretical methods available to us, we conclude that the Stevens rearrangement in the gas phase proceeds via dissociation to radical pairs and recombination to the corresponding amine. This mechanism holds for all of the methods we have used and, from our earlier studies at the CCSD and MP4 levels, higher levels of theory are not expected to alter our findings. The concerted and ion-pair pathways are considerably higher in energy in each case.

Lithium cations from the base used to generate the ylide do not lower the activation energy of the rearrangement when they are complexed to the intermediates, and hence would not act as a catalyst. It is possible that a lithium ion could co-ordinate to the ylide through the oxygen atom in a carbonyl substituent.

Table 5.9. Structural parameters and energies for $C_2H_7NLi^+$ amine (C_s)

	RHF/3-21G	RHF/6-31G(d)	MP2/6-31G(d)
CN	1.525	1.491	1.501
CC	1.533	1.522	1.519
LiN	1.932	1.990	2.006
H _C C _B	1.083	1.084	1.093
HN	1.015	1.008	1.025
H _A C _A	1.081	1.084	1.094
H _D C _B	1.084	1.085	1.094
CCN	112.3	113.4	113.1
LiNC	112.5	114.9	114.8
H _C C _B C _A	109.8	110.0	110.2
HNC _A	108.7	108.3	107.6
H _A C _A C _B	110.6	110.4	110.7
H _D C _B C _A	110.9	111.2	111.1
HNC _A C _B	57.61	56.18	55.61
H _A C _A C _B H _C	60.20	59.37	59.61
H _D C _B C _A N	60.55	60.50	60.52
E/a.u.	-140.782331	-141.556326	-141.988521

Table 5.10. Structural parameters and energies for $C_2H_7NLi^+$ ylide (C_s)

	RHF/3-21G	RHF/6-31G(d)	MP2/6-31G(d)
NC_B	1.518	1.488	1.498
NC_A	1.574	1.525	1.520
C_BH_C	1.080	1.081	1.091
C_BH_D	1.078	1.079	1.089
C_AH	1.088	1.087	1.097
NH	1.012	1.006	1.025
C_ALi	2.073	2.077	2.086
C_BNC_A	114.4	116.5	116.3
NC_BH_C	109.8	109.8	109.9
NC_BH_D	107.8	108.4	107.9
NC_AH	103.4	104.1	104.1
C_ANH	109.5	108.8	108.8
NC_ALi	123.0	125.1	125.2
$C_ANC_BH_C$	59.36	59.50	59.32
$C_ANC_BH_D$	55.46	55.17	55.29
$H_A C_A NH$	58.55	57.04	57.05
E/a.u.	-140.710300	-141.484730	-141.916699

Table 5.11. Structural parameters and energies for CH_4NLi^+ radical (C_s)

	ROHF/ 3-21G	UHF/ 3-21G	ROHF/ 6-31G(d)	UHF/ 6-31G(d)	UMP2/ 6-31G(d)
CN	1.446	1.455	1.430	1.430	1.420
LiN	1.945	1.944	2.004	2.004	2.041
HN	1.011	1.011	1.006	1.006	1.021
HC	1.070	1.071	1.072	1.072	1.082
LiNC	94.69	95.56	93.13	94.47	84.42
HNC	113.2	113.0	112.5	112.3	114.0
HCN	117.3	117.7	117.4	117.8	118.0
HNCLi	118.0	118.1	119.4	119.7	117.1
HCNLi	102.2	99.80	103.5	101.2	100.9
E/a.u.	-101.326394	-101.329514	-101.882311	-101.886252	-102.163920
$\langle s^2 \rangle$		0.7611		0.7609	0.7609

Table 5.12. Structural parameters and energies for fully concerted $C_2H_7NLi^+$ transition geometry (C_s)

	RHF/3-21G	RHF/6-31G(d)	MP2/6-31G(d)
NC_B	1.971	1.998	1.850
NC_A	1.665	1.595	1.577
$C_A C_B$	2.172	2.178	2.048
$C_B H_C$	1.076	1.074	1.097
$C_B H_D$	1.068	1.068	1.083
$C_A H$	1.084	1.088	1.092
NH	1.007	1.001	1.019
$C_A Li$	1.986	2.055	2.127
$C_B N C_A$	72.81	73.67	72.89
$NC_B H_C$	88.64	87.80	90.98
$NC_B H_D$	109.8	108.8	114.0
$NC_A H$	106.6	107.3	110.7
$C_A N H$	97.53	101.4	104.5
$NC_A Li$	71.21	69.12	67.22
$C_A N C_B H_C$	63.50	63.35	65.62
$C_A N C_B H_D$	115.7	118.3	113.4
$H_A C_A N H$	58.20	58.86	60.32
E/a.u.	-140.546242	-114.311315	-141.753835

Table 5.13. Structural parameters and energies for CH₂NH₂Li

	RHF/3-21G	RHF/6-31G(d)	MP2/6-31G(d)
CN	1.586	1.535	1.533
LiN	1.870	1.919	1.934
NH _A	1.009	1.004	1.021
NH _B	1.009	1.004	1.020
CH _A	1.087	1.087	1.094
CH _B	1.087	1.089	1.097
LiNC	67.79	66.79	67.11
CNH _A	112.5	113.9	114.1
CNH _B	112.5	110.1	109.1
NCH _A	107.0	109.6	110.5
NCH _B	107.0	106.2	106.0
LiCNH _A	118.7	132.4	135.2
LiCNH _B	241.3	251.3	253.3
LiNCH _A	122.2	135.3	137.8
LiNCH _B	237.8	250.3	253.8
E	-101.482807	-102.093275	-102.349344

Table 5.14. Structural parameters and energies for CH₃Li⁺ radical (C_{3v})

	ROHF/ 3-21G	UHF/ 3-21G	ROHF/ 6-31G(d)	UHF/ 6-31G(d)	UMP2/ 6-31G(d)
LiC	2.359	2.359	2.386	2.384	2.399
CH	1.077	1.077	1.076	1.076	1.089
LiCH	98.75	97.99	98.39	97.64	97.36
E	-46.552583	-46.554642	-46.801700	-46.803773	-46.881229
<s ² >		0.7574		0.7573	0.7578

Table 5.15. Structural parameters and energies for CH₃Li (C_{3v})

	RHF/3-21G	RHF/6-31G(d)	MP2/6-31G(d)
LiC	2.001	2.001	2.011
CH	1.094	1.093	1.097
LiCH	111.9	112.6	111.8
E	-46.752481	-47.015544	-47.162106

Table 5.16. Structural parameters and energies for C₃H₇NOLi⁺ ylide **1a**

	RHF/3-21G	RHF/6-31G(d)	MP2/6-31G(d)
C _B N	1.519	1.492	1.499
C _A N	1.543	1.507	1.500
C _C C _A	1.464	1.565	1.459
O _C C	1.225	1.200	1.242
H _B C _B	1.080	1.081	1.091
H _C C _B	1.078	1.079	1.089
H _D C _B	1.078	1.078	1.089
H _E N	1.027	1.013	1.043
H _F N	1.008	1.005	1.023
H _A C _A	1.082	1.084	1.094
H _G C _C	1.084	1.093	1.106
LiC _A	2.125	2.144	2.157
C _A NC _B	113.9	115.8	114.8
C _C C _A N	104.6	106.4	105.6
O _C C _C A	122.2	123.1	122.2
H _B C _B N	109.2	109.2	109.7
H _C C _B N	108.5	108.7	108.7
H _D C _B N	107.5	108.1	107.5
H _E NC _A	102.6	104.9	102.4
H _F NC _A	112.5	111.7	113.2
H _A C _A N	108.7	108.5	110.3
H _G C _C C _A	116.2	116.0	117.2
LiC _A N	119.0	121.0	121.8
C _C C _A NC _B	92.80	84.64	89.28
O _C C _C A _N	18.31	19.10	19.25
H _B C _B NC _A	182.1	182.2	183.3
H _C C _B NC _A	61.48	61.94	62.71
H _D C _B NC _A	301.8	302.0	303.0
H _E NC _A CC	336.2	326.0	332.9
H _F NC _A CC	218.7	210.2	216.2
H _A C _A NC _B	331.2	323.7	325.4
H _G C _C C _A N	195.7	196.1	196.0
LiC _A NC _B	209.4	204.5	203.3
E/a.u.	-252.808785	-254.220703	-254.955249

Table 5.17. Structural parameters and energies for $C_3H_7NOLi^+$ ylide **1b**

	RHF/3-21G	RHF/6-31G(d)	MP2/6-31G(d)
C_{BN}	1.521	1.491	1.498
C_{AN}	1.491	1.467	1.465
C_{CC_A}	1.329	1.336	1.353
OC_C	1.318	1.288	1.319
H_{BC_B}	1.079	1.081	1.091
H_{CC_B}	1.078	1.079	1.089
H_{DC_B}	1.077	1.078	1.088
H_{EN}	1.021	1.012	1.040
H_{FN}	1.014	1.009	1.028
H_{AC_A}	1.064	1.068	1.080
H_{GC_C}	1.076	1.082	1.093
LiO	1.647	1.717	1.742
$C_{AN}C_B$	113.7	115.2	114.9
$C_{CC}C_{AN}$	115.0	116.9	114.1
OC_{CC_A}	123.6	124.6	122.4
$H_{BC_B}N$	109.1	109.3	109.3
$H_{CC_B}N$	108.1	108.5	108.4
$H_{DC_B}N$	107.5	108.0	107.5
$H_{EN}C_A$	103.2	104.9	102.4
$H_{FN}C_A$	111.0	110.6	111.6
$H_{AC}C_{AN}$	116.8	116.3	117.9
$H_{GC}C_{CC_A}$	117.5	116.8	118.5
$LiOC_C$	152.6	145.3	141.9
$C_{CC}C_{AN}C_B$	117.9	118.6	115.8
$OC_{CC}C_{AN}$	0.560	0.435	0.847
$H_{BC_B}N C_A$	181.5	180.7	182.0
$H_{CC_B}N C_A$	61.12	60.49	61.59
$H_{DC_B}N C_A$	302.3	301.3	302.6
$H_{EN}C_A C_C$	358.2	177.6	356.1
$H_{FN}C_A C_C$	242.4	243.2	241.5
$H_{AC}C_{AN}C_B$	298.4	298.9	298.5
$H_{GC}C_{CC}C_{AN}$	180.6	180.4	180.7
$LiOC_{CC}C_A$	178.9	178.1	177.9
E/a.u.	-252.875087	-245.266780	-254.998716

Table 5.18. Structural parameters and energies for $C_3H_7NOLi^+$ amine 1c

	RHF/3-21G	RHF/6-31G(d)	MP2/6-31G(d)
C _A N	1.502	1.476	1.485
C _C C _A	1.507	1.512	1.509
O C _C	1.224	1.202	1.236
C _B C _A	1.547	1.535	1.534
H _A C _A	1.084	1.086	1.098
H _B C _B	1.082	1.083	1.093
H _C C _B	1.083	1.085	1.093
H _D C _B	1.084	1.085	1.094
H _E N	1.011	1.005	1.024
H _F N	1.011	1.005	1.022
H _G C _C	1.079	1.086	1.100
LiN	2.014	2.071	2.070
LiO	1.827	1.880	1.933
C _C C _A N	108.8	109.4	109.5
O C _C C _A	122.3	122.9	123.1
C _B C _A C _C	108.7	109.0	108.1
H _A C _A C _C	108.4	107.1	107.9
H _B C _B C _A	109.8	109.9	109.9
H _C C _B C _A	110.7	111.0	111.0
H _D C _B C _A	110.6	111.1	110.6
H _E N C _A	111.3	110.2	109.4
H _F N C _A	110.9	110.2	109.3
H _G C _C C _A	117.0	107.8	117.5
LiN C _A	105.7	105.8	106.1
O C _C C _A N	354.5	351.3	346.7
C _B C _A C _C O	116.0	114.2	108.0
H _A C _A C _C O	234.5	231.4	225.3
H _B C _B C _A C _C	176.5	174.9	175.0
H _C C _B C _A C _C	57.38	55.81	55.86
H _D C _B C _A C _C	297.0	295.3	295.5
H _E N C _A C _C	247.8	253.6	260.9
H _F N C _A C _C	127.9	137.7	146.5
H _G C _C C _A N	175.7	172.6	169.3
LiN C _A C _C	6.087	10.97	17.12
E/a.u.	-252.909657	-254.311981	-255.039634

Table 5.19. Structural parameters and energies for C₃H₇NOLi⁺ amine 1d

	RHF/3-21G	RHF/6-31G(d)	MP2/6-31G(d)
C _A N	1.454	1.446	1.455
C _C C _A	1.500	1.504	1.496
OC _C	1.234	1.212	1.241
C _B C _A	1.551	1.536	1.537
H _A C _A	1.084	1.087	1.100
H _B C _B	1.082	1.084	1.093
H _C C _B	1.082	1.084	1.093
H _D C _B	1.083	1.085	1.093
H _E N	1.001	1.002	1.017
H _F N	1.001	1.000	1.018
H _G C _C	1.081	1.086	1.101
OLi	1.702	1.778	1.811
C _C C _A N	106.2	106.6	106.2
OC _C C _A	125.2	124.3	124.2
C _B C _A C _C	107.0	107.4	106.4
H _A C _A C _C	109.5	108.1	108.7
H _B C _B C _A	108.6	109.1	108.7
H _C C _B C _A	111.4	111.5	111.5
H _D C _B C _A	110.2	110.9	110.4
H _E NC _A	116.6	112.9	111.8
H _F NC _A	116.0	112.6	111.2
H _G C _C C _A	113.9	115.9	115.7
C _C OLi	174.9	168.5	163.6
OC _C C _A N	147.9	139.3	141.9
C _B C _A C _C O	265.2	258.2	259.3
H _A C _A C _C O	23.66	16.02	16.96
H _B C _B C _A C _C	180.3	178.6	179.7
H _C C _B C _A C _C	60.86	59.52	60.60
H _D C _B C _A C _C	299.2	297.8	298.6
H _E NC _A C _C	268.5	269.1	270.4
H _F NC _A C _C	131.6	146.1	150.3
H _G C _C C _A N	326.7	318.6	320.9
C _A C _C OLi	192.3	184.3	181.8
E/a.u.	-252.875915	-254.283580	-255.004568

Table 5.20. Structural parameters and energies for transition geometry between the two structures of C₃H₇NOLi⁺ amine (**1d–1e**)

	RHF/3-21G	RHF/6-31G(d)	MP2/6-31G(d)
C _A N	1.475	1.461	1.477
LiO	1.702	1.778	1.808
LiOC _C	166.9	159.9	154.8
OC _C C _A N	290.9	278.2	271.9
C _B C _A CCO	49.98	38.43	30.36
H _A C _A CCO	171.6	158.9	152.5
H _G CC _C A _N	107.9	94.91	87.21
LiOC _C C _A	70.86	62.63	55.44
C _C C _A	1.514	1.517	1.509
OC _C	1.230	1.208	1.236
C _B C _A	1.535	1.525	1.519
H _A C _A	1.081	1.086	1.098
H _B C _B	1.082	1.083	1.093
H _C C _B	1.083	1.084	1.093
H _D C _B	1.083	1.084	1.093
H _E N	1.003	1.001	1.019
H _F N	1.003	1.001	1.019
H _G CC	1.082	1.087	1.101
C _C C _A N	103.5	103.2	100.6
OC _C C _A	122.8	123.5	123.4
C _B C _A CC	110.9	112.1	112.9
H _A C _A CC	109.0	107.9	108.7
H _B C _B C _A	109.3	109.4	109.5
H _C C _B C _A	111.5	111.4	111.4
H _D C _B C _A	110.0	111.1	110.7
H _E NC _A	115.2	112.4	111.3
H _F NC _A	114.2	111.2	109.7
H _G CC _C A	118.3	118.2	118.4
H _B C _B C _A CC	181.0	177.2	178.1
H _C C _B C _A CC	61.28	58.00	58.70
H _D C _B C _A CC	300.4	296.6	297.2
H _E NC _A CC	260.2	268.9	269.9
H _F NC _A CC	128.1	148.4	152.0
E/a.u.	-252.872047	-254.279249	-255.001131

Table 5.21. Structural parameters for C₂H₄NOLi⁺ radical **1e** (C_s)

	ROHF/ 3-21G	UHF/ 3-21G	ROHF/ 6-31G(d)	UHF/ 6-31G(d)
C _A N	1.451	1.458	1.428	1.432
C _C C _A	1.446	1.398	1.452	1.432
OC _C	1.234	1.287	1.211	1.227
LiN	2.056	2.024	2.119	2.101
LiO	1.831	1.880	1.878	1.898
HN	1.014	1.014	1.009	1.008
H _A C _A	1.070	1.071	1.073	1.075
H _G C _C	1.075	1.071	1.083	1.081
C _C C _A N	115.7	117.6	116.6	117.4
OC _C C _A	119.9	119.5	120.7	120.4
LiNC _A	101.9	102.5	101.9	102.2
HNC _A	111.7	111.2	110.1	110.0
H _A C _A C _C	122.5	121.9	121.9	121.7
H _G C _C C _A	118.6	120.9	118.5	119.4
HNC _A C _C	119.6	120.0	122.2	122.4
E/a.u.	-213.457978	-213.472649	-214.647619	-214.656070
<s ² >		0.9536		0.8439

Table 5.22. Structural parameters for $C_2H_4NOLi^+$ radical **1f** (C_s)

	ROHF/ 3-21G	UHF/ 3-21G	ROHF/ 6-31G(d)	UHF/ 6-31G(d)	UMP2/ 6-31G(d)
C_{AN}	1.326	1.328	1.326	1.327	1.336
C_{CC_A}	1.394	1.388	1.402	1.396	1.406
OC_C	1.270	1.273	1.246	1.248	1.277
$H_{A_C A}$	1.070	1.071	1.073	1.073	1.085
H_{EN}	1.000	1.001	0.996	0.996	1.013
H_{FN}	1.002	1.002	0.997	0.998	1.015
H_{GC_C}	1.079	1.078	1.085	1.084	1.098
LiO	1.666	1.674	1.733	1.738	1.748
$C_{CC_{AN}}$	123.6	123.7	123.4	123.4	122.7
OC_{CC_A}	122.5	122.4	122.6	122.5	122.1
$H_{A_C A C_C}$	118.7	118.8	119.1	119.3	119.8
$H_{EN C_A}$	121.1	121.1	121.1	121.1	121.3
$H_{FN C_A}$	122.4	122.3	122.3	122.3	121.9
$LiOC_C$	172.5	172.5	167.9	167.5	166.8
$H_{GC_C C_A}$	117.9	118.3	118.1	118.4	118.7
E/a.u.	-213.470095	-213.475261	-214.654387	-214.659671	-215.237415
$\langle s^2 \rangle$		0.7792		0.7728	0.7741

Table 5.23. Structural parameters and energies for $C_3H_7NOLi^+$ transition geometry

1g between ylide and amine.

	RHF/3-21G	RHF/6-31G(d)	MP2/6-31G(d)
LiO	1.643	1.708	1.745
LiOC _C	159.6	150.6	147.9
LiOC _C CA	157.0	153.5	171.0
C _A N	1.482	1.457	1.463
C _B N	2.096	2.149	1.938
C _C CA	1.349	1.351	1.378
OC _C	1.303	1.283	1.303
H _B C _B	1.067	1.067	1.086
H _C C _B	1.072	1.070	1.090
H _D C _B	1.069	1.070	1.085
H _E N	1.006	1.003	1.023
H _F N	1.005	1.002	1.019
H _A CA	1.068	1.072	1.083
H _G CC	1.078	1.083	1.094
C _B NC _A	70.64	73.33	69.51
C _C CA _N	118.4	120.7	117.2
OC _C CA	124.0	124.5	121.3
H _B C _B N	84.24	83.62	89.48
H _C C _B N	125.9	120.8	129.6
H _D C _B N	91.65	91.88	96.79
H _E NC _A	111.8	111.0	110.8
H _F NC _A	114.3	112.4	115.3
H _A CA _N	117.2	116.8	117.3
H _G CCCA	117.2	117.1	118.8
C _C CA _N C _B	93.27	90.95	99.61
OC _C CA _N	354.9	357.1	355.2
H _B C _B NC _A	146.1	148.8	147.6
H _C C _B NC _A	28.49	31.13	30.04
H _D C _B NC _A	263.1	266.5	261.5
H _E NC _A CC	339.6	335.3	345.8
H _F NC _A CC	209.9	212.4	214.6
H _A CA _N C _B	260.5	261.7	261.6
H _G CCCA _N	178.4	180.1	179.8
C _B CA	2.128	2.224	1.978
E/a.u.	-252.751215	-254.141986	-254.883334

Chapter 6. The effects of solvation on the Stevens rearrangement

6.1. Introduction

In the previous chapters we have shown that the preferred mechanism for the Stevens rearrangement in the gas phase involves a dissociative radical pathway. In Chapter 2, some of the approaches available for incorporating solvation were detailed. These will now be applied in order to determine if this prediction is changed in the presence of solvent.

In this study, the specific solvent-solute effects of acetonitrile (a commonly used solvent) on the Stevens rearrangement of methylammonium formylmethylide will be investigated by optimising the positions of up to six solvent molecules around the solute. From Chapters 3 and 4, it was seen that methylammonium formylmethylide is the smallest ylide which displays the important electronic effects necessary in order to compare rearrangement pathways. The geometry optimisations of the resulting supermolecules are done using the semi-empirical PM3 Hamiltonian, which was seen in Chapter 4 to give results comparable to high level ab initio calculations on these systems. COSMO is an attractive method for incorporating solvation in the calculation as energy derivatives are easily obtained and hence geometry optimisation within the continuum is possible. COSMO is used to incorporate solvent effects upon both the individual solute molecules and the solvated clusters.

The SCRF formalism is a useful method for determining the electrostatic effects of solvation at an ab initio level. In this study, the energies of the transition structures and radical intermediates relative to the amines for the rearrangements already studied in the gas phase in Chapters 3 and 4 have been calculated using a dielectric constant $\epsilon = 35.9$, corresponding to acetonitrile. The solvated relative energies are to be compared with those gas-phase energies, and with each other, in

order to determine if the solvent effects are significant in assigning a mechanism to the Stevens rearrangement.

The optimised supermolecule geometries are displayed in Tables 6.1-6.9 and Figure 6.1. The complexation energies of these molecules are given as a graph in Figure 6.3. Relative SCRF energies of the Stevens rearrangement are shown in Table 6.10 and Figure 6.4. Geometries optimised using COSMO are presented in Tables 6.11-6.20 and Figure 6.8, and the complexation energies calculated using COSMO in Figure 6.6. A comparison of methods of solvation on the relative energies of the Stevens rearrangement of methylammonium methylene are presented in Figure 6.7.

6.2. Supermolecule studies of the Stevens rearrangement of methylammonium formylmethylenide

6.2.1. Geometries of complexed species

Supermolecule optimisations were done in two stages. First the positions of the acetonitrile molecules were optimised with the parameters describing the solute molecule held constant. All molecular parameters were then freed for a complete geometry optimisation. The concerted transition structure was characterised by geometry optimisation towards the starting ylide and product amine along the reaction co-ordinate. The acetonitrile molecules in this case were described by five parameters, shown in Figure 6.1: the distance R from the solute nitrogen to the central carbon of the acetonitrile (C_{AC}); the angle θ_1 between $N-C_{AC}$ and $N-C_A$; the torsional angle ϕ_1 between $N-C_{AC}$ and C_A-H_N where H_N is one of the hydrogen atoms on the amine group (R , θ_1 and ϕ_1 are, in effect, polar coordinates of C_{AC} relative to N); the angle θ_2 between the solute nitrogen, the C_{AC} and the acetonitrile nitrogen (hence $0 < \theta_2 < 90$ indicates the nitrogen end of the acetonitrile is oriented towards the solute, $90 < \theta_2 < 180$ indicates it is oriented away from the solute); and the torsional angle ϕ_2 between the

N–C of the acetonitrile and N–C_A, which gives an indication of the conical movement of the solvent molecule.

The geometries reported in this study are for the lowest-energy conformation of the cluster, generated by a systematic search for local minima using several positions of solvent molecules as starting points. Typically twenty starting geometries were used with acetonitrile molecules occupying different positions about the solute. When optimisations involve several polar solvent molecules, there are two interactions which affect the energy of the system, and hence the optimised geometry: the interaction of the solvent molecule with the solute molecule, and the interaction of the solvent molecule with other solvent molecules. Tables 6.1-6.5 list the positions of the acetonitrile molecules (by their five parameters defined previously) and a pictorial representation of each of the largest complexes is given as Figure 6.2. It can be seen that when there are a large number of acetonitrile molecules in the calculation, most of the solvent molecules gather on one "side" of the solvent molecule. The lowest-energy conformation thus resembles an appropriate *n*-mer co-ordinated to the solute molecule.

By and large, the geometries of the reacting species (the solutes) have changed very little from our previous study, as seen in Tables 6.6-6.9. The bond distances and angles of all species in general show little variation with the number of complexing acetonitrile molecules, apart from the two dihedral angles OC_CC_AN and OC_CC_AC_B describing the orientation of the carbonyl group on the amine (rotation about the C_CC_A bond). It is worth noting that a parameter one might expect to change noticeably, the C_AN C_B angle (in effect, the reaction co-ordinate) of the concerted transition structure, remains unaltered with the addition of several co-ordinating acetonitrile molecules.

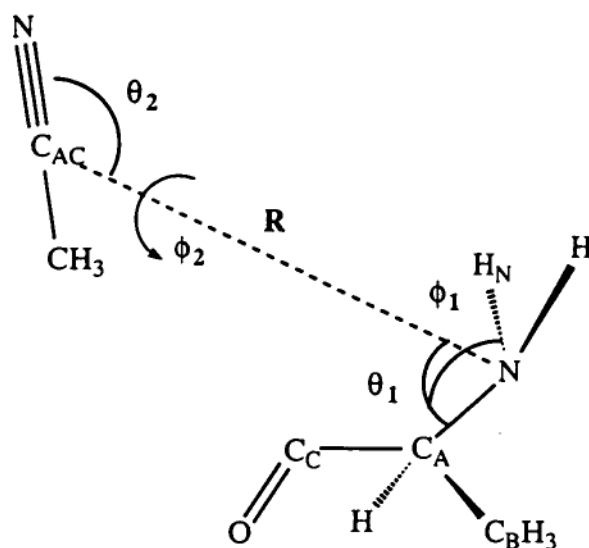


Figure 6.1. The five parameters used to describe solvent position

Table 6.1. PM3 optimised parameters of 1-6 acetonitrile molecules around amine

	R	θ_1	ϕ_1	θ_2	ϕ_2
1	6.05	69.9	43.6	137.4	136.1
2	5.30	81.1	29.1	116.0	186.2
	4.69	129.5	38.5	17.7	120.4
3	5.58	52.0	180.8	152.0	271.0
	5.34	84.1	33.9	126.1	168.3
	4.75	128.6	51.9	11.8	112.0
4	5.55	54.1	164.5	129.5	332.6
	5.12	81.6	29.0	110.6	184.6
	4.05	125.0	159.1	111.9	12.7
	4.78	133.1	38.4	28.4	132.4
5	5.81	52.1	128.0	94.2	132.3
	4.88	83.2	185.7	122.7	87.1
	5.57	88.4	37.4	116.1	169.6
	4.67	133.7	52.4	1.6	122.7
	4.71	140.8	135.2	137.9	269.7
6	6.34	29.1	160.5	106.5	227.8
	4.76	66.3	213.5	128.1	17.3
	4.07	90.0	312.3	115.8	374.8
	4.07	123.6	156.5	119.4	75.8
	4.17	129.0	262.5	79.02	143.8
	4.11	142.9	16.85	63.39	97.37

Table 6.2. PM3 optimised position of 1-6 acetonitrile molecules around ylide

	R	θ_1	ϕ_1	θ_2	ϕ_2
1	3.97	111.8	165.4	57.17	188.2
2	5.19	98.6	155.6	87.6	205.5
	4.20	145.3	115.2	19.54	227.4
3	4.53	97.4	117.5	73.5	146.5
	5.20	98.2	159.0	95.8	200.5
	4.21	146.1	124.7	16.6	234.0
4	4.89	54.2	36.0	105.9	178.2
	5.35	99.6	219.4	133.0	182.5
	3.99	109.2	35.9	9.3	209.5
	4.02	110.5	162.0	59.8	199.8
5	5.88	27.2	22.4	137.3	140.1
	4.87	64.6	320.8	48.5	185.5
	5.02	101.9	158.8	93.4	146.5
	5.41	102.2	218.0	136.6	167.3
	4.21	144.1	111.6	16.3	229.5
6	5.82	38.7	239.7	101.0	75.3
	5.15	51.5	352.3	110.3	158.5
	5.29	67.0	293.0	54.5	195.6
	5.72	93.9	220.9	151.2	155.2
	4.51	102.4	6.24	14.0	168.9
	4.02	111.1	163.0	60.3	208.0

Table 6.3. PM3 optimised position of 1-6 acetonitrile molecules around concerted TS

	R	θ_1	ϕ_1	θ_2	ϕ_2
1	5.04	59.3	330.8	118.2	154.2
2	5.42	96.7	192.6	125.7	150.5
	4.02	111.3	129.3	62.6	223.1
3	5.34	53.9	14.1	117.9	172.9
	5.73	55.7	302.4	132.9	172.5
	4.68	102.3	19.9	7.4	179.6
4	6.79	22.4	205.7	132.9	181.0
	5.94	47.4	294.9	146.5	189.7
	5.24	61.9	7.7	120.1	178.3
	4.68	110.1	15.9	0.9	69.5
5	6.65	20.9	215.8	130.5	185.1
	5.86	50.0	301.0	147.9	193.0
	5.04	67.3	12.3	118.8	173.5
	4.47	113.6	45.5	8.83	356.4
	4.40	117.7	109.5	121.4	193.4
6	5.72	31.2	224.8	103.7	188.1
	5.56	34.6	22.8	134.0	38.4
	5.86	53.9	306.1	145.7	190.6
	4.77	97.6	209.6	102.6	156.1
	4.61	103.8	345.7	32.3	18.7
	4.64	134.2	288.3	105.3	94.8

Table 6.4. PM3 optimised positions of 1-5 acetonitrile molecules around amine radical.

	R	θ_1	ϕ_1	θ_2	ϕ_2
1	5.25	76.3	0.7	111.6	167.5
2	5.03	73.8	25.4	106.1	141.3
	4.43	115.5	62.8	20.5	139.9
3	5.21	64.0	165.0	105.4	200.2
	5.46	73.6	0.2	118.4	172.9
	4.46	111.1	142.2	10.1	231.4
4	6.43	40.9	5.1	81.7	173.1
	4.59	72.7	183.1	92.4	178.3
	4.64	99.4	17.6	103.9	144.5
	4.40	132.3	72.0	16.9	92.6
5	6.62	31.5	94.8	106.9	217.8
	5.09	65.2	152.1	108.3	202.1
	4.56	72.5	18.1	76.7	174.7
	4.35	113.0	126.0	1.0	319.1
	4.51	144.8	60.9	125.7	101.0

Table 6.5. PM3 optimised positions of 1-5 acetonitrile molecules around methyl radical.

	R	θ_1	ϕ_1	θ_2	ϕ_2
1	4.68	12.6	83.5	131.5	166.9
2	4.64	109.7	179.7	129.8	357.1
	4.06	161.9	345.1	111.9	197.5
3	3.96	41.8	161.6	108.5	172.4
	4.45	97.1	5.0	122.3	6.4
	4.49	133.3	166.7	124.4	188.8
4	3.92	47.1	146.2	109.0	162.7
	4.52	78.8	67.2	68.1	12.8
	4.49	133.3	166.7	124.4	188.8
	3.84	122.5	119.9	106.6	262.7
5	6.62	31.5	94.8	106.9	217.8
	5.09	65.2	152.1	108.3	202.1
	4.56	72.5	18.1	76.7	174.7
	4.35	113.0	126.0	1.0	319.1
	4.51	144.8	60.9	125.7	101.0

Table 6.6. Geometries of amine with varying number of acetonitrile molecules

	0	1	2	3	4	5	6
C _A N	1.484	1.484	1.484	1.483	1.484	1.485	1.483
C _C C _A	1.528	1.529	1.528	1.527	1.528	1.526	1.524
OC _C	1.207	1.209	1.209	1.208	1.209	1.210	1.208
C _B C _A	1.522	1.522	1.522	1.523	1.523	1.522	1.524
C _C C _A N	107.5	107.5	107.5	109.1	108.4	108.3	112.6
OC _C C _A	123.4	123.2	123.4	123.5	123.1	122.8	124.1
C _C C _A C _B	112.1	111.9	112.0	110.3	110.8	112.6	108.4
OC _C C _A N	274.4	274.5	274.2	294.1	289.3	200.6	330.4
OC _C C _A C _B	40.5	40.5	40.5	60.7	55.4	327.1	97.8

Table 6.7. Geometries of ylide with varying number of acetonitrile molecules

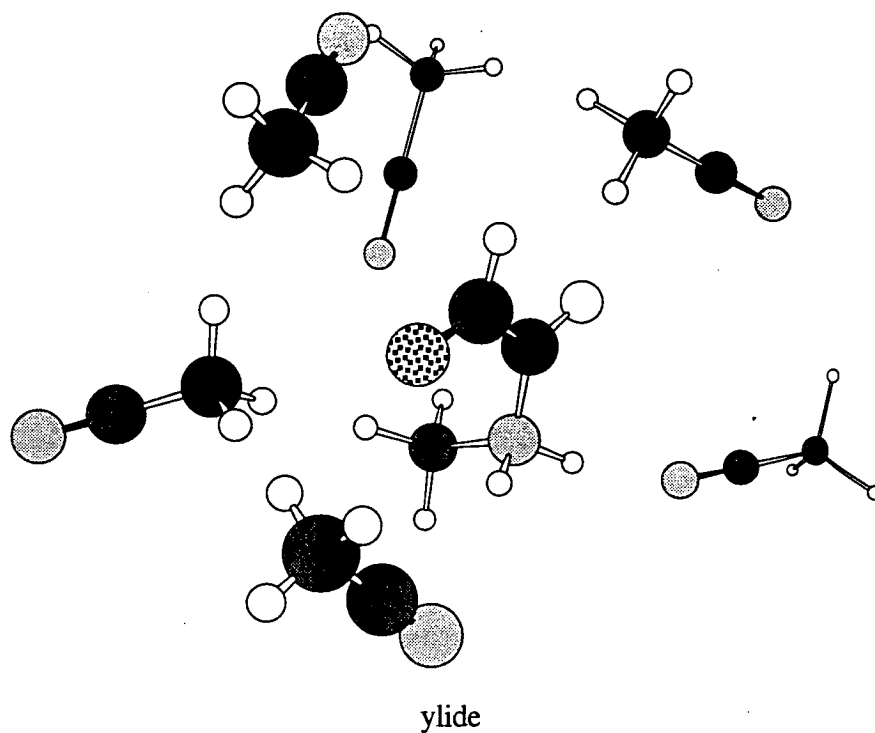
	0	1	2	3	4	5	6
C _B N	1.516	1.513	1.513	1.511	1.512	1.510	1.510
C _A N	1.409	1.415	1.417	1.421	1.426	1.422	1.424
C _C C _A	1.420	1.415	1.413	1.409	1.409	1.410	1.406
OC _C	1.233	1.236	1.237	1.240	1.239	1.238	1.241
C _A NC _B	114.3	113.9	113.6	113.2	113.2	113.8	113.9
C _C C _A N	120.8	121.2	121.2	121.8	121.5	121.4	121.7
OC _C C _A	123.4	123.8	124.0	124.4	124.4	124.3	124.7
C _C C _A NC _B	96.3	97.8	98.7	110.8	90.1	88.6	86.1
OC _C C _A N	359.5	0.2	359.8	359.7	358.3	358.0	356.9

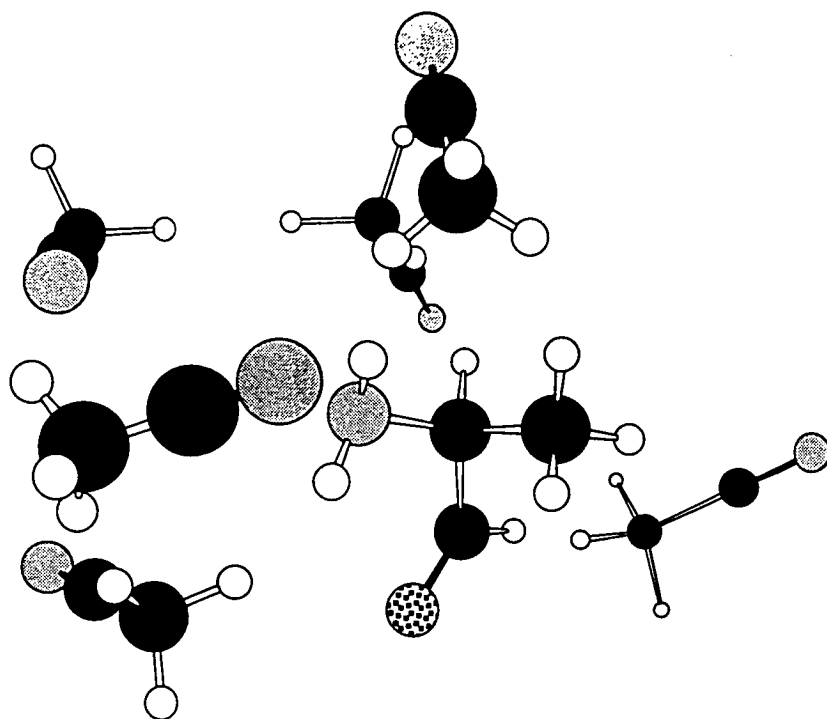
Table 6.8. Concerted TS geometries with varying number of acetonitrile molecules

	0	1	2	3	4	5	6
C _B N	1.792	1.794	1.801	1.795	1.797	1.800	1.794
C _A N	1.474	1.474	1.475	1.476	1.476	1.476	1.475
C _C C _A	1.449	1.451	1.445	1.450	1.450	1.449	1.450
OC _C	1.222	1.221	1.226	1.221	1.220	1.222	1.221
C _A NC _B	72.1	71.9	71.5	71.2	71.2	71.2	71.2
C _C C _A N	119.9	119.9	120.4	119.9	119.9	119.9	120.0
OC _C C _A	124.0	124.0	124.2	124.4	124.7	124.6	124.3
C _C C _A NC _B	108.8	109.0	107.7	107.7	107.8	107.4	107.2
OC _C C _A N	355.7	355.2	352.4	353.8	357.1	357.0	354.0

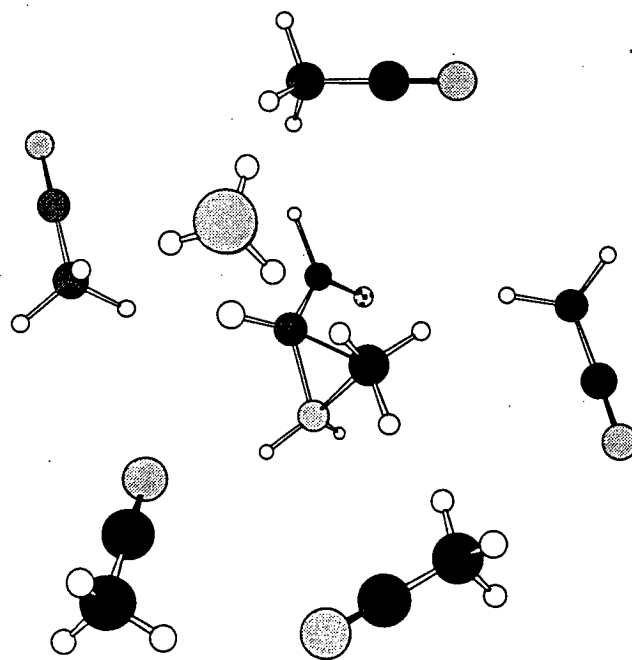
Table 6.9. Amine radical geometries with varying number of acetonitrile molecules

	0	1	2	3	4	5
C _A N	1.373	1.372	1.370	1.369	1.369	1.370
C _C C _A	1.456	1.456	1.453	1.450	1.448	1.447
O _C C	1.205	1.216	1.218	1.218	1.219	1.220
C _A C _C N	121.1	121.4	121.6	121.4	121.3	121.3
O _C C _C A	122.2	121.8	121.9	122.4	122.8	122.8
O _C C _C A _N	184.1	184.7	183.6	184.8	184.4	182.4

**Figure 6.2.** PM3 optimised geometries of largest clusters (six solvating acetonitrile molecules for closed-shell species, five for open-shell)



amine



concerted TS

Figure 6.2. (cont.)

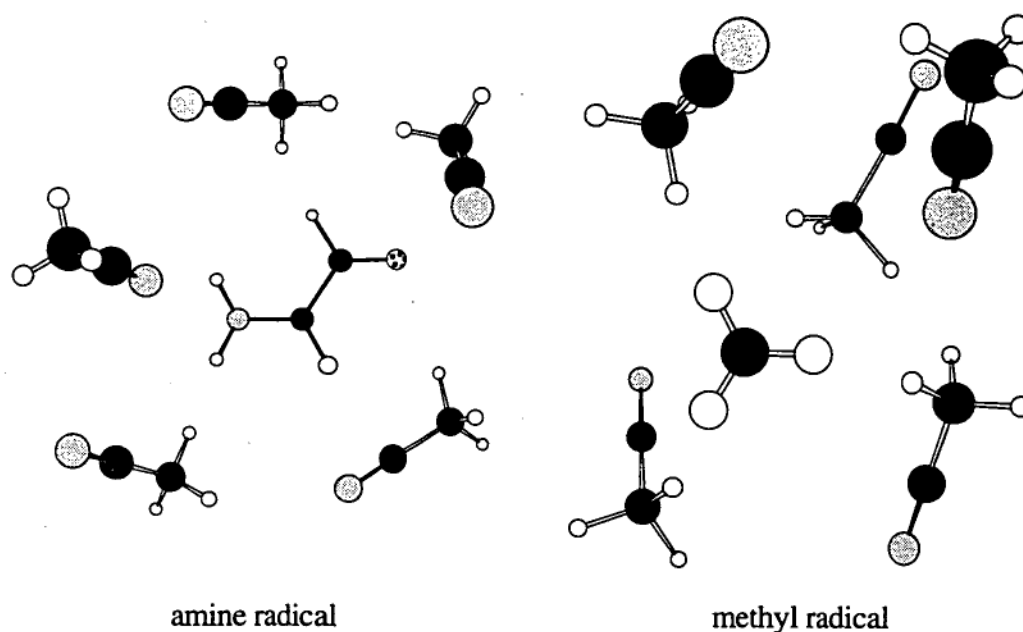


Figure 6.2. (cont.) PM3 optimised geometries of largest clusters (six solvating acetonitrile molecules for closed-shell species, five for open-shell)

6.2.2. Complexation energies of supermolecules

The complexation energy of the five species as a function of number of coordinating acetonitrile molecules is given in Figure 6.3. The energies are all relative to the energies of the solute molecule and the appropriate n -mer of acetonitrile calculated at PM3. The lines indicating the complexation energy start to flatten out at three or four solvent molecules for the radicals and at five or six solvent molecules for the singlet species and hence it is anticipated that the major specific interactions between solvent and solute are adequately covered at these numbers of solvent molecules. The coordination to the ylide is the strongest, this could be expected from the charge separation seen in this molecule. By extrapolating these lines one would expect a specific solvent-solute energy of between 10 and 20 kJ mol⁻¹ for the amine and the radical species, between 20 and 30 kJ mol⁻¹ for the concerted transition geometry, and 40-60 kJ mol⁻¹ for the ylide.

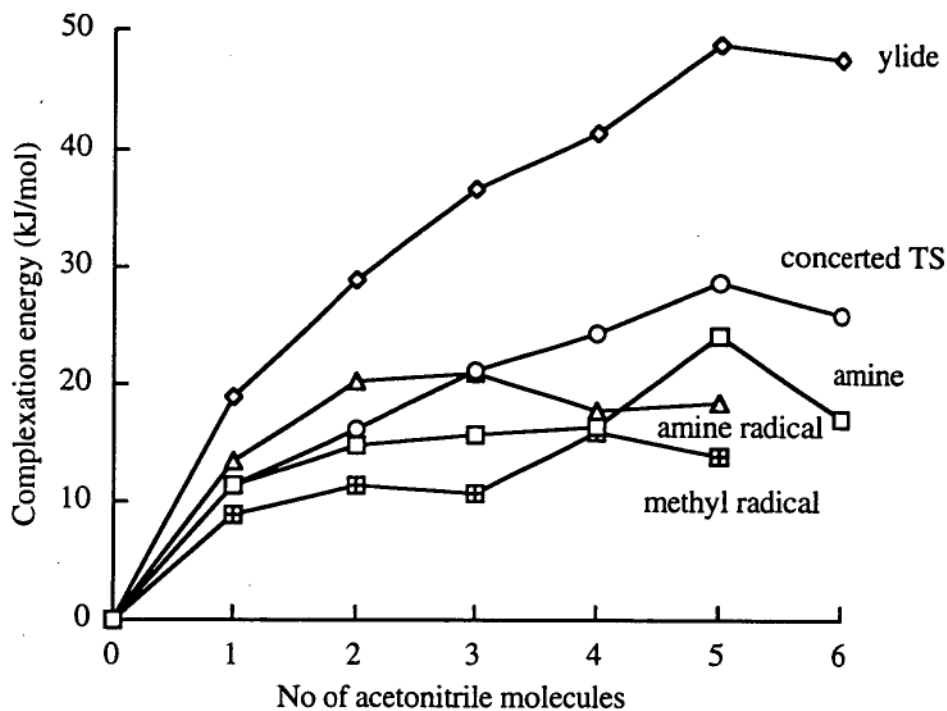


Figure 6.3. Complexation energy of supermolecules calculated at PM3

6.3. SCRF studies of ylide rearrangements

Studies of molecules using the SCRF formalism have generally involved large basis sets incorporating several polarisation and diffuse functions⁸⁷. Since we are interested in relative energies more than individual enthalpies of solvation, we have calculated the relative energies of the species involved in the rearrangement of methylammonium methyllide at several basis sets of increasing complexity (Table 6.10). The difference between the gas-phase and SCRF relative energies is similar across all of the basis sets, and hence the MP2/6-31G(d) level of theory, which is small enough to be applied to all of our rearrangement systems has been used to study the solvation effects on the four ylide rearrangements.

The effects of solvation as calculated at the SCRF MP2/6-31G(d) level for these four Stevens rearrangement systems are shown in Figure 6.4. The effect of

SCRF on most of the species is to lower their energies slightly with respect to the solvated amine. This is most evident for the charge-separated species (i.e. the ylides), however in no case is there any indication that the concerted pathway is to be favoured over the radical mechanism. There is an large SCRF effect seen in the aminoformylmethyl radical obtained by dissociation of methylammonium formylmethylide. This is due to an abnormally large dipole moment caused by an uneven charge distribution which would not be present in the larger experimental systems. For the rearrangement of methylammonium formylmethylide, the effects of SCRF on the absolute energy is to lower it by 1 kJ mol⁻¹ (amine), 24 kJ mol⁻¹ (ylide), 85 kJ mol⁻¹ (amine radical) and 16 kJ mol⁻¹ (concerted transition geometry). As the methyl radical has no dipole moment, there is no change in energy.

Table 6.10. Relative SCRF energies ($\epsilon = 35.9$) and gas-phase energies ($\epsilon = 1$) for the methylammonium methylide system at several levels of theory (RHF for closed-shell species, UHF for radicals).

	ylide		radicals		concerted TS	
	$\epsilon = 1$	$\epsilon = 35.9$	$\epsilon = 1$	$\epsilon = 35.9$	$\epsilon = 1$	$\epsilon = 35.9$
HF/6-31G(d)	167	151	208	181	485	453
HF/6-311+G(d)	298	272	281	262	583	579
MP2/6-31G(d)	323	300	383	384	549	546
MP2/6-311+G(d)	293	265	377	375	532	524
MP2/6-31+G(d,p)	305	278	377	378	547	543

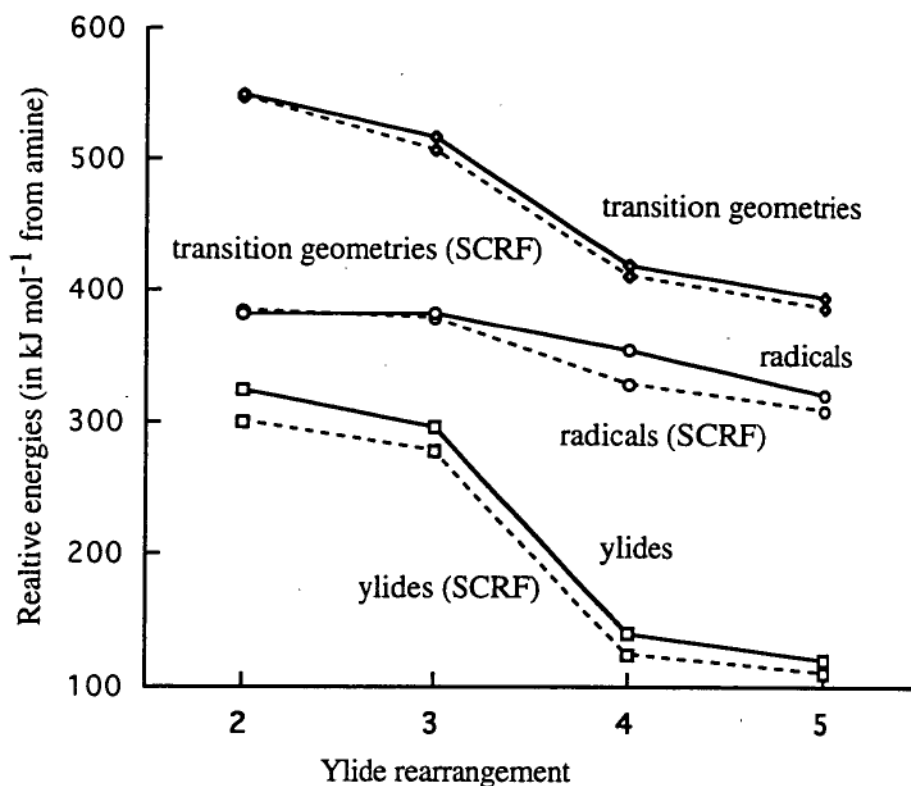


Figure 6.4. Relative MP2/6-31G(d) gas phase and SCRF energies for rearrangements (rearrangement numbers are as for Chapter 4)

6.4. COSMO studies of methylammonium formylmethylide

Optimising the solute molecules within COSMO leads to some changes in geometry, as seen in Table 6.11. The effect on the geometry of the continuum is small, but significant, the largest geometry changes being in the concerted transition geometry and the aminofornyl methyl radical. These changes can be rationalised in the sense of the large charge separation seen in the radical, and the relaxation of the small heterocycle of the transition state.

Using COSMO to calculate the electrostatic effect on the molecular energy, the energy of solvation of the isolated species is 1 kJ mol⁻¹ for the methyl radical, 65 kJ mol⁻¹ for the amine radical, 56 kJ mol⁻¹ for the concerted transition geometry, 42 kJ

mol⁻¹ for the amine and 113 kJ mol⁻¹ for the ylide. Comparing these numbers to the supermolecule energies above, we can see that the electrostatic effects are in general larger than specific solute-solvent effects, however of the same order of magnitude, hence specific effects are of some importance. The electrostatic effects are larger than those calculated at SCRF, with the exception of the amine radical (for reasons explained above).

Table 6.11. PM3 and COSMO optimised geometries for species involved in the rearrangement of methylammonium formylmethylide

	$\epsilon=1$	$\epsilon=35.9$	$\epsilon=1$	$\epsilon=35.9$	$\epsilon=1$	$\epsilon=35.9$	$\epsilon=1$	$\epsilon=35.9$
C _B N			1.516	1.502	1.792	1.848		
C _A N	1.484	1.489	1.409	1.441	1.474	1.473	1.373	1.350
C _C C _A	1.528	1.525	1.420	1.386	1.449	1.425	1.456	1.426
OC _C	1.207	1.217	1.233	1.262	1.222	1.245	1.205	1.242
C _A C _B	1.522	1.522						
C _A NC _B			114.3	112.3	72.1	70.2		
C _C C _A N	107.5	107.7	120.8	123.5	119.9	122.1	121.1	122.3
OC _C C _A	123.4	123.0	123.4	124.9	124.0	124.7	122.2	121.6
C _C C _A C _B	112.1	112.3						
C _C C _A NC _B			96.3	96.3	108.8	107.2		
OC _C C _A N	274.4	274.8	359.5	0.5	355.7	356.0	184.1	182.1
OC _C C _A C _B	40.5	40.4						

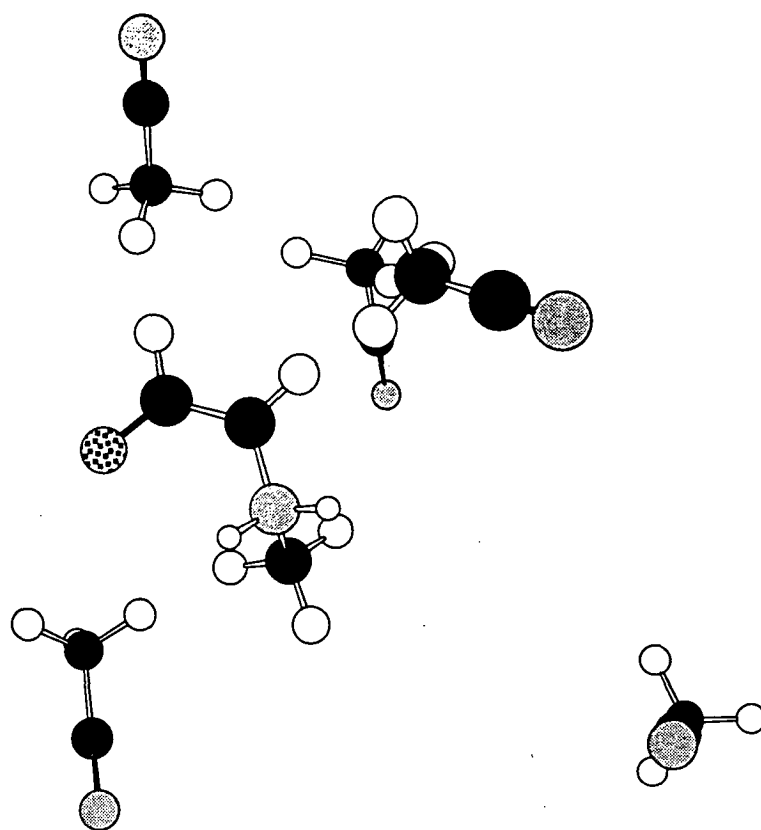
6.5. Hybrid COSMO-supermolecule studies of solvation.

6.5.1. Geometries of solvated clusters

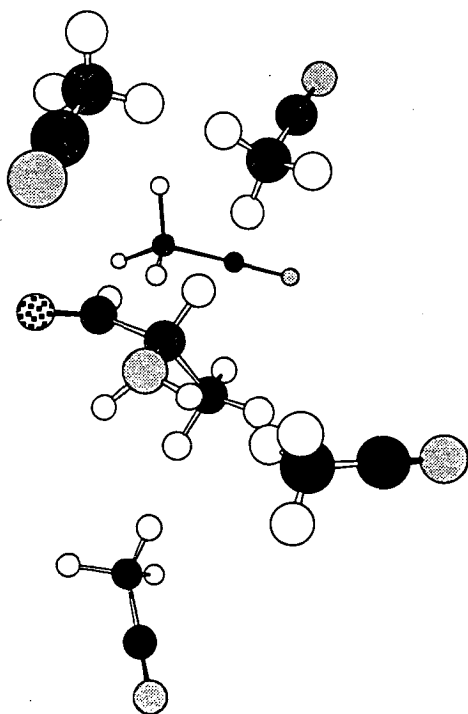
In the second stage of this study, we have optimised the gas-phase supermolecules within COSMO. As was seen for the gas-phase cluster, there is little effect on the original COSMO solute geometry from the incorporation of solvent molecules (Table 6.12-6.15). In the amine, again, there is variation in the values of $OC_C C_A N$ and $OC_C C_A C_B$ due to the facility of rotation about $C_C C_A$. Optimisations of the complex in the continuum show considerable changes in the positions of the acetonitrile molecules (Tables 6.16-6.20). This is not surprising, as the continuum should have an effect on the polar solvent molecules as well as the solute. The optimised solvated supermolecules are pictured in Figure 6.5.

Table 6.12. COSMO geometries of amine with varying number of acetonitrile molecules ($\epsilon = 35.9$)

	0	1	2	3	4	5
$C_A N$	1.489	1.489	1.486	1.484	1.486	1.486
$C_C C_A$	1.525	1.527	1.523	1.519	1.516	1.516
OC_C	1.217	1.217	1.215	1.216	1.217	1.216
$C_A C_B$	1.522	1.522	1.522	1.524	1.525	1.525
$C_C C_A N$	107.7	108.0	110.9	112.8	113.2	113.3
$OC_C C_A$	123.0	122.6	123.6	124.1	124.0	124.2
$C_C C_A C_B$	112.3	112.2	109.0	108.4	108.8	108.9
$OC_C C_A N$	274.8	276.3	319.2	338.5	2.7	6.6
$OC_C C_A C_B$	40.4	42.5	85.7	105.6	129.6	133.9



ylide



amine

Figure 6.5. Optimised COSMO supermolecule geometries for each species

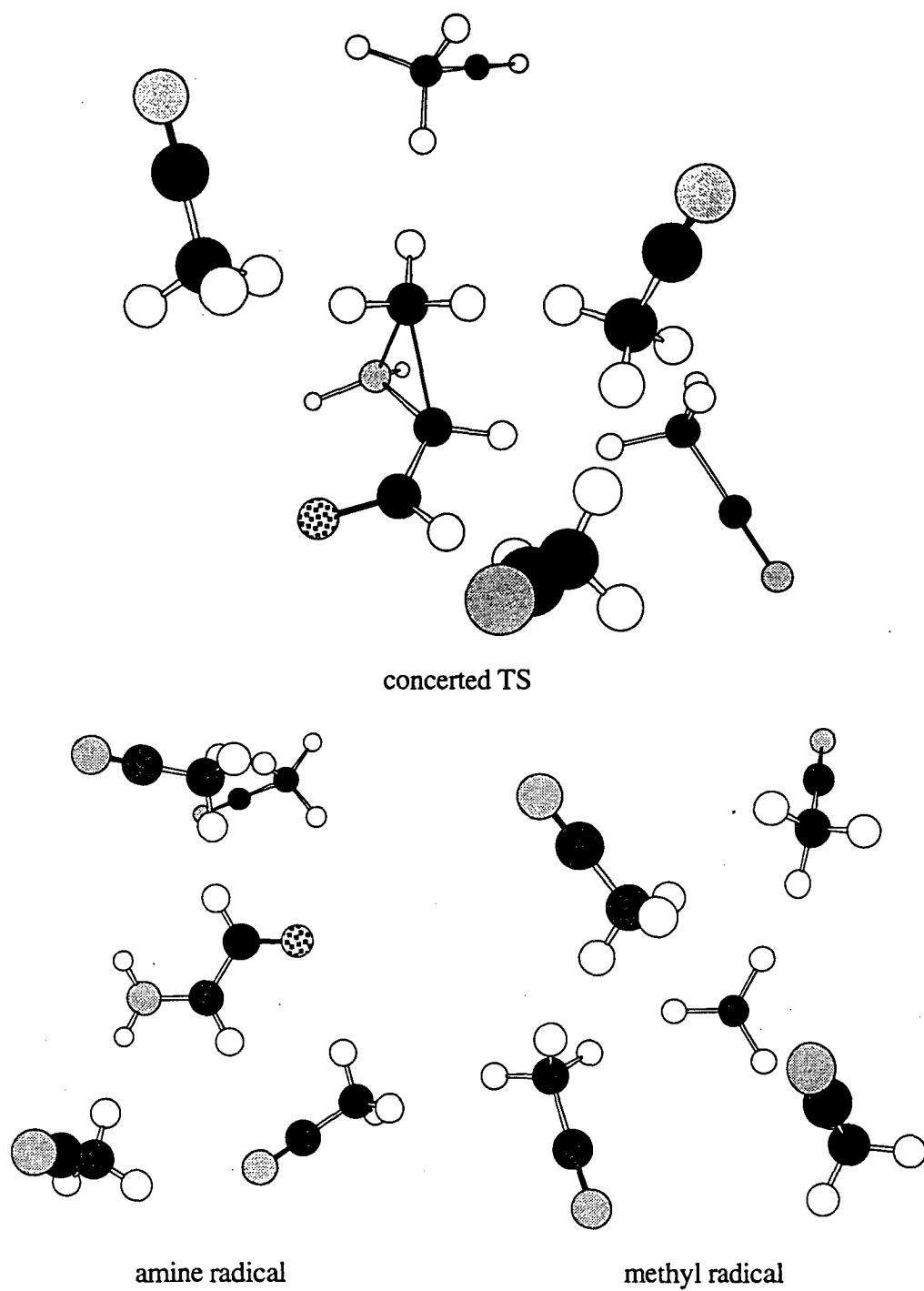


Figure 6.8. (cont.) Optimised COSMO supermolecule geometries for each species

Table 6.13. COSMO geometries of ylide with varying number of acetonitriles ($\epsilon = 35.9$)

	0	1	2	3	4	5
C _B N	1.502	1.503	1.504	1.503	1.504	1.504
C _A N	1.441	1.443	1.444	1.444	1.442	1.440
C _C C _A	1.386	1.386	1.383	1.387	1.389	1.390
OC _C	1.262	1.262	1.265	1.261	1.258	1.258
C _A NC _B	112.3	112.0	112.4	112.1	111.5	113.0
C _C C _A N	123.5	123.6	123.4	123.6	123.1	122.9
OC _C C _A	124.9	125.0	125.0	125.0	124.9	125.1
C _C C _A NC _B	96.3	98.2	97.4	94.0	99.4	81.1
OC _C C _A N	0.5	2.3	359.3	0.8	0.4	3.2

Table 6.14. COSMO concerted TS geometries with varying number of acetonitrile molecules ($\epsilon = 35.9$)

	0	1	2	3	4	5
C _B N	1.848	1.851	1.845	1.846	1.844	1.840
C _A N	1.473	1.473	1.473	1.473	1.473	1.473
C _C C _A	1.425	1.427	1.425	1.426	1.427	1.427
OC _C	1.245	1.244	1.243	1.243	1.243	1.242
C _A NC _B	70.2	69.4	70.3	70.2	70.1	70.1
C _C C _A N	122.1	122.1	122.2	122.0	122.0	122.0
OC _C C _A	124.7	124.7	124.9	124.9	124.8	124.8
C _C C _A NC _B	107.2	107.7	107.8	107.4	107.3	107.7
OC _C C _A N	356.0	355.8	357.5	357.0	358.0	357.7

Table 6.15. COSMO optimised amine radical geometries with varying number of acetonitrile molecules ($\epsilon = 35.9$)

	0	1	2	3	4
C _A N	1.350	1.352	1.362	1.365	1.370
C _C C _A	1.426	1.426	1.435	1.441	1.449
OC _C	1.242	1.240	1.236	1.227	1.218
C _C C _A N	122.3	122.4	122.3	121.1	121.6
OC _C C _A	121.6	122.5	121.7	122.9	122.4
OC _C C _A N	182.1	183.0	183.1	187.5	187.9

Table 6.16. COSMO optimised positions of acetonitrile molecules around amine.

	R	θ_1	ϕ_1	θ_2	ϕ_2
1	5.50	69.0	181.9	146.6	21.6
2	5.77	48.7	164.7	151.9	268.9
	5.96	83.0	44.4	139.9	125.0
3	5.73	62.4	164.5	135.7	217.2
	5.33	94.0	41.7	106.9	195.1
	4.67	133.2	133.1	134.6	96.6
4	5.70	64.4	173.6	145.4	335.2
	5.82	84.6	51.0	121.3	177.3
	5.02	88.4	234.3	75.5	92.3
	4.69	134.2	132.1	136.6	57.1
5	6.64	34.7	127.1	122.3	190.8
	5.63	66.1	183.4	147.7	325.8
	4.94	84.4	247.4	81.8	136.7
	5.75	84.5	51.1	119.3	188.8
	4.74	129.5	123.5	140.6	18.1

Table 6.17. COSMO optimised positions of acetonitrile molecules around ylide.

	R	θ_1	ϕ_1	θ_2	ϕ_2
1	5.47	127.9	123.9	113.0	198.8
2	4.67	62.9	75.5	105.2	190.0
	5.37	120.1	125.7	94.8	197.6
3	6.54	23.9	129.0	115.1	187.0
	4.55	71.5	6.5	100.7	162.1
	6.38	116.3	187.8	69.7	238.8
4	6.83	1.49	130.0	129.7	125.5
	5.23	52.3	302.3	88.0	204.0
	5.05	64.6	16.0	118.3	179.0
	4.78	111.6	218.3	109.9	320.0
5	6.91	1.77	167.8	136.4	112.4
	4.92	54.9	200.4	96.8	210.5
	5.03	68.0	17.9	122.7	175.9
	5.24	114.3	214.1	120.9	188.8
	7.37	130.6	331.6	80.5	123.9

Table 6.18. COSMO optimised positions of acetonitrile molecules around concerted transition geometry.

	R	θ_1	ϕ_1	θ_2	ϕ_2
1	5.31	54.8	333.2	127.2	147.6
2	6.20	34.8	267.3	154.7	198.5
	5.44	55.0	348.4	124.0	193.1
3	6.97	17.0	197.1	139.4	194.7
	6.31	48.7	283.1	147.8	194.2
	5.36	58.9	355.1	122.9	174.8
4	6.96	17.9	197.5	137.6	192.4
	5.71	45.7	5.2	143.8	77.7
	6.29	48.2	283.7	148.1	195.9
	4.99	122.7	306.6	114.6	102.7
5	6.94	19.0	197.5	135.7	191.3
	5.73	44.3	6.9	143.2	76.4
	6.28	47.9	284.2	147.6	194.7
	5.68	98.3	221.1	132.1	134.2
	5.07	118.6	307.3	116.9	91.5

Table 6.19. COSMO optimised positions of acetonitrile molecules about amine radical

	R	θ_1	ϕ_1	θ_2	ϕ_2
1	4.70	65.6	172.0	89.1	194.9
2	4.33	72.6	167.4	85.5	192.3
	5.35	82.8	3.0	116.3	162.3
3	5.70	43.8	235.1	86.4	165.2
	5.32	59.7	167.7	104.6	174.6
	4.41	140.5	49.2	122.8	67.5
4	5.92	47.5	233.8	84.1	160.2
	5.27	61.2	168.8	103.7	181.3
	4.63	71.6	2.8	76.1	168.8
	4.47	137.8	49.1	125.3	88.0

Table 6.20. COSMO optimised positions of acetonitrile molecules around methyl radical.

	R	θ_1	ϕ_1	θ_2	ϕ_2
1	4.71	109.4	185.5	133.4	11.2
2	4.66	115.0	347.8	131.2	299.2
	4.50	139.5	161.9	124.0	221.5
3	4.05	45.9	150.8	118.4	158.5
	4.57	58.4	41.7	140.1	287.0
	4.54	139.0	159.3	126.7	232.8
4	4.06	44.4	150.5	115.8	164.3
	4.88	55.2	40.8	151.7	287.9
	4.49	111.0	356.4	125.8	281.9
	3.69	119.5	121.0	103.2	294.4

6.5.2. Interactions of solvent molecules with the solute

From the optimisations within the continuum, some specific solvent-solute effects are in evidence. In the amine (Table 6.16), there are two acetonitrile molecules interacting with the lone pair on the amine nitrogen. These appear at θ_1 values of around 130° and 66° and are common to the COSMO complexes of 3, 4, and 5 solvent molecules. A third acetonitrile molecule common to the two largest clusters is aligned "side-on" to the methyl group at $\theta_1 = 85^\circ$. In the ylide (Table 6.17), there are two acetonitrile molecules in similar positions in the two largest COSMO clusters, with θ_1 values of 55° and 68° in the largest solvated ylide. These are above and below the N-C-C-O plane, with the methyl end of the solvent molecule oriented towards the plane (and hence, one assumes, a delocalised π -type orbital). The concerted transition geometry (Table 6.18), satisfyingly shows two acetonitrile molecules above and below the N-C-C-O plane, as in the ylide ($\theta_1 = 44^\circ, 48^\circ$) and an acetonitrile molecule at $\theta_1 = 119^\circ$, which behaves similarly to that near the methyl group in the amine. In the amine radical (Table 6.19), there are again acetonitrile molecules above and below the N-C-C-O plane ($\theta_1 = 48^\circ, 61^\circ$), as well as a common solvent molecule oriented towards the nitrogen atom at $\theta_1 = 138^\circ$. Specific interactions can now be assumed: two solvating acetonitrile molecules co-ordinate to the delocalised orbital in the ylide; these remain coordinated in the transition geometries, with a third solvent molecule becoming important, coordinating to the migrating methyl group in the concerted transition geometry, or to the amine end of the radical in the dissociative pathway. The delocalisation, and hence the interaction of the two solvating acetonitriles, is lost with the formation of the amine, and solvent molecules cluster at the methyl group and at the amine lone pair. Unfortunately, the calculation of the influence on the energy of these specific effects individually is beyond the scope of this study, however it explains the differences in complexation energies discussed below.

It is also worth noting that we have neglected the timescale of reaction, and treated the ideal situation that the solvent is always in equilibrium with the solute.

Although this is not likely to be the case, it is done to obtain the maximum solvent effect - presumably energies presented here are an upper bound to the true energy of the individual species.

6.5.3. Complexation energy of solvated clusters

The effect of acetonitrile molecules inside the cavity on solvation is presented in Figure 6.6. There is little effect on the energy of the methyl radical, as could be expected. The solvation energy of the amine radical decreases with coordinating acetonitrile molecules, the solvation energy of the amine and concerted transition geometry is increased and then flattens out, and the ylide solvation energy seems to increase and decrease with number of acetonitrile molecules. It can be seen from this graph that there is a definite change in solvation energy by incorporating solvent molecules in the cavity, and that it may require several co-ordinating solvent molecules to get an idea of the contributions of specific solvent-solute interactions to the molecular energy.

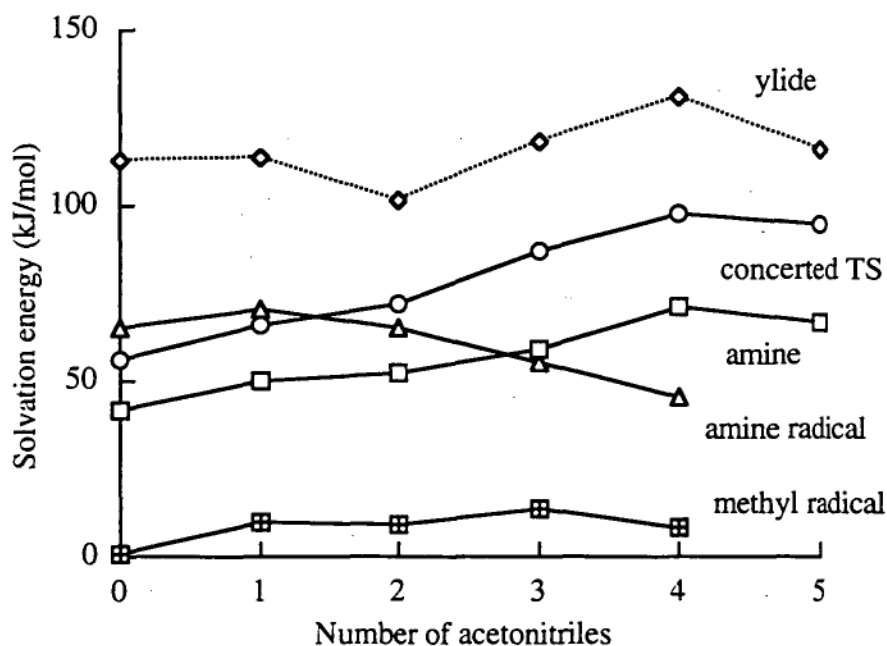


Figure 6.6. COSMO solvation energy as a function of number of solvent molecules

6.6. Comparison of solvation methods on the Stevens rearrangement.

The relative energies for the rearrangement are presented in Table 6.21, and graphically as a function of the number of acetonitrile molecules in Figure 6.7. COSMO is shown to have a similar effect on relative energies as the SCRF MP2/6-31G(d) method of solvation previously reported; the energies of all species are lowered, however COSMO lowers the relative energy of the amine considerably more than SCRF.

For the supermolecule calculations, it is difficult to assign an appropriate energy for the radical pair pathway, as there are two species involved in the transition structure. The energies reported in this paper are the lowest obtained from all possible combinations of the two radicals and the appropriate number of solvent molecules (for six acetonitriles, this corresponds to three solvent molecules on each radical species). From the relative energies of the largest supermolecule calculations presented in Table 6.21, it can be seen that there is some difference between the supermolecule calculations and the single-molecule calculations, both in the "gas phase" and with COSMO. The overall effect of all methods for incorporating solvation effects is that the radical pair rearrangement is favoured over the concerted pathway, the supermolecule methods lowering the difference between the two pathways slightly, but not enough for the concerted pathway to be considered as the rearrangement mechanism.

Figure 6.7 shows the behaviour of the two supermolecule methods as a function of number of solvent molecules. It is satisfying to note that, for the radical pair and for the ylide, the two methods are converging - indicating that adding the continuum to a supermolecule calculation brings the energy towards that which an infinite number of solvent molecules would achieve. Energies for the concerted transition geometry are not converging, this may be because of the different geometries seen between the gas phase complex and COSMO geometry.

Table 6.21. Relative energies (in kJ mol^{-1} relative to amine) of species involved in the Stevens rearrangement of methylammonium formylmethylide at several levels of theory

	ylide	concerted TS	radical pairs
PM3	99	227	325
MP2/6-31G(d)	139	355	420
COSMO PM3	28	203	310
SCRF MP2/6-31G(d)	124	327	410
PM3 (+6 CH_3CN)	68	228	316
COSMO PM3 (+5 CH_3CN)	50	216	297

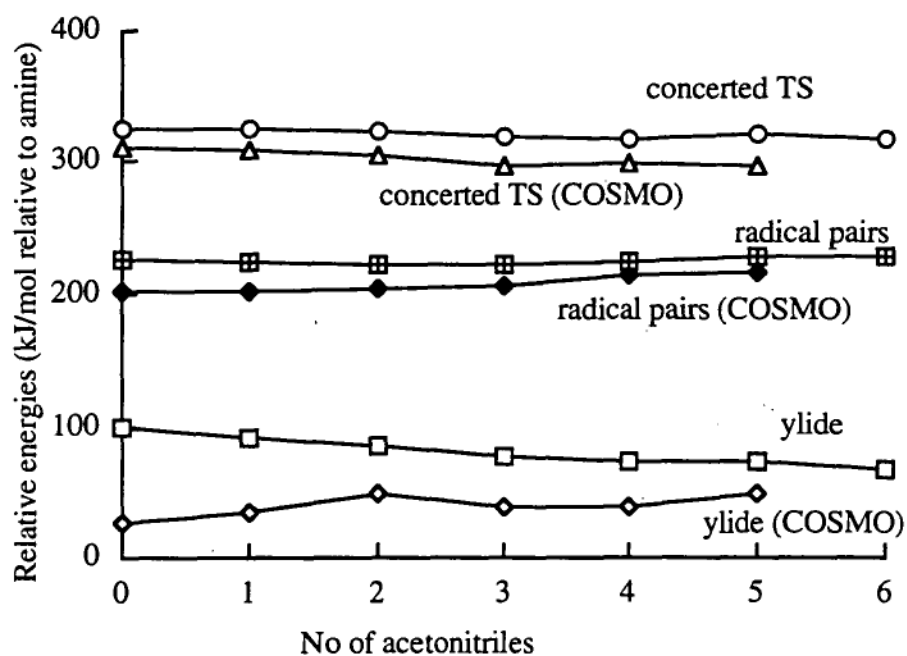


Figure 6.7. Relative energies of all species with varying number of solvating acetonitrile molecules

6.7. Conclusions

We have used the supermolecule approach and a polarisable continuum method in concert to obtain a solvation energy which takes into account both specific solvent-solute effects and the electrostatic contribution to solvation. The changes in relative energy due to solvation become apparent after between four and six solvent molecules have been incorporated in the wavefunction, which puts the calculations comfortably in reach using semi-empirical methods. The COSMO method is shown to be a reliable and useful tool in calculating solvation energies as the molecular geometry of the supermolecule can be optimised for a large system in the presence of an electric field.

From these calculations, the solvent effect on the Stevens rearrangement of methylammonium formylmethylide has been calculated. There are specific solvent-solute interactions in evidence; two solvent molecules coordinate to the delocalised orbital on the ylide, and remain coordinated in the transition geometry. Energetically, however it has been determined that there is no effect on the pathway of the reaction, which proceeds via a radical pair mechanism.

Chapter 7. Competing rearrangements of ammonium ylides

7.1. Introduction

In this study, we will use our previous *ab initio* and semi-empirical calculations on ammonium ylides and the Stevens rearrangement as a basis for a study of the Sommelet-Hauser rearrangement. Comparison of the radical intermediates of the Stevens rearrangement with the concerted transition geometry of the Sommelet-Hauser rearrangement should give an indication as to which pathway is preferred, and which orbital interactions are important in promoting each rearrangement pathway.

In this study, we have chosen to perform semi-empirical and *ab initio* molecular orbital calculations on the competing rearrangement of a prototype ylide, N-methyl-3-propenyl ammonium methyllide **1**, shown in Figure 7.1. This ylide has the novel property that both the Stevens and the Sommelet-Hauser rearrangement will give the same product amine, N-methyl-4-butenylamine **2**. This is particularly attractive for a theoretical study, in that any errors in calculation of the initial and final energies should fortuitously cancel out, and any activation energies calculated would be expected to be accurate. The Stevens rearrangement involves two radical intermediates: the N-methyl aminomethyl radical **3**, and the allyl radical **4**. The Sommelet-Hauser rearrangement will proceed via a transition geometry **5**. Once the intermediates have been characterised, the important factors in each rearrangement will be taken into account by modifying the skeleton rearrangement so as to approach the ylides used in experiment.

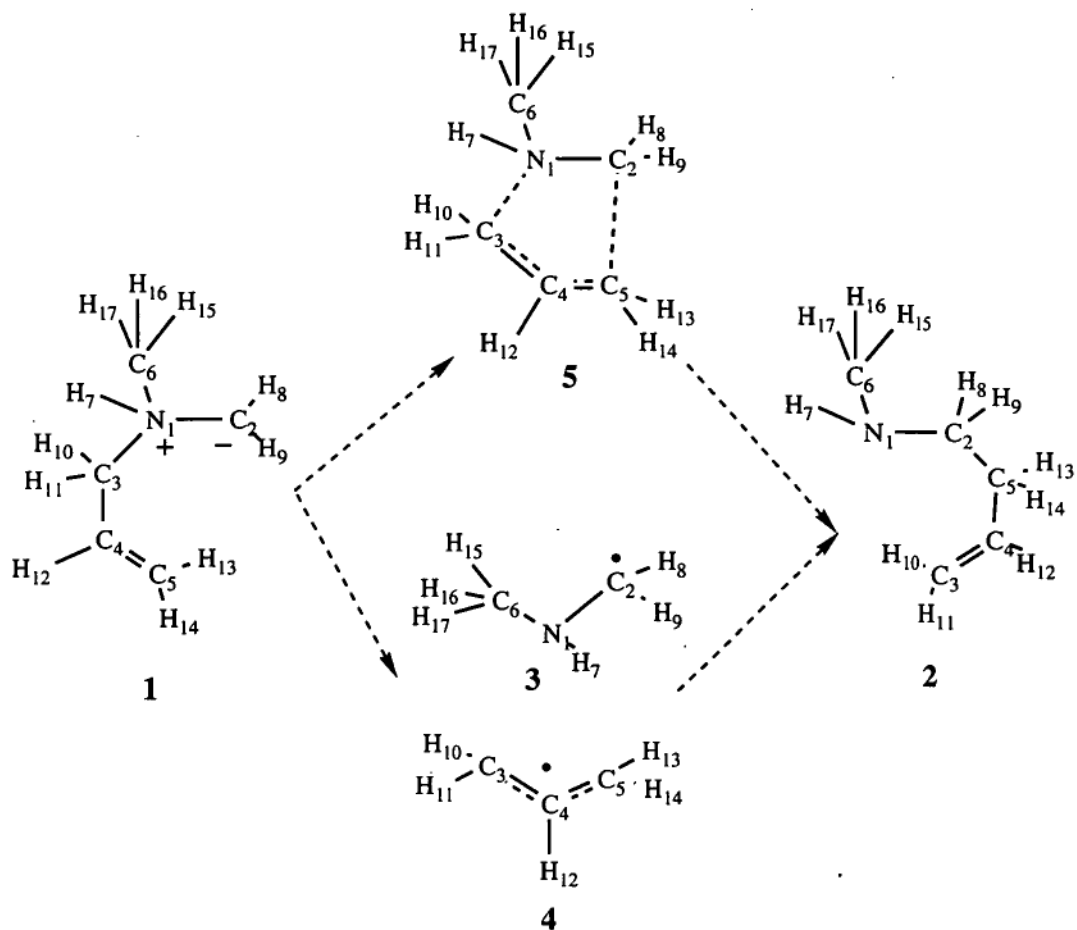


Figure 7.1. The competing rearrangements of N-methyl-3-propenyl ammonium methylide (with atom labels to be used through this Chapter)

7.2. The rearrangement ylide and product amine

7.2.1. N-methyl-3-propenyl ammonium methylyde (**1**)

Determining the minimum-energy structure of organic molecules is often difficult, as there are several conformers possible, usually close in energy. It is also the case that low levels of theory sometimes predict the minimum energy conformation incorrectly, particularly in the case of substituted amines⁸⁰. Since there is no spectroscopic or previous theoretical work on this particular ylide, a conformational analysis was carried out at the PM3 level of theory, and each local minimum found was optimised at the HF level with the 3-21G and 6-31G(d) basis set, and at MP2/6-31G(d). Three local minima (**1a-1c**, as shown in Figure 7.2) were located at PM3, however at the HF level, no minimum corresponding to **1c** could be located. Relative energies at the four levels of theory are shown in Table 7.1. It can be seen that **1a** and **1b** are very close in energy, **1b** being slightly favoured, and hence **1b** has been used as a starting point for all higher-level calculations. Optimised bond distances, angles and torsional angles for **1b** at the higher levels of theory are presented in Table 7.2.

The general structural features of ammonium ylides have been discussed in Chapters 3-6. This particular ylide has the characteristic long C-N bond distance. The double bond is aligned away from the electron lone pair on the carbanion, which puts it in an unfavourable position for the Sommelet-Hauser rearrangement.

Table 7.1. Relative energies (in kJ mol⁻¹) of ylide conformers

	ylide 1a	ylide 1b	ylide 1c
PM3	0	5	6
RHF/3-21G	2	0	- ^a
RHF/6-31G(d)	1	0	-
MP2/6-31G(d)	2	0	-

^a No minimum corresponding to **1c** was located at the HF or MP2 level

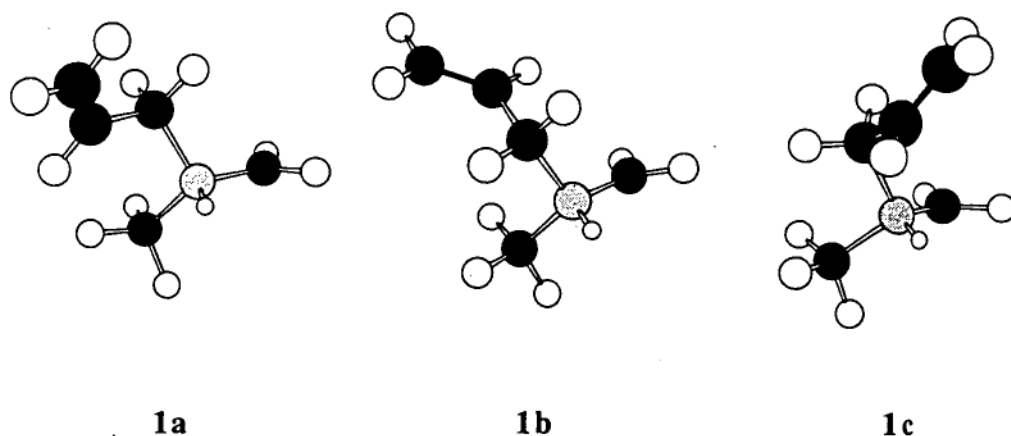


Figure 7.2. Structures of ylides **1a-1c** optimised at PM3

Table 7.2. Structural parameters and energies for ylide **1b** optimised at MP2

	6-31G(d)	6-31+G(d)	6-311G(d)	6-311+G(d)	6-311+G(d,p)
N ₁ C ₂	1.5259	1.5139	1.5212	1.5140	1.5145
N ₁ C ₃	1.5168	1.5237	1.5157	1.5193	1.5175
C ₃ C ₄	1.4973	1.4981	1.5000	1.5001	1.5007
C ₄ C ₅	1.3410	1.3446	1.3421	1.3439	1.3438
N ₁ C ₆	1.4832	1.4861	1.4817	1.4827	1.4828
C ₂ N ₁ C ₃	117.8	117.8	117.4	117.6	117.5
N ₁ C ₃ C ₄	113.8	113.4	113.7	113.3	113.4
C ₃ C ₄ C ₅	122.5	122.4	122.5	122.4	122.2
C ₃ N ₁ C ₆	111.2	110.6	110.9	110.4	110.7
C ₂ N ₁ C ₃ C ₄	187.8	187.9	187.4	187.5	187.4
N ₁ C ₃ C ₄ C ₅	99.14	95.84	97.82	95.16	96.57
C ₄ C ₃ N ₁ C ₆	61.46	61.08	61.11	61.00	60.90
MP2 /a.u.	-250.846518	-250.872795	-250.949152	-250.960833	-251.044600
CCSD	-250.913976				
CCSD(T)	-250.943282				
a ₀ /Å	4.06				4.12

7.2.2. N-methyl-4-butenylamine (2)

As with the ylide, a conformational search of the amine, using staggered conformations along the (N₁C₂C₃C₄) backbone as initial geometries, was carried out at the PM3 level, and six local minima were located, **2a-2f** in Figure 7.3. Relative energies of all six conformations at PM3, RHF/3-21G, RHF/6-31G(d) and MP2/6-31G(d) are reported in Table 7.3. **2b** is predicted to be lowest in energy at MP2/6-31G(d), and all higher level calculations were carried out using this geometry as a starting point. Optimised MP2 geometries and energies for the amine are presented in Table 7.4. Although the amine is important for calculating reaction enthalpy, and in characterising the correct transition geometry, there is no real insight into the competing rearrangements to be gained from calculations on the amine, as it is the reaction barriers that are more important. Since there is a large difference in energy between the ylide and the amine, the concerted transition geometry is expected to resemble the reactant more closely than the product.

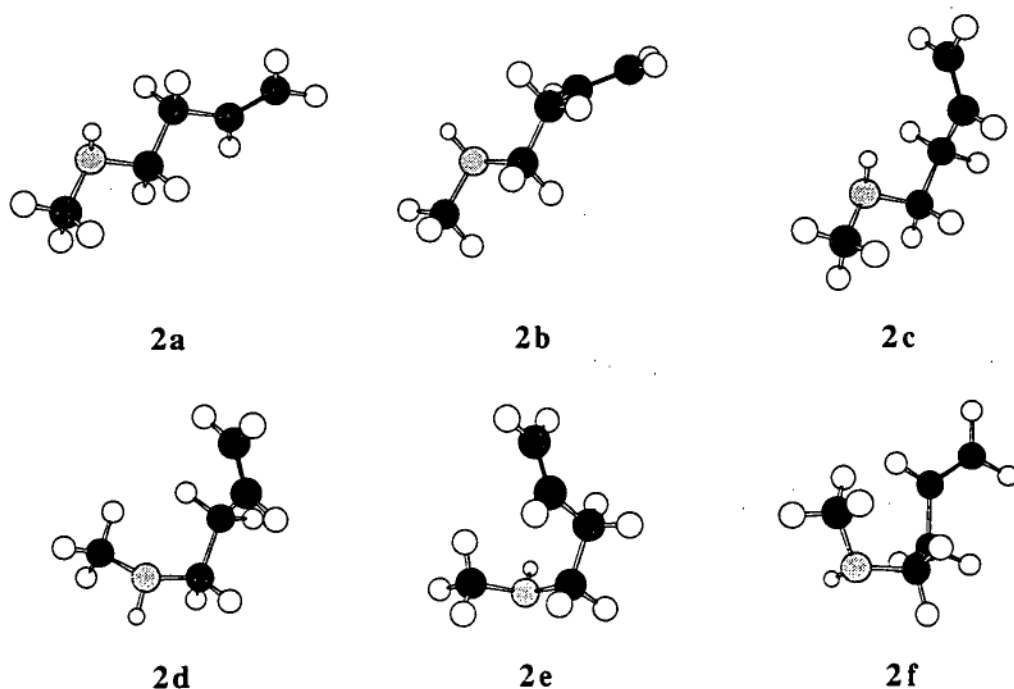


Figure 7.3. Structures of amines **2a-2f** optimised at PM3

Table 7.3. Relative energies (in kJ mol⁻¹) of amine conformers **2a-2f**

	2a	2b	2c	2d	2e	2f
PM3	6	4	9	2	0	4
RHF/3-21G	0	1	9	13	14	4
RHF/6-31G(d)	2	0	10	15	18	2
MP2/6-31G(d)	4	0	8	15	18	5

Table 7.4. Structural parameters and energies for amine **2b** optimised at MP2

	6-31G(d)	6-31+G(d)	6-311G(d)	6-311+G(d)	6-311+G(d,p)
C ₂ N ₁	1.4564	1.4577	1.4555	1.4556	1.4560
C ₅ C ₂	1.5300	1.5302	1.5313	1.5312	1.5321
C ₄ C ₅	1.5002	1.5004	1.5014	1.5014	1.5020
C ₃ C ₄	1.3402	1.3436	1.3411	1.3429	1.3430
C ₆ N ₁	1.4580	1.4603	1.4579	1.4581	1.4585
C ₅ C ₂ N ₁	110.2	110.4	110.3	110.5	110.5
C ₄ C ₅ C ₂	111.6	111.7	111.5	111.5	111.5
C ₃ C ₄ C ₅	124.5	124.6	124.6	124.5	124.4
C ₆ N ₁ C ₂	112.2	112.6	111.9	112.4	112.4
C ₄ C ₅ C ₂ N ₁	65.92	65.14	65.69	64.94	65.44
C ₃ C ₄ C ₅ C ₂	249.3	248.6	249.9	249.8	248.4
C ₆ N ₁ C ₂ C ₅	185.0	183.1	183.1	182.7	184.8
MP2 /a.u.	-250.962597	-250.979849	-251.056467	-251.065823	-251.149411
CCSD	-251.027493				
CCSD(T)	-251.055390				
a ₀ /Å	4.06				4.10

7.3. The Stevens [1,2] rearrangement of N-methyl-3-propenyl ammonium methylide

The structures and molecular energies of the Stevens rearrangement intermediates, the N-methyl aminomethyl radical, **3**, and the allyl radical, **4**, are presented in Tables 7.5 and 7.6 respectively. The structure of the amine radical is as expected from previous studies of amine radicals, and the allyl radical has been well-characterised by experiment⁸⁸ and theory^{89,90}. We have repeated the calculations in this study in order to make consistent comparisons with other species.

The allyl radical shows a high degree of spin contamination in the UHF and UMP2 wavefunction. In order to justify our single point ROMP2 energy calculations on this geometry, full geometry optimisation has been carried out at ROMP2/6-31+G(d). The only geometry change was a slight lengthening of the C-C bond, and the difference in ROMP2 energy between the UMP2 optimised geometry and the ROMP2 geometry is only 0.3 kJ mol⁻¹. At ROMP2 and the largest basis set, the barrier to formation of the radicals is 37 kJ mol⁻¹.

There is another possible Stevens rearrangement of **1**, involving a methyl radical as opposed to an allyl radical as the migrating species. There is some precedent for more than one Stevens rearrangement being observed.

Geometry optimisation of the resulting N-propenyl aminomethyl radical shows that the barrier to the formation of this radical pair is 267 kJ mol⁻¹ at PM3 and 374 kJ mol⁻¹ at ROHF/3-21G. These values are considerably higher than those for the previously discussed dissociation and hence no further calculations were performed on this rearrangement.

Table 7.5. Structural parameters and energies of N-methyl aminomethyl radical **3** calculated at MP2

	6-31G(d)	6-31+G(d)	6-311G(d)	6-311+G(d)	6-311+G(d,p)
C ₂ N ₁	1.3940	1.3911	1.3908	1.3885	1.3886
C ₆ N ₁	1.4553	1.4571	1.4546	1.4552	1.4553
C ₆ N ₁ C ₂	117.1	117.7	117.2	117.7	117.6
<s ² >	0.7598	0.7618	0.7610	0.7622	0.7622
UMP2	-134.018928	-134.030886	-134.071384	-134.078633	-134.125687
PUMP2	-134.020633	-134.032736	-134.073193	-134.080520	-134.127582
ROMP2	-134.017617	-134.031216	-134.071695	-134.079001	-134.126150
CCSD	-134.055896				
CCSD(T)	-134.067274				
a ₀ /Å	3.42				3.45

Table 7.6. Structural parameters and energies of the allyl radical **4** calculated at MP2

	6-31G(d)	6-31+G(d)	6-311G(d)	6-311+G(d)	6-311+G(d,p)	6-31+G(d) ^a
H ₁₂ C ₄	1.0883	1.0890	1.0882	1.0884	1.0881	1.090
H ₁₀ C ₃	1.0825	1.0830	1.0820	1.0822	1.0824	1.084
H ₁₁ C ₃	1.0845	1.0852	1.0842	1.0844	1.0847	1.087
C ₃ C ₄	1.3781	1.3806	1.3791	1.3803	1.3802	1.390
C ₃ C ₄ H ₁₂	117.8	117.8	117.8	117.8	117.9	117.7
H ₁₀ C ₃ C ₄	121.8	121.6	121.6	121.6	121.5	121.6
H ₁₁ C ₃ C ₄	121.0	121.0	120.9	121.0	120.8	120.8
<s ² >	0.9606	0.9522	0.9554	0.9521	0.9509	
UMP2/a.u	-116.810216	-116.819168	-116.852147	-116.855480	-116.892630	
PUMP2	-116.824836	-116.833176	-116.866501	-116.869581	-116.906592	
ROMP2	-116.821064	-116.830281	-116.863695	-116.867176	-116.904958	-116.830385
CCSD	-116.856761					
CCSD(T)	-116.869524					
a ₀ /Å	3.38				3.42	

7.4. The Sommelet-Hauser [3,2] rearrangement of N-methyl-3-propenyl ammonium methylyde

The transition geometry for the Sommelet-Hauser rearrangement of **1b** to **2b** was located using the saddle-point algorithm of Dewar, Healey and Stewart⁹¹ and the PM3 Hamiltonian. Vibrational frequencies were calculated to verify the character of the saddle point, and the transition geometry was optimised to the ylide and amine by a slight increase and decrease in the $N_1C_3C_4$ bond angle. This geometry was successfully used as a starting point for ab initio transition geometries, which were similarly followed to the ylide and amine. Optimised structural parameters and energies for the transition geometry **5** are presented in Table 7.7.

As there is a difference in the bond distances in ylide geometries depending on the method used to calculate them (PM3, HF, or MP2 wavefunctions), there is also a difference in the Sommelet-Hauser transition geometry, as seen in Figure 7.4. PM3 in particular predicts a much shorter bond distance in the ylide, and hence allows for more orbital overlap between C_2 and C_5 in the transition structure. At all levels, however, there are consistent differences between the ylide and the transition structure. The NC_3 bond, formally broken in the rearrangement, is lengthened in the transition geometry, and the NC_2 bond is shortened, consistent with the C–N charge-separated bond becoming a formal C–N single bond. The two angles NC_3C_4 and $C_3C_4C_5$ both tighten to allow C_5 and C_2 to come into position to form a bond, and there is a change in the dihedral angles which describe rotation about NC_3 and C_3C_4 . There is little interaction between C_2 and C_5 in the transition geometry: the energy barrier seems to arise from rotating the molecule (in particular the double bond, which is in a sterically unfavourable environment) to a position where the bond formation occurs.

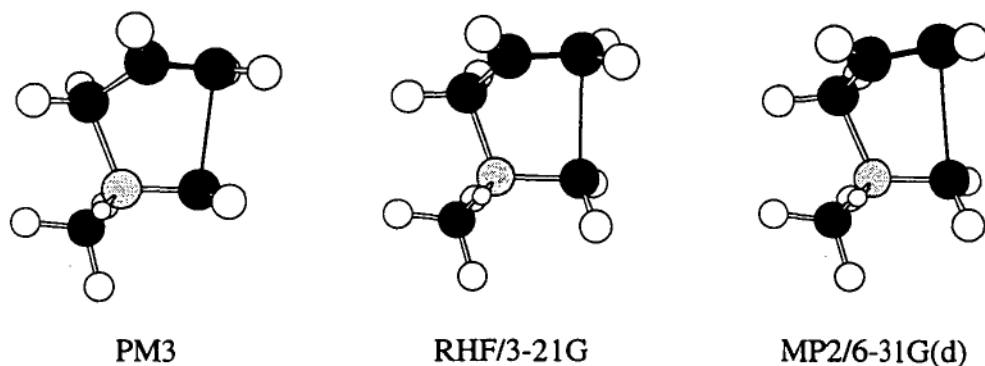


Figure 7.4. Optimised Sommelet-Hauser transition geometries **5** at different levels of theory.

Table 7.7. Structural parameters and energies for the Sommelet-Hauser transition geometry **5** calculated at MP2

	6-31G(d)	6-31+G(d)	6-311G(d)	6-311+G(d)	6-311+g(d,p)
C ₂ C ₅	2.7051	2.9586	2.7148	2.8727	2.8809
N ₁ C ₂	1.4515	1.4315	1.4470	1.4369	1.4364
N ₁ C ₃	1.6394	1.6759	1.6458	1.6681	1.6626
C ₃ C ₄	1.4526	1.4563	1.4539	1.4559	1.4572
C ₄ C ₅	1.3570	1.3550	1.3588	1.3560	1.3561
N ₁ C ₆	1.4881	1.4888	1.4865	1.4838	1.4856
C ₂ N ₁ C ₃	113.4	115.4	113.4	114.9	115.2
N ₁ C ₃ C ₄	106.2	107.0	106.2	106.8	107.0
C ₃ C ₄ C ₅	116.3	119.8	116.8	119.1	118.9
C ₃ N ₁ C ₆	107.2	105.6	106.7	105.8	105.9
C ₂ N ₁ C ₃ C ₄	302.8	303.9	304.2	307.9	306.2
N ₁ C ₃ C ₄ C ₅	66.41	73.81	66.99	72.61	71.95
C ₄ C ₃ N ₁ C ₆	171.4	174.9	173.6	180.2	177.3
MP2 /a.u.	-250.833905	-250.858979	-250.935942	-250.947026	-251.031248
CCSD	-250.896258				
CCSD(T)	-250.928558				
a ₀ /Å	4.04				4.10

7.5. Relative energies of competing pathways

7.5.1. Effect of level of theory on activation energies

Relative energies for intermediates in each of the two rearrangements (in kJ mol^{-1} relative to amine **2**) are given in Table 7.8. At the PM3 level, the Stevens rearrangement is favoured by 48 kJ mol^{-1} . This value is expected to be artificially large, since semi-empirical methods overestimate the stability of open-shell species. The HF methods predict the Stevens rearrangement to be favoured by over 100 kJ mol^{-1} ; again, HF is an inappropriate method for comparison of a pair of radicals with a closed-shell concerted rearrangement, and there is expected to be considerable correlation energy in all species. At MP2/6-31G(d), the Stevens rearrangement is favoured by 30 kJ mol^{-1} at PUMP2 and 13 kJ mol^{-1} at ROMP2. As this energy separation is quite small, the effects of further correlation and larger basis sets have been investigated.

Further electron correlation effects were taken into account by calculations at the CCSD(T)/6-31G(d) level using the optimised MP2/6-31G(d) geometries. The relative energy of the Stevens pathway is lowered considerably; there is little change in the Sommelet-Hauser relative energy. Higher levels of electron correlation seem to favour the Stevens rearrangement over the Sommelet-Hauser.

Table 7.8. Relative energy of rearrangements, in kJ mol⁻¹ with respect to amine **2b**, at various levels of theory.

	ylide 1	Sommelet-Hauser 5	Stevens (3+4)
PM3	224	275	227
UHF/3-21G	292	360	182
ROHF/3-21G			257
UHF/6-31G(d)	315	399	187
ROHF/6-31G(d)			263
UMP2/6-31G(d)	306	338	350
PUMP2 ^a			308
ROMP2			325
UMP2/6-31+G(d)	281	317	341
PUMP2			299
ROMP2			311
UMP2/6-311G(d)	281	316	349
PUMP2			307
ROMP2			318
UMP2/6-311+G(d)	276	312	346
PUMP2			304
ROMP2			314
UMP2/6-311+G(d,p)	275	310	344
PUMP2			303
ROMP2			312
CCSD/6-31G(d) ^b	298	345	301
CCSD(T)/6-31G(d) ^b	294	333	311

^a PUMP2 and ROMP2 energies calculated at the appropriate optimised MP2 geometry

^b Calculated at optimised MP2/6-31G(d) geometry

7.5.2. Effect of basis set on activation energies

Increasing the flexibility of the basis set (by adding further primitives, polarisation and diffuse functions) has the effect of lowering the relative energy of the Sommelet-Hauser rearrangement at MP2, as seen in Table 7.8. The effect on the radicals is a slight lowering in relative energy, not as pronounced as in the concerted process. The activation energy of the Stevens rearrangement is raised as the basis set

increases, the activation energy of the Sommelet-Hauser process remains much the same. MP2 optimisations at the largest basis set, 6-311+G(d,p), involving polarisation on all of the hydrogen atoms, predict the Stevens rearrangement to be favoured by 7 kJ mol⁻¹ at PUMP2, but the Sommelet-Hauser rearrangement to be favoured by 2 kJ mol⁻¹ at the ROMP2 level. In general, larger basis sets tend to favour the Sommelet-Hauser rearrangement over the Stevens rearrangement.

7.5.3. Effect of solvation on activation energies

In Chapter 6, solvation effects were shown to be of minor significance on the activation energy of the Stevens rearrangement, however the effect on the [3,2] transition geometry is unknown. To investigate the electrostatic effects of solvation, SCRF energies have been calculated at the MP2/6-31G(d) level, with dielectric constants values $\epsilon = 2.95$ (corresponding to THF), $\epsilon = 30.0$ (corresponding to HMPA), $\epsilon = 35.9$ (acetonitrile), $\epsilon = 36.7$ (DMF) and $\epsilon = 78.5$ (water - although not a common solvent in this type of rearrangement, it is worth including to see an extreme case of solvent polarisability). The relative energies are shown in Table 7.9. Although there are some small changes in going from the gas phase to a low polarity solvent and then to one of higher polarity (such as HMPA), there is little additional electrostatic effect from solvents with a large dielectric constant. As a final test of solvation, the SCRF energies were calculated at MP2/6-311+G(d,p) (the basis set recommended by Wong⁸⁷ for SCRF calculations), and essentially the same difference in relative energies was found (in keeping with our findings of Chapter 6).

Since there is a large change in the molecular energy of the ylide, there is an overall increase in activation energy for both pathways, however the Sommelet-Hauser rearrangement appears to be favoured by the inclusion of the electrostatic effects of solvation.

Table 7.9. Relative SCRF energies (in kJ mol⁻¹ from amine 2) for rearrangement of **1** at MP2/6-31G(d)

solvent	ϵ	ylide 1	[1,2] (3 + 4)	[3,2] 5
none	1.0	306	350	338
THF	2.95	290	348	327
HMPA	30.0	284	348	324
CH ₃ CN	35.9	283	348	324
DMF	36.7	283	348	324
H ₂ O	78.5	283	348	324
CH ₃ CN ^a	35.9	258	345	303

^a MP2/6-311+G(d) SCRF energy calculated at optimised UMP2/6-311+G(d,p) geometry

7.6. Effect of substitution on competing rearrangements

Now that the two sets of intermediates have been characterised, it is clear that they are very close in energy, with larger basis sets and more electron correlation tending to act in opposite ways. In order to investigate what causes a preference for one rearrangement over the other, this prototype rearrangement has been modified by substituting selected hydrogens with other functional groups.

Since the Stevens rearrangement is radical in nature, ylides which dissociate to form stable radicals would be expected to prefer the Stevens rearrangement. Ylides which are very unstable would also tend to favour breaking of the NC₃ bond to the two radical fragments. However, since this bond is also broken in the Sommelet-Hauser rearrangement, choosing an ylide which will dissociate easily may not cause the Stevens pathway to become any more preferred than the Sommelet-Hauser.

In the transition geometry of the Sommelet-Hauser rearrangement, the lone pair on the carbanion C₂ must be able to orient itself with the empty antibonding orbital corresponding to the C₄C₅ double bond. It is possible that this could be done sterically, using rigid cyclic systems, or electronically, by delocalising the C₄C₅ double bond and promoting its rotation, or by raising the energy of the lone pair on C₂ and thus encouraging bond formation of some description. Using electron-

withdrawing groups to stabilise the lone pair could have the effect of raising the activation energy of the Sommelet-Hauser rearrangement and thus causing a preference for the Stevens rearrangement. Heavily localising the double bond and making its rotation unfavourable could have the same effect.

In order to investigate these possibilities, a study of substituent effects, involving a variety of electron-withdrawing and electron-donating groups replacing the hydrogen atoms H₇ (being β to the lone pair on C₂) and H₁₂ (being β to C₅) has been undertaken at the PM3 level of theory. The absolute energies are not expected to be reliable, for the reasons seen in the study of the prototype rearrangement system; however our previous studies on ammonium ylides show that the trends in energies across a range of substituents should be similar to those predicted by ab initio calculations. Calling our original rearrangement of 1-2 rearrangement A, the substituted rearrangements are B-O. Structural geometries and energies for the ylides involved in these rearrangements calculated are presented in Table 7.10 and the concerted Sommelet-Hauser transition geometries in Table 7.11 along with energies of the Stevens rearrangement radicals. The Sommelet-Hauser transition geometries are presented in Figure 7.5, and the relative energies for each rearrangement calculated at PM3 are presented in Table 7.12.

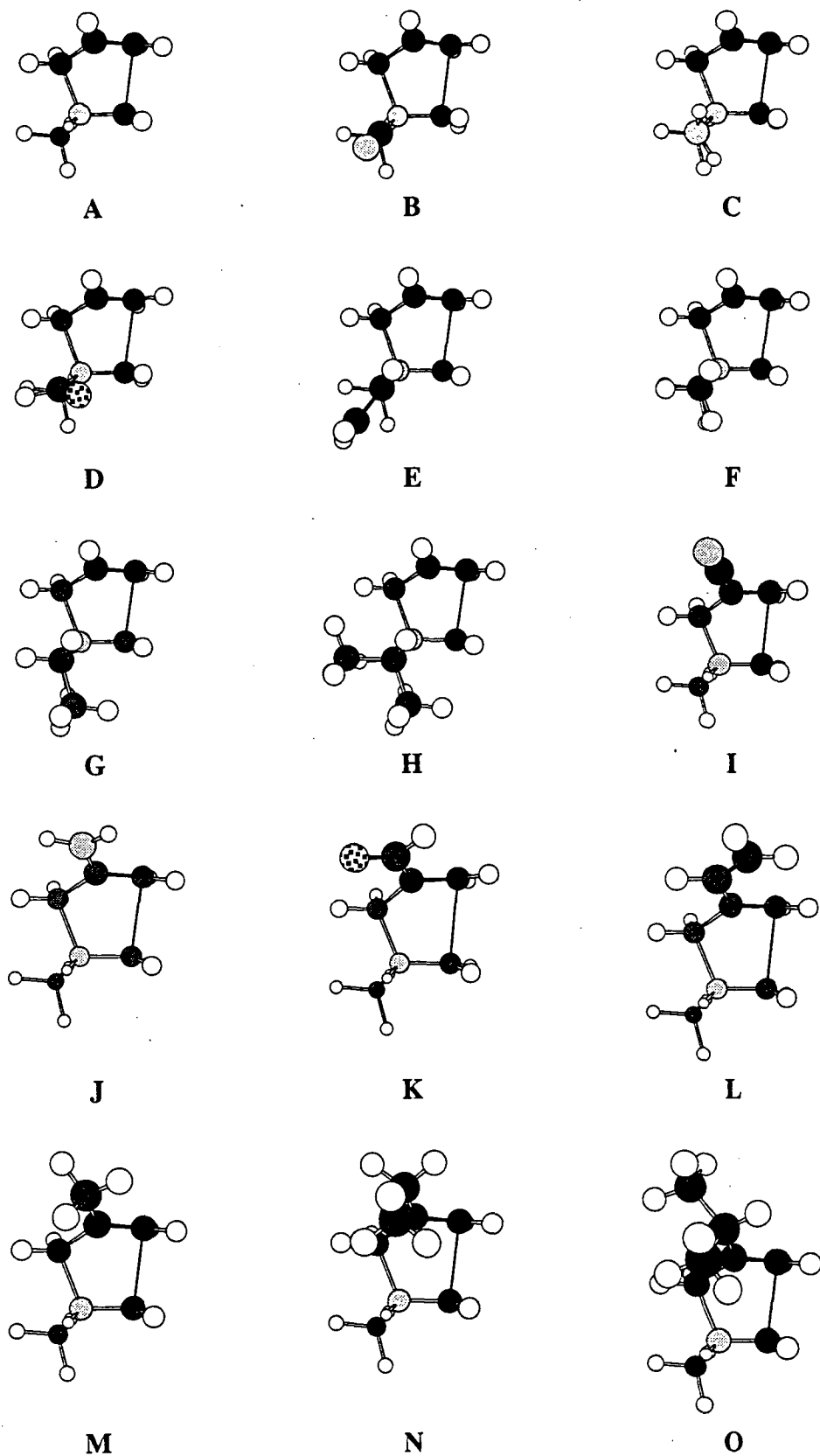


Figure 7.5. PM3 optimised geometries for Sommelet-Hauser transition geometries for rearrangements A-O

Table 7.10. Optimised structures for ylides involved in rearrangements A-O calculated at PM3

	A	B	C	D	E
NC ₂	1.370	1.353	1.365	1.376	1.376
NC ₃	1.567	1.537	1.534	1.536	1.600
C ₃ C ₄	1.486	1.491	1.494	1.491	1.485
C ₄ C ₅	1.327	1.327	1.328	1.328	1.329
NC ₆	1.524	1.522	1.516	1.518	1.523
C ₂ NC ₃	113.8	113.8	114.6	113.4	114.1
NC ₃ C ₄	112.5	112.9	115.0	112.8	112.4
C ₃ C ₄ C ₅	123.1	122.5	123.5	122.6	122.7
C ₃ NC ₆	106.1	109.1	109.1	108.9	103.8
C ₂ NC ₃ C ₄	190.3	301.8	294.0	301.4	300.6
NC ₃ C ₄ C ₅	131.4	121.8	69.07	124.0	89.35
C ₄ C ₃ NC ₆	64.67	174.7	165.9	175.3	179.6

	F	G	H	I	J
NC ₂	1.378	1.376	1.377	1.370	1.370
NC ₃	1.584	1.594	1.579	1.579	1.582
C ₃ C ₄	1.487	1.486	1.487	1.493	1.496
C ₄ C ₅	1.329	1.329	1.329	1.337	1.341
NC ₆	1.533	1.522	1.517	1.524	1.515
C ₂ NC ₃	113.8	113.7	113.0	114.1	113.3
NC ₃ C ₄	112.7	112.8	113.1	110.9	112.5
C ₃ C ₄ C ₅	122.6	122.6	122.7	122.7	121.3
C ₃ NC ₆	104.0	104.2	106.1	105.0	107.0
C ₂ NC ₃ C ₄	295.0	298.1	302.9	288.8	203.7
NC ₃ C ₄ C ₅	69.12	76.68	85.07	68.18	76.15
C ₄ C ₃ NC ₆	173.6	176.5	180.9	163.8	78.24

Table 7.10. (cont.)

	K	L	M	N	O
NC ₂	1.374	1.372	1.372	1.371	1.372
NC ₃	1.564	1.573	1.573	1.575	1.574
C ₃ C ₄	1.490	1.495	1.493	1.494	1.494
C ₄ C ₅	1.337	1.337	1.334	1.334	1.334
NC ₆	1.530	1.526	1.526	1.526	1.524
C ₂ NC ₃	114.1	114.6	114.7	114.8	114.7
NC ₃ C ₄	110.8	110.8	110.7	110.7	110.8
C ₃ C ₄ C ₅	120.9	120.7	121.2	121.0	120.8
C ₃ NC ₆	105.3	105.5	105.5	105.5	105.5
C ₂ NC ₃ C ₄	289.5	279.8	280.2	278.1	257.8
NC ₃ C ₄ C ₅	70.94	69.03	69.73	70.05	73.44
C ₄ C ₃ NC ₆	164.4	154.8	155.3	152.9	152.7

Table 7.11. Optimised geometries of concerted Sommelet-Hauser transition structures for rearrangements A-O.

	A	B	C	D	E
C ₂ C ₅	2.204	2.250	2.216	2.338	2.257
NC ₂	1.401	1.392	1.407	1.381	1.401
NC ₃	1.696	1.768	1.717	1.792	1.734
C ₃ C ₄	1.441	1.434	1.440	1.436	1.441
C ₄ C ₅	1.365	1.361	1.364	1.354	1.359
NC ₆	1.499	1.506	1.507	1.505	1.505
C ₂ NC ₃	111.2	110.3	110.4	110.6	110.2
NC ₃ C ₄	101.8	101.7	101.9	101.7	102.3
C ₃ C ₄ C ₅	114.9	116.2	115.1	117.3	115.8
C ₃ NC ₆	106.9	105.5	106.3	104.2	104.8
C ₂ NC ₃ C ₄	330.8	337.7	332.1	335.9	333.0
NC ₃ C ₄ C ₅	55.95	55.59	56.58	58.03	56.89
C ₄ C ₃ NC ₆	205.1	213.7	208.6	213.3	211.4

Table 7.11. (cont.)

	F	G	H	I	J
C ₂ C ₅	2.237	2.247	2.244	2.322	2.206
NC ₂	1.403	1.400	1.403	1.394	1.400
NC ₃	1.712	1.729	1.723	1.637	1.689
C ₃ C ₄	1.442	1.441	1.441	1.465	1.450
C ₄ C ₅	1.361	1.361	1.360	1.362	1.372
NC ₆	1.507	1.506	1.507	1.505	1.500
C ₂ NC ₃	110.2	109.8	109.3	112.1	111.3
NC ₃ C ₄	102.3	102.2	102.7	103.8	102.1
C ₃ C ₄ C ₅	115.3	115.5	115.5	116.4	114.4
C ₃ NC ₆	105.6	104.8	105.5	116.4	114.4
C ₂ NC ₃ C ₄	330.6	330.7	331.6	327.4	328.9
NC ₃ C ₄ C ₅	57.10	57.57	57.47	58.13	55.78
C ₄ C ₃ NC ₆	208.0	208.7	210.4	201.6	203.3

	K	L	M	N	O
C ₂ C ₅	2.355	2.254	2.202	2.206	2.207
NC ₂	1.396	1.399	1.402	1.401	1.402
NC ₃	1.612	1.645	1.686	1.684	1.681
C ₃ C ₄	1.467	1.461	1.447	1.448	1.449
C ₄ C ₅	1.360	1.368	1.369	1.368	1.369
NC ₆	1.507	1.504	1.500	1.500	1.500
C ₂ NC ₃	112.4	112.0	111.4	111.5	111.5
NC ₃ C ₄	104.2	103.1	102.1	102.3	102.3
C ₃ C ₄ C ₅	115.5	114.0	114.3	114.2	113.8
C ₃ NC ₆	115.5	114.0	114.3	114.2	113.8
C ₂ NC ₃ C ₄	324.3	327.2	330.2	331.1	330.3
NC ₃ C ₄ C ₅	60.66	57.73	55.85	55.73	56.28
C ₄ C ₃ NC ₆	198.4	201.4	204.5	205.2	204.4

Table 7.12. Relative energies of competing pathways (in kJ mol⁻¹) of rearrangements A-O at PM3

	N-sub	C-sub	ΔE (Stevens)	ΔE (S-H)	ΔE (S-H - Stevens)
A	H	H	4	51	47
B	CN	H	-19	60	79
C	NH ₂	H	1	60	59
D	CHO	H	-48	51	99
E	CH=CH ₂	H	-36	33	69
F	CH ₃	H	-26	37	63
G	CH ₂ CH ₃	H	-30	37	67
H	CH(CH ₃) ₂	H	-31	37	68
I	H	CN	1	25	24
J	H	NH ₂	9	54	45
K	H	CHO	4	22	18
L	H	CH=CH ₂	2	36	34
M	H	CH ₃	7	52	45
N	H	CH ₂ CH ₃	4	44	40
O	H	CH(CH ₃) ₂	4	46	42

7.6.1. Effects of substitution at nitrogen

Experimentally, direct substitution at N would be a difficult process. In most syntheses, groups directly substituted at N are alkyl or aryl in nature. From Table 7.12, it can be seen that the effect of all substituents at N (with the exception of NH₂) is a considerable lowering of the activation energy of the Stevens rearrangement. This is most likely due to highly substituted ylides being sterically, as well as electronically, unstable: dissociation to radicals would most likely occur with no energy barrier. Electron withdrawing groups on N show no clear trend with respect to the relative energy of the Sommelet-Hauser rearrangement; CN, NH₂ and CHO each stabilise the ylide relative to the Sommelet-Hauser transition geometry, however all substitutions at N indicate an increased preference for the Stevens rearrangement over the Sommelet-Hauser.

Looking at this from the point of view of molecular geometries, most substituents on N give rise to geometry changes in the Sommelet-Hauser transition state. The NC_3 bond is slightly longer in all cases, accompanied by a smaller C_2NC_3 angle, indicating that the transition state occurs further along the reaction pathway than in the unsubstituted case. Again, these changes are consistent with a higher degree of steric instability of the ylide, and are reflected in the facility of dissociation to the Stevens radical.

7.6.2. Effects of substitution at the double bond

Inspection of the relative energies of pathways involving substitution at C_4 show a number of interesting results. The range of substituents have very little effect on the activation energy of the Stevens rearrangement. This is to be expected, since the substituents are far enough removed from the NC_3 bond as to have little effect on the strength of that bond. Electron withdrawing groups (with the exception of NH_2) lower the activation energy of the Sommelet-Hauser rearrangement considerably, however electron-donating groups have little effect on the Sommelet-Hauser rearrangement barrier. This can be rationalised in terms of the double bond between C_4 and C_5 . The presence of electron withdrawing groups on C_4 would reduce the double bond character and allow more freedom of rotation, which is required for C_2 and C_5 to come into alignment for the Sommelet-Hauser rearrangement. Electron-donating groups may be expected to localise the double bond and hinder rotation, however that effect is not seen with the mildly electron-donating groups studied.

Inspection of the geometries of these species supports this hypothesis. The C_4C_5 bond is slightly longer in the substituted ylides, an indication of increased delocalisation. The C_3C_4 bond is also longer. The Sommelet-Hauser transition is an earlier transition structure, with a more open C_2NC_3 and NC_3C_4 angle.

7.6.3. *ab initio* studies of solvation

The *ab initio* optimisation of rearrangements **B-O** is, in general, beyond the computational power available. Single point MP2/6-31G(d) calculations on the optimised PM3 geometries, as outlined in chapter 4, would be possible, yet impractical as there are great differences between the PM3 and MP2/6-31G(d) optimised geometries involved in rearrangement **A**, and hence the single point energies would be unreliable.

In an attempt to have some *ab initio* results to back up the PM3 findings, transition geometries for **B** and **I** (involving a nitrile group) and **F** and **M** (involving a methyl group) have been optimised at RHF/6-31G(d). The only concerted transition geometry which has been successfully optimised at MP2/6-31G(d) is that for rearrangement **I**. Optimised geometries for the concerted transition structures are given in Table 7.13, and relative energies in Table 7.14.

At RHF/6-31G(d), rearrangements **B** and **I** show the same behaviour as they did at PM3. The difference in energy between the two pathways is increased in the case of electron-withdrawing functionality at N, and decreased when the nitrile group is co-ordinated to the double bond. The NC₃ bond is longer in **B**, however it is the NC₃C₄ angle which is tighter. In **I**, the Sommelet-Hauser transition structure resembles **A**, and at MP2/6-31G(d) it is predicted to be considerably favoured over the Stevens (recalling in **A**, the Sommelet-Hauser was favoured at UMP2, and the Stevens at ROMP2).

For methyl substitution (**F** and **M**), there is little real change to the energy differences, consistent with the trend seen at PM3. In each case the Stevens rearrangement is slightly favoured compared to **A**. The concerted transition geometries of **F** and **M** are very similar along the skeleton, both resembling more the substituted N geometries than the substituted double bond geometries.

Table 7.13. Optimised geometries for concerted [3,2] transitions at ab initio levels.

	A	B	F	I	M	F (MP2)
C ₂ C ₅	2.314	2.954	2.932	2.489	2.910	2.785
NC ₂	1.498	1.349	1.360	1.517	1.357	1.491
NC ₃	1.586	1.971	1.978	1.533	1.981	1.543
C ₃ C ₄	1.460	1.425	1.427	1.482	1.429	1.482
C ₄ C ₅	1.363	1.340	1.341	1.354	1.343	1.357
NC ₆	1.471	1.484	1.467	1.476	1.463	1.494
C ₂ NC ₃	111.2	117.5	115.6	111.2	117.8	111.1
NC ₃ C ₄	105.9	101.7	102.2	106.3	101.2	107.1
C ₃ C ₄ C ₅	110.9	120.9	121.9	114.3	119.3	117.9
C ₃ NC ₆	111.1	102.1	100.3	110.8	101.9	109.0
C ₂ NC ₃ C ₄	311.4	320.0	316.5	305.8	323.6	245.3
NC ₃ C ₄ C ₅	58.50	71.29	69.55	64.00	70.69	70.06
C ₄ C ₃ NC ₆	179.9	195.1	193.8	174.8	194.6	164.3

Table 7.14. Relative energy of the Sommelet-Hauser transition geometry (in kJ mol⁻¹ with respect to the Stevens transition intermediates) at various levels of theory.

	PM3	UHF/ 6-31G(d)	ROHF/ 6-31G(d)	UMP2/ 6-31G(d)	ROMP2/ 6-31G(d) ^a
A	47	212	136	-12	13
B	79	290	213		
F	63	233	156		
I	24	166	79	-70	-20
M	45	229	151		

^a Based on geometry optimised at UMP2/6-31G(d)

7.7. Conclusions

The competing transition geometries for both the [1,2] (Stevens) and [3,2] (Sommelet-Hauser) rearrangements of N-methyl-3-propenyl ammonium methylide have been characterised at semi-empirical and ab initio levels of theory. The Stevens rearrangement intermediates are the two radical species (as predicted over previous chapters), the Sommelet-Hauser intermediate involves orienting the lone pair of the

carbanion with the double bond in preparation for the formation of a carbon-carbon bond, and hence the barrier to the Sommelet-Hauser rearrangement is primarily controlled by steric factors. Electronic effects are important in determining geometries and hence can influence the steric effects.

The two rearrangements are predicted to be very close in energy. Too close, indeed, to assign a mechanism for this particular ylide. Increasing the size of the basis set shows a preference for the concerted [3,2] rearrangement, while increased levels of electron correlation show a stabilisation of the radical rearrangement. Calculations including the electrostatic effects of solvation using the SCRF formalism show a stabilisation of the concerted transition structure.

Investigation of the effects of substitution on this prototype rearrangement show that the degree of preference can be influenced by the functional groups present. The preference for the Stevens rearrangement occurs when there is an unstable onium part of the ylide assisting the breaking of the N-C bond before rotation. This is achieved with substitution about the amine causing a sterically favoured dissociation. The Sommelet-Hauser rearrangement can be promoted by delocalisation of the double bond involved in the rearrangement, since this bond has to rotate (and effectively lose its double-bond character). This seems to be favoured by electron-withdrawing substituents on the double bond. This would concur with the experimental evidence (described in Chapter 2) where there are several electron-donating and electron-withdrawing substituents around the aromatic ring. The effects of electron-donating groups are difficult to consider theoretically, however it is probable that electron-donating groups could localise the double-bond and prevent its rotation.

Chapter 8. Sulfonium ylides

8.1. Introduction

Ammonium ylides are not the only ylides used in synthesis - the Michael and Wittig reactions of phosphorus ylides are quite common, as are the Stevens and Sommelet-Hauser rearrangements of sulfonium ylides. Tanzawa⁹² and Hayashi⁹³ reported that there was no observed competition from a Stevens rearrangement in the rearrangement of S-methylbenzylsulfonium S-alkylides to the corresponding substituted benzylthiols, whereas we have seen that in the ammonium case, there can be considerable competition. Calculations have been performed on the sulfur analogue of the prototype ylide from Chapter 7, S-methyl-S-propenylsulfonium methylene. Optimised geometries for the Stevens and Sommelet-Hauser transition states, as well as the ylide and product thiol are found in Tables 8.1 and 8.2, a diagram of the [3,2] rearrangement in Figure 8.1 and the relative energies of ylides and the two rearrangements pathways in Table 8.3. For simplicity in comparison, the numbering system for individual atoms is the same as used for the nitrogen analogue (refer to Figure 7.1).

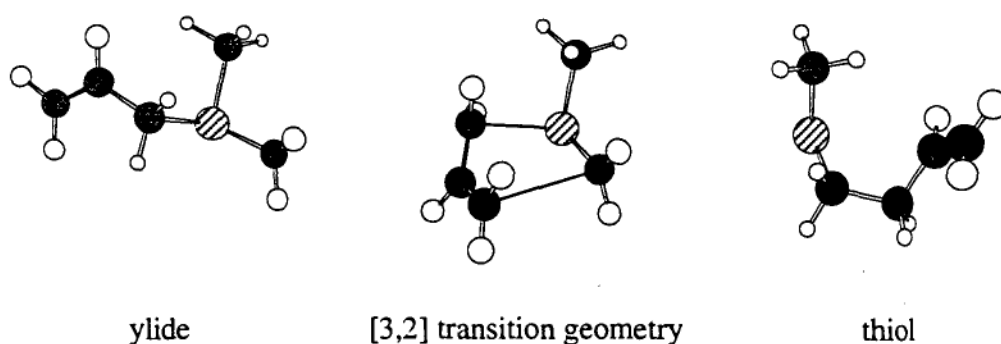


Figure 8.1. Optimised MP2/6-31G(d) geometries for species involved in the rearrangement of S-methyl S-propenyl sulfonium methylene

8.2. The Stevens [1,2] rearrangement of S-methyl-S-propenylsulfonium methylide

The most significant difference between the nitrogen and sulfonium ylide is in the nature of the charge-separated bond. In nitrogen ylides, this bond is quite long, but in the case of the sulfonium ylide, there is definite double bond character in C₂-S, both at PM3 and MP2/6-31G(d). This has been observed in previous theoretical calculations on ylides of heavier main-group elements⁹⁴. Dissociation of the ylide to the radical is predicted to have a slightly larger barrier (at the correlated level) than in the nitrogen case. Consistent with the bonding characteristic of the ylide, there is a longer C₂-S bond in the thiol radical. In the product thiol, this bond distance is typical of a C-S single bond.

8.3. The [3,2] rearrangement of S-methyl-S-propenylsulfonium methylide

The very short C₂-S bond is maintained in the optimised [3,2] transition geometry. In essence, the transition structure is similar to the nitrogen transition structure, the major difference between the ylide and the transition geometry being in bond rotation to orient the vacant π^* orbital of the double bond with the carbonyl lone pair. This lone pair is in a favourable position in the case of sulfonium ylides: due to the interaction with vacant p orbitals on the sulfur, the lone pair is expected to reside more perpendicular to the C-S bond. The lesser steric hindrance on S (which is also a considerably "larger" atom than N) allows for the smaller bond angles, this facilitates the orientation into position for the [3,2] rearrangement.

Table 8.1. PM3 optimised geometries for species involved in rearrangements of S-methyl S-propenyl sulfonium methyliide

	ylide	thiol	[3,2] transition	[1,2] radical
SC ₂	1.577	1.823	1.656	1.647
SC ₃	1.861		1.973	
C ₃ C ₄	1.478	1.327	1.433	
C ₄ C ₅	1.328	1.489	1.363	
SC ₆	1.826	1.802	1.813	1.807
C ₂ C ₅		1.520	2.240	
C ₂ SC ₃	104.9		99.16	
SC ₃ C ₄	112.4		103.9	
C ₃ C ₄ C ₅	123.5	123.2	117.7	
C ₆ SC ₃	96.37		101.9	
C ₆ SC ₂	105.5	103.6	103.3	104.2
SC ₂ C ₅		115.7		
C ₂ C ₅ C ₄		112.4		
C ₂ SC ₃ C ₄	168.7		339.9	
SC ₃ C ₄ C ₅	126.1		57.35	
C ₄ C ₃ SC ₆	60.78		234.1	
SC ₂ C ₅ C ₄		82.87		
C ₅ C ₂ SC ₆		129.7		
C ₃ C ₄ C ₅ C ₂		280.5		
E/eV	-930.77548	-932.66605	-930.20606	-499.51461

Table 8.2. MP2/6-31G(d) optimised geometries for species involved in rearrangements of S-methyl S-propenyl sulfonium methylene

	ylide	thiol	[3,2] transition	[1,2] radical
SC ₂	1.650	1.820	1.646	1.719
SC ₃	1.915		2.174	
C ₃ C ₄	1.487	1.340	1.438	
C ₄ C ₅	1.343	1.500	1.359	
SC ₆	1.806	1.811	1.803	1.808
C ₂ C ₅		1.533	2.944	
C ₂ SC ₃	117.5		110.9	
SC ₃ C ₄	112.6		100.8	
C ₃ C ₄ C ₅	123.7	124.2	122.0	
C ₆ SC ₃	95.06		92.73	
C ₆ SC ₂	104.9	100.2	104.5	100.3
SC ₂ C ₅		114.9		
C ₂ C ₅ C ₄		113.9		
C ₂ SC ₃ C ₄	172.1		321.5	
SC ₃ C ₄ C ₅	83.51		69.41	
C ₄ C ₃ SC ₆	62.43		214.8	
SC ₂ C ₅ C ₄		60.19		
C ₅ C ₂ SC ₆		110.1		
C ₃ C ₄ C ₅ C ₂		265.2		
E/a.u.	-593.413936	-593.413936	-593.310229	-476.470257 ^a

^a PUMP2 energy is -476.472558 a.u. ROMP2 energy is -476.470700 a.u.

Table 8.3. Relative energies (in kJ mol⁻¹ from thiol) of the competing rearrangement pathways of S-methyl S-propenyl sulfonium methylene

	ylide	[1,2] rearrangement	[3,2] rearrangement
PM3	182	220	237
UMP/6-31G(d)	269	350	272
PUMP2/6-31G(d) ^a		306	
ROMP2/6-31G(d) ^a		321	

^a Based on geometries optimised at UMP2/6-31G(d)

8.4. Conclusions

At the correlated level, the [3,2] rearrangement is considerably favoured over the [1,2]. There is a very small barrier to rearrangement calculated at MP2/6-31G(d) level, due to the facility of rotation and changes in the angles of C–S bonds as opposed to C–N. This would explain why there has been no competition observed from the [1,2] rearrangement, which is predicted to have an activation energy 50 kJ mol⁻¹ higher than the concerted process at ROMP2/6-31G(d).

There is still scope for more work to be done on the substituent and solvent effects, however the experimental evidence suggests that Sommelet-Hauser rearrangement of sulfonium ylides to be universally favoured over the Stevens, and further calculations are therefore unlikely to be necessary.

References

- (1) Markó, I. E. In *Comprehensive Organic Synthesis, Vol. 3*; Pergamon: Oxford, 1991; pp 913-974.
- (2) Bonneau, R.; Reuter, I. *J. Am. Chem. Soc.* **1994**, *116*, 3145-3146.
- (3) West, F. G.; Naidu, B. N. *J. Am. Chem. Soc.* **1993**, *115*, 1177-1178.
- (4) Tomioka, H.; Yamada, S.; Hirai, K. *J. Org. Chem.* **1995**, *60*, 1298-1302.
- (5) Vedejs, E.; Martinez, G. R. *J. Am. Chem. Soc.* **1979**, *101*, 6452.
- (6) Sato, Y.; Sakakibara, H. *J. Organomet. Chem.* **1979**, *166*, 303.
- (7) Shirai, N.; Watanabe, Y.; Sato, Y. *J. Org. Chem.* **1990**, *55*, 2767-2770.
- (8) Chelain, E.; Goumont, R.; Hamon, L.; Parlier, A.; Rudler, M.; Rudler, H.; Daran, J.-C.; Vaissermann, J. *J. Am. Chem. Soc.* **1992**, *114*, 8088-8098.
- (9) Stevens, T. S.; Creighton, E. M.; Gordon, A. B.; MacNicol, M. *J. Chem. Soc.* **1928**, 3193.
- (10) Mageswaran, S.; Ollis, W. D.; Sutherland, I. O. *J. Chem. Soc. Perkin. Trans I* **1981**, 1953.
- (11) West, F. N.; Glaeske, K. W.; Naidu, B. N. *Synthesis* **1993**, 977.
- (12) West, F. G.; Naidu, B. N. *J. Org. Chem.* **1994**, *59*, 6051.
- (13) Thomson, T.; Stevens, T. S. *J. Chem. Soc.* **1930**, 2107.
- (14) Campbell, A.; Houston, A. H. J.; Kenyon, J. *J. Chem. Soc.* **1947**, 93.
- (15) Wittig, G.; Mangold, R.; Felletschin, G. *Justus Liebig Ann. Chem.* **1948**, *560*, 116.
- (16) Hauser, C. R.; Kantor, S. W. *J. Am. Chem. Soc.* **1951**, *73*, 1437.
- (17) Woodward, R. B.; Hoffmann, R. *Angew. Chem., Int. Ed. Engl.* **1969**, *8*, 781.
- (18) Jemison, R. W.; Morris, D. G. *J. Chem. Soc. Chem. Commun.* **1969**, 1227.
- (19) Dewar, M. J. S.; Ramsden, C. A. *J. Chem. Soc. Perkin Trans. I* **1974**, 1839.

- (20) Ollis, W. D.; Rey, M.; Sutherland, I. O.; Closs, G. L. *J. Chem. Soc. Chem. Commun.* **1975**, 543.
- (21) Dolling, U. H.; Closs, G. L.; Cohen, A. H.; Ollis, W. D. *J. Chem. Soc. Chem. Commun.* **1975**, 545.
- (22) Stamegna, A. P.; McEwen, W. E. *J. Org. Chem.* **1981**, *46*, 1653-1655.
- (23) Ollis, W. D.; Rey, M.; Sutherland, I. O. *J. Chem. Soc. Perkin. Trans. 1* **1983**, 1009.
- (24) Stará, I. G.; Stary, I.; Tichy, M.; Závada, J.; Hanus, V. *J. Am. Chem. Soc.* **1994**, *116*, 5084-5088.
- (25) Mander, L. N.; Turner, J. V. *J. Org. Chem.* **1973**, *38*, 2915.
- (26) Bailey, T. S. Thesis, University of Tasmania, 1995.
- (27) Maeda, Y.; Shirai, N.; Sato, Y.; Tatewaki, H. *J. Org. Chem.* **1994**, *59*, 7897-7901.
- (28) Tao, Y.-T.; Saunders, W. H. *J. Am. Chem. Soc.* **1983**, *105*, 3183.
- (29) Sato, Y.; Shirai, N. *J. Pharm. Soc. Japan.* **1994**, *114*, 880-887.
- (30) Tanaka, T.; Shirai, N.; Sugimori, J.; Sato, Y. *J. Org. Chem.* **1992**, *57*, 5034-5036.
- (31) Usami, T.; Shirai, N.; Sato, Y. *J. Org. Chem.* **1992**, *57*, 5419-5425.
- (32) Kitano, T.; Shirai, N.; Motoi, M.; Sato, Y. *J. Chem. Soc. Perkin Trans. 1* **1992**, 2851.
- (33) Sato, Y.; Shirai, N.; Machida, Y.; Ito, E.; Yasui, T.; Kurono, Y.; Hatano, K. *J. Org. Chem.* **1992**, *57*, 6711-6716.
- (34) Sakuragi, A.; Shirai, N.; Sato, Y.; Kurono, Y.; Hatano, K. *J. Org. Chem.* **1994**, *59*, 148-153.
- (35) Szabo, A.; Ostlund, N. S. *Modern Quantum Chemistry: Introduction to Advanced Electronic Structure Theory*; McGraw-Hill: 1982.
- (36) Hehre, W. J.; Radom, L.; Schleyer, P. v. R.; Pople, J. A. *Ab Initio Molecular Orbital Theory*; Wiley-Interscience: 1986.
- (37) Stewart, J. J. P. *Reviews in Computational Chemistry* **1990**, *1*, 45.

- (38) Stewart, J. J. P. *Mopac 93.00 Manual*; Fujitsu Limited: Tokyo, Japan, 1993.
- (39) McWeeny, R.; Dierksen, G. *J. Chem. Phys.* **1968**, *49*, 4852.
- (40) Dewar, M. J. S.; Thiel, W. *J. Am. Chem. Soc.* **1977**, *99*, 4899.
- (41) Dewar, M. J. S.; Zoebisch, E. G.; Healy, E. F.; Stewart, J. J. P. *J. Am. Chem. Soc.* **1985**, *107*, 3902.
- (42) Stewart, J. J. P. *J. Comp. Chem.* **1989**, *10*, 209.
- (43) Binkley, J. S.; Pople, J. A.; Hehre, W. J. *J. Am. Chem. Soc.* **1980**, *102*, 939.
- (44) Frisch, M. J.; Pople, J. A.; Binkley, J. S. *J. Chem. Phys.* **1984**, *80*, 3265.
- (45) Hariharan, P. C.; Pople, J. A. *Chem. Phys. Lett.* **1972**, *66*, 217.
- (46) Krishnan, R.; Binkley, J. S.; Seeger, R.; Pople, J. A. *J. Chem. Phys.* **1980**, *72*, 651.
- (47) Amos, R. D.; Andrews, J. S.; Handy, N. C.; Knowles, P. J. *Chem. Phys. Lett.* **1991**, *185*, 256.
- (48) Cizek, J. *Adv. Chem. Phys.* **1969**, *35*, 148.
- (49) Pople, J. A.; Head-Gordon, M.; Raghavachari, K. *J. Chem. Phys.* **1987**, *87*, 5968.
- (50) Purvis, D.; Bartlett, R. J. *J. Chem. Phys.* **1982**, *76*, 1910.
- (51) Scuseria, G. E.; Janssen, C. L.; Schaefer III, H. F. *J. Chem. Phys.* **1989**, *89*, 7382.
- (52) Scuseria, G. E.; Schaefer III, H. F. *J. Chem. Phys.* **1989**, *89*, 7382.
- (53) Baker, J. J. *Comp. Chem.* **1986**, *7*, 385.
- (54) Cramer, C. J.; Truhlar, D. G. *Reviews in Computational Chemistry* **1995**, *6*, 1.
- (55) Rivail, J. L.; Terryn, B.; Ruiz-Lopez, M. F. *J. Mol. Struct. (Theochem)* **1985**, *120*, 387.
- (56) Klamt, A.; Schüürmann, G. *J. Chem. Soc. Perkin Trans 2* **1993**, 799-805.
- (57) Szafran, M.; Karelson, M. M.; Katritzky, A. R.; Koput, J.; Zerner, M. C. *J. Comp. Chem.* **1993**, *14*, 371-377.

- (58) Furuki, T.; Sakurai, M.; Inoue, Y. *J. Comp. Chem.* **1995**, *16*, 378-384.
- (59) Coolidge, M. B.; Stewart, J. J. P., MOPAC 6, QCPE #455
- (60) Stewart, J. J. P., MOPAC 93, Fujitsu Limited 1993
- (61) Frisch, M. J.; Head-Gordon, M.; Trucks, G. W.; Foresman, J. B.; Schlegel, H. B.; Raghavachari, K.; Robb, M.; Binkley, J. S.; Gonzalez, J. S.; Defrees, D. J.; Fox, D. J.; Whiteside, R. A.; Seeger, R.; Melius, C. F.; Baker, J.; Martin, R. L.; Kahn, L. R.; Stewart, J. J. P.; Topiol, S.; Pople, J. A., Gaussian 90, Revision F, Gaussian Inc. 1990
- (62) Frisch, M. J.; Trucks, G. W.; Head-Gordon, M.; Gill, P. M. W.; Wong, M. W.; Foresman, J. B.; Johnson, B. G.; Schlegel, H. B.; Robb, M. A.; Replogle, E. S.; Gomperts, R.; Andres, J. L.; Raghavachari, K.; Binkley, J. S.; Gonzalez, C.; Martin, R. L.; Fox, D. J.; Defrees, D. J.; Baker, J.; Stewart, J. J. P.; Pople, J. A., Gaussian 92, Revision B, Gaussian Inc 1992
- (63) Frisch, M. J.; Trucks, G. W.; Schlegel, H. B.; Gill, P. M. W.; Johnson, B. G.; Robb, M. A.; Cheeseman, J. R.; Keith, T.; Petersson, G. A.; Montgomery, J. A.; Raghavachari, K.; Al-Laham, M. A.; Zakrewski, V. G.; Ortiz, J. V.; Foresman, J. B.; Cioslowski, J.; Stefanov, B. B.; Nanayakkara, A.; Challacombe, M.; Peng, C. Y.; Ayala, P. Y.; Chen, W.; Wong, M. W.; Andres, J. L.; Replogle, E. S.; Gomperts, R.; Martin, R. L.; Fox, D. J.; Binkley, J. S.; Defrees, D. J.; Baker, J.; Stewart, J. J. P.; Head-Gordon, M.; Gonzalez, C.; Pople, J. A., Gaussian 94, Revision B.1, Gaussian Inc 1995
- (64) Rodriguez, C.; Hopkinson, A. *THEOCHEM* **1987**, *37*, 55.
- (65) Batista, L. A. E.; De Carvalho, A. M.; Amorim Da Costa, A. M.; Teixeira-Dias, J. J. C. *THEOCHEM* **1990**, *64*, 327.
- (66) Durig, J. R.; Li, Y. S. *J. Chem. Phys.* **1975**, *63*, 4110.
- (67) Hamada, Y.; Hashiguchi, K.; Hirakawa, A. Y.; Tsuboi, M. *J. Mol. Spectrosc.* **1983**, *102*, 123.
- (68) Fischer, E.; Botskor, I. *J. Mol. Spectrosc.* **1984**, *104*, 226.

- (69) Hamada, Y.; Tsuboi, M.; Yamanouchi, K.; Kuchitsu, K. *J. Mol. Struct.* **1986**, *146*, 253.
- (70) Boese, R.; Blaser, D.; Niederprum, N.; Nusse, M.; Brett, W. A.; Schleyer, P. v. R.; Buhl, M.; Hommes, N. J. R. v. E. *Angew. Chem. Intl. Ed. Engl.* **1992**, *31*, 314.
- (71) Yates, B. F.; Bouma, W. J.; Radom, L. *J. Am. Chem. Soc.* **1987**, *109*, 2250.
- (72) Pasto, D. *J. Am. Chem. Soc.* **1988**, *110*, 8164.
- (73) Peeters, D.; Leroy, G.; Matagne, M. *THEOCHEM* **1988**, *43*, 267.
- (74) Shinya, N.; Takasaki, M.; Sakata, N.; Harada, K. *Tetrahedron Lett.* **1983**, *24*, 3357.
- (75) Balenovic, K.; Bregant, D.; Cerar, D.; Fles, D.; Jambesic, I. *J. Org. Chem.* **1953**, *18*, 297.
- (76) Leroy, G.; Sana, M.; Wilante, C. *THEOCHEM* **1991**, *80*, 303.
- (77) Briend, M.; Lamy, A.; Peltre, M.-J.; Man, P. P.; Barthomeuf, D. *Zeolites* **1993**, *13*, 201.
- (78) Ter Brake, J. H. M.; Mom, V.; Mijlhoff, F. C. *J. Mol. Struct.* **1980**, *65*, 303.
- (79) Durig, J. R.; Cox, F. O. *J. Mol. Struct.* **1982**, *95*, 85.
- (80) Shephard, M. J.; Paddon-Row, M. N. *Aust. J. Chem.* **1993**, *46*, 547.
- (81) de Carvalho, B.; Teixiera-Dias, L. A. E. *THEOCHEM* **1993**, *282*, 211.
- (82) Frenking, G.; Kohler, K. F.; Reetz, M. T. *Tetrahedron* **1993**, *49*, 3971.
- (83) Peeters, D.; Leroy, G.; Wilante, C. *THEOCHEM* **1984**, *16*, 157.
- (84) Shaffer, S. A.; Furecek, F.; Cerny, R. L. *J. Am. Chem. Soc.* **1993**, *115*, 12115.
- (85) Kochi, J. K. E. *Free Radicals*; Wiley Interscience: New York, 1973.
- (86) Pine, S. *J. Chem. Educ.* **1971**, *48*, 99.
- (87) Wong, M. W.; Frisch, M. J.; Wiberg, K. B. *J. Am. Chem. Soc.* **1991**, *113*, 4776.

- (88) Vadja, E.; Tremmel, J.; Rozsondai, B.; Hargittai, I.; Maltsev, A. K.; Kagramanov, N. D.; Nefedov, O. M. *J. Am. Chem. Soc.* **1986**, *108*, 4352.
- (89) Gobbi, A.; Frenking, G. *J. Am. Chem. Soc.* **1994**, *116*, 9275-9286.
- (90) Glaser, R.; Choy, G. S.-C. *J. Phys. Chem.* **1994**, *98*, 11379-11393.
- (91) Dewar, M. J. S.; Healy, E. F.; Stewart, J. J. P. *J. Chem. Soc. Faraday Trans. II* **1984**, *3*, 227.
- (92) Tanzawa, T.; Ichioka, M.; Shirai, N.; Sato, Y. *J. Chem. Soc. Perkin. Trans. I* **1995**, 431.
- (93) Hayashi, Y.; Oda, R. *Tetrahedron Lett* **1968**, 5381.
- (94) Naito, T.; Nagase, S.; Yamakata, H. *J. Am. Chem. Soc.* **1994**, *116*, 10080.

Appendix A: Geometries and energies not explicitly incorporated in the text.

Table A.1. Energies of the planar methyl radical at various levels of theory (used throughout Chapters 3-6)

Basis set	ROHF	UHF	UMP2
3-21G	-39.339391	-39.342610	
6-31G(d)	-39.554723	-39.558992	-39.673031 (FU) ^a -39.668750 (FC) ^b
6-311G(d)	-39.562807	-39.567115	-39.702819 (FU)
6-311+G(d)	-39.563499	-39.567704	-39.703947 (FU) -39.685874 (FC)
6-311G(2d)		-39.567101	
6-31+G(d)		-39.561101	-39.703947 (FU) -39.685874 (FC)
6-311G(2df)		-39.569861	-39.709134 (FU)
6-31+G(d,p)			-39.694201 (FC)

^a Higher-level energies from this wavefunction: UMP3 -39.685136 a.u., UMP4 -39.684633 a.u., CCSD -39.688911 a.u.

^b PUMP2 energy is -39.561992 a.u., ROMP2 energy is -39.668540 a.u.

Table A.2. Optimised semi-empirical energies (in eV) for species involved in rearrangements 1-12 from Chapter 4.

	MNDO	AM1	PM3
1a	-406.53235	-404.13270	-358.04240
1y	-403.68833	-401.74543	-356.34439
1r	-391.20520	-389.47495	-341.58481
1c	-402.55074	-400.87755	-354.85864
2a	-563.00852	-560.00700	-507.66551
2y	-559.68870	-557.13208	-505.52124
2c	-558.73629	-555.51452	-503.59738
3a	-875.22505	-870.76833	-806.45188
3y	-871.15529	-867.45324	-803.83956
3r	-703.49156	-700.18547	-640.30314
3c	-870.63945	-866.17359	-802.25584
4a	-1012.56905	-1008.11669	-919.54883

Table A.2. (cont) Optimised semi-empirical energies (in eV) for species involved in rearrangements 1-12 from Chapter 4.

	MNDO	AM1	PM3
4y	-1010.60437	-1006.66512	-918.52567
4r	-841.11676	-837.94569	-753.85181
4c	-1008.95807	-1004.30273	-916.18547
5a	-1168.71479	-1163.53163	-1068.93249
5y	-1166.46754	-1161.92299	-1067.71069
5r	-997.38843	-993.40265	-903.17016
5c	-1165.05375	-1159.68598	-1065.52559
6a	-1324.64823	-1318.82065	-1218.31342
6y	-1321.94881	-1317.01113	-1216.79501
6r	-1153.32935	-1148.71871	-1052.52932
6c	-1320.73951	-1314.85125	-1214.69156
7a	-2147.62579	-2141.57273	-1990.30178
7y	-2144.93728	-2139.77238	-1988.80786
7r	-1976.32316	-1971.46179	-1824.53400
7c	-2143.71275	-2137.60538	-1986.71256
8a	-2147.62579	-2141.62404	-1990.22014
8y	-2144.68421	-2139.81329	-1988.76432
8c	-2143.35084	-2137.66587	-1986.64726
9a	-2970.42913	-2964.38259	-2762.23843
9y	-2967.66987	-2962.57540	-2760.77716
9c	-2966.32017	-2960.43249	-2758.73085
10a	-1658.33630	-1658.28922	-1556.63011
10y	-1655.85730	-1656.67993	-1555.34845
10r	-1487.04999	-1487.94417	-1390.79159
10c	-1654.52222	-1654.43732	-1553.20417
11a	-1658.12947	-1658.37754	-1556.26276
11y	-1655.34028	-1656.52742	-1554.74435
11c	-1654.86408	-1656.52742	-1554.74435
12a	-1991.76884	-1997.82412	-1894.51686
12y	-1989.21358	-1996.16330	-1893.26784
12c	-1988.38336	-1994.03710	-1892.051784
H	-11.90628	-11.39643	-13.07246
CH ₃	-169.28352	-167.83811	-163.34594
CH ₂ Ph	-992.39098	-990.91753	-935.53022
CH ₂ Br	-503.00416	-507.75788	-501.25590

Table A.3. Single-point MP2/6-31G(d)//PM3 and optimised MP2-631G(d) energies (in parentheses) for species involved in rearrangements 1-9 in Chapter 4.

	amine	ylide	radical ^a	concerted TS
1	-95.505752 (-95.506531)	-95.355375 (-95.338205)	-94.857825 (-94.860771)	-95.344505 (-95.357184)
2	-134.674246 (-134.675532)	-134.523613 (-134.552462)	--94.857825 (-94.860771)	-134.450101 (-134.466589)
3	-212.991760 (-212.995424)	-212.851394 (-212.883085)	-173.177908 (-173.181133)	-212.786778 (-212.799898)
4	-247.692260 (-247.697787)	-247.622473 (-247.644736)	-207.901875 (-207.894227)	-247.524864 (-247.538038)
5	-286.848591 (-286.854997)	-286.788062 (-286.809709)	--247.065284 (-247.064645)	-286.691930 (-286.737676)
6	-326.011523 (-326.016228)	-325.949707 (-325.964586)	-286.227014 (-286.222357)	-325.852955 (-325.895388)
7	-556.318123	-556.261822	-516.532665	-556.165656
8	-556.313576	-556.254107	-286.227014	-556.161650
9	-786.623965	-786.566548	-516.532665	-786.474121

^a Radical pair energies are the sum of the energies of the appropriate amino radical and either a hydrogen radical ($E=-0.498223$ a.u.), methyl radical ($E=-39.668408$ a.u. single point, -39.668750 a.u. optimised), or benzyl radical ($E=-269.983254$ a.u.).

Table A.4. Optimised PM3, and single point MP2/6-31G(d)//PM3 energies of ion-pair species involved in Chapter 5.

	PM3 (eV)	MP2/6-31G(d)//PM3 (a.u)
CH ₃ ⁺	-153.51315	-39.325174
CH ₃ ⁻	-162.40076	-39.583197
(CHO)HC-N(CH ₃) ₂ ⁺	-1045.33723	-286.007144
(CHO)HC-N(CH ₃) ₂ ⁻	-1053.81011	-286.231953
(PhCO)HC-N(CH ₃) ₂ ⁺	-1817.56566	-516.334285
(PhCO)HC-N(CH ₃) ₂ ⁻	-1825.91821	-516.547395
CH ₂ Ph ⁺	-927.94856	-269.741459
CH ₂ Ph ⁻	-937.00673	-269.974012

Table A.5. Optimised MP2/6-31G(d) geometries and energy for species involved in the rearrangement of H₃N-CH₂ (Chapter 5).

	ylide	amine	concerted TS
NC	1.563	1.465	1.666
H _A N	1.036		1.101
H _B N	1.020	1.018	1.015
H _C C	1.101	1.092	1.092
H _A C		1.100	1.463
H _A NC	121.5		59.74
H _B NC	107.3	109.5	103.5
H _C CN	101.8	108.8	116.3
H _A CN		115.4	
H _A NCH _C	54.23		123.4
H _B NCH _C	177.4	296.3	12.82
H _A CNH _B		57.87	
E/a.u.	-95.388205	-95.506531	-95.357184

Table A.6. Optimised energies (in a.u.) of methyl anion and cation (Chapter 5)

	CH ₃ ⁺	CH ₃ ⁻
RHF/3-21G	-39.009130	-39.237079
RHF/6-31G(d)	-39.230640	-39.465466
MP2/6-31G(d)	-39.325376	-39.602726

Table A.7. Energies (in eV) of the lowest energy conformations (by number of solvent molecules) of all species at PM3

	amine	ylide	concerted TG	amine radical	methyl radical	(CH ₃ CN) _n
0	-919.55246	-918.53052	-916.18989	-753.85556	-163.34787	
1	-1364.45496	-1363.51022	-1361.09168	-1198.77851	-608.22562	-444.78432
2	-1809.35789	-1808.48006	-1806.00841	-1643.71649	-1053.11691	-889.65163
3	-2254.25388	-2253.44715	-2250.94727	-2088.61076	-1497.99804	-1334.53882
4	-2699.15002	-2698.38716	-2695.86987	-2533.46653	-1942.94176	-1779.42817
5	-3144.09455	-3143.32749	-3140.77760	-2978.33753	-2387.78415	-2224.29214
6	-3588.97328	-3588.26886	-3585.70203			-2269.24406

Table A.8. Structural parameters, energies, a_0 values and dipole moments for ethanamine (C_s). SCRF results are at $\epsilon=35.9$ (Chapter 6).

	SCRF RHF/ 3-21G	SCRF RHF/ 6-31G(d)	SCRF RHF/ 6-311+G(d)	MP2/ 6-31+G(d,p)
$C_A C_B$	1.541	1.529	1.527	1.527
$C_A N$	1.476	1.456	1.457	1.464
$C_B H_C$	1.085	1.086	1.086	1.091
$C_B H_D$	1.085	1.087	1.086	1.091
$C_A H$	1.083	1.086	1.086	1.091
NH	1.006	1.003	1.000	1.015
$C_B C_A N$	114.4	115.6	115.5	115.7
$C_A C_B H_C$	111.1	111.2	111.1	111.2
$C_A C_B H_D$	110.5	111.1	111.2	110.6
$C_B C_A H$	109.7	109.6	109.7	109.7
$C_A N H$	112.8	110.2	110.9	110.5
$N C_A C_B H_D$	59.83	59.95	60.01	59.79
$H_C C_B C_A H$	58.79	58.15	58.13	58.39
$C_B C_A N H$	62.99	58.60	54.34	59.18
E/a.u.	-133.505448	-134.249075	-134.280720	-134.745040
(MP2-SCRF)		-134.676208	-134.736010	-134.745734
a_0	3.42	3.45	3.42	3.46
μ	1.6	1.7	1.7	1.7

Table A.9. Structural parameters, energies, a_0 values and dipole moments for methylammonium methylene (C_s). SCRF results are at $\epsilon=35.9$ (Chapter 6).

	SCRF RHF/ 3-21G	SCRF RHF/ 6-31G(d)	SCRF RHF/ 6-311+G(d)	MP2/ 6-31+G(d,p)
NC_B	1.506	1.480	1.481	1.497
NC_A	1.636	1.565	1.547	1.524
C_BH_C	1.082	1.083	1.083	1.091
C_BH_D	1.078	1.080	1.079	1.086
C_AH	1.101	1.097	1.094	1.095
NH	1.009	1.004	1.001	1.018
C_BNC_A	117.7	120.0	119.8	120.7
NC_BH_C	111.2	111.2	110.7	111.1
NC_BH_D	107.8	108.3	108.6	107.5
NC_AH	100.0	101.4	102.9	104.3
C_ANH	110.3	109.2	109.0	108.9
$C_ANC_BH_C$	59.11	59.20	59.36	58.79
$C_ANC_BH_D$	53.75	53.72	54.79	56.98
$H_A C_A NH$	58.98	57.00	56.97	57.00
E/a.u.	-133.412507	-134.146867	-134.177084	-134.630314
(MP2-SCRF)		-134.561797	-134.635166	-134.641272
a_0	3.46	3.45	3.48	3.51
μ	6.6	6.5	7.2	7.2

Table A.10. Structural parameters, energies, a_0 values and dipole moments for aminofmethyl radical (C_s). SCRF results are at $\epsilon=35.9$ (Chapter 6).

	SCRF UHF/ 3-21G	SCRF UHF/ 6-31G(d)	SCRF UHF/ 6-311+G(d)	UMP2/ 6-31+G(d,p)
CN	1.404	1.402	1.399	1.398
CH	1.074	1.076	1.076	1.079
NH	0.998	0.999	0.996	1.009
HCN	116.4	115.8	116.0	115.8
CNH	118.1	113.2	114.0	115.1
cis-HCNH	134.4	46.31	44.70	42.03
tr-HCNH	145.2	124.9	127.3	131.3
E/a.u.	-94.063789	-94.587199	-94.613304	-94.907097
(MP2-SCRF)		-94.861291	-94.907275	-94.907560
a_0	1.02	3.08	3.02	3.11
μ	1.0	1.1	1.0	1.2

Table A.11. Structural parameters, energies, a_0 values and dipole moments for concerted transition geometry between methylammonium methylene and ethanamine. SCRF results are at $\epsilon=35.9$ (Chapter 6).

	SCRF RHF/ 3-21G	SCRF RHF/ 6-31G(d)	SCRF RHF/ 6-311+G(d)	MP2/ 6-31+G(d,p)
NC _B	1.894	1.892	1.938	1.842
NC _A	1.552	1.498	1.493	1.492
C _B C _A	2.068	2.075	2.119	2.081
C _B H _C	1.080	1.079	1.074	1.094
C _B H _D	1.072	1.070	1.069	1.082
C _B H _E	1.070	1.071	1.070	1.082
C _A H _A	1.092	1.095	1.094	1.095
C _A H _B	1.086	1.086	1.086	1.084
NH _F	1.014	1.004	1.008	1.037
NH _G	1.005	1.000	0.996	1.011
CNC	72.98	74.48	75.07	76.46
NC _B H _C	90.79	91.06	89.69	92.97
NC _B H _D	124.7	121.0	120.3	120.9
NC _B H _E	103.3	105.5	103.5	108.6
NC _A H _A	110.9	111.8	112.3	113.7
NC _A H _B	135.8	139.7	140.1	139.9
C _B NH _F	105.9	106.7	107.3	108.6
C _B NH _G	101.2	99.08	98.24	94.49
C _A NC _B H _C	159.0	161.9	159.3	162.3
C _A NC _B H _D	42.33	45.85	42.49	46.88
C _A NC _B H _E	272.5	275.7	274.0	275.9
C _B NC _A H _A	147.4	151.4	153.0	154.8
C _B NC _A H _B	266.0	269.1	271.4	277.6
H _C C _B NH _F	43.85	43.76	41.38	38.18
H _C C _B NH _G	268.8	272.0	269.9	273.8
E/a.u.	-133.298328	-134.025441	-134.060087	-134.539967
(MP2 SCRF)		-134.468425	-134.535102	-134.542151
a_0	3.44	3.46	3.44	3.50
μ	3.0	3.2	3.6	3.3

Table A.12. SCRf ($\epsilon=35.9$) energies and cavity radius (in Å) at MP2/6-31G(d) for species involved in rearrangements 3, 4, 5 (Chapter 6).

		rearrangement 3	rearrangement 4	rearrangement 5
amine	E	-212.993928	-247.699539	-286.856509
	a_0	3.94	3.75	3.95
ylide	E	-212.888237	-247.652398	-286.814717
	a_0	3.95	3.70	3.92
radical	E	-173.181361	-207.906305	-247.071013
	a_0	3.69	3.40	3.69
concerted TS	E	-212.801152	-247.543137	-286.709266
	a_0	3.93	3.71	3.94

Table A.13. Energies (in eV) of the lowest energy conformations of all species at COSMO PM3 as a function of number of acetonitrile molecules (Chapter 6)

	amine	ylide	concerted TG	amine radical	methyl radical	(CH ₃ CN) _n
0	-919.98747	-919.70171	-916.77013	-754.53010	-163.35848	
1	-1365.23495	-1364.87056	-1362.03621	-1199.74740	-608.61534	-445.16197
2	-1810.57992	-1810.00205	-1807.35327	-1644.95582	-1053.86689	-890.42279
3	-2255.74902	-2255.33946	-2252.67862	-2090.07515	-1499.07328	-1335.58370
4	-2701.03144	-2700.62832	-2697.94264	-2535.07103	-1944.18155	-1780.74021
5	-3146.26732	-3145.75068	-3143.19066			-2226.02265

Table A.14. SCRf MP2/6-31G(d) energies (in a.u.) at a range of ϵ values of species 1-5 from Chapter 7.

ϵ	1	2	3	4	5
2.95	-250.849753	-250.960282	-134.017520	-116.810216	-250.835556
30.0	-250.852374	-250.960366	-134.017703	-116.810217	-250.836885
35.9	-250.852432	-250.960368	-134.017707	-116.810217	-250.836914
36.7	-250.852439	-250.960368	-134.017707	-116.810217	-250.836918
78.5	-250.852545	-250.960373	-134.017718	-116.810217	-250.836997
35.9 ^a	-251.051184	-251.149601	-134.125697	-116.892631	-251.034247

^a MP2/6-311+G(d,p) energy

Table A.15. PM3 optimised energies (in eV) of species involved in rearrangements A-O from Chapter 7.

	ylide	[1,2] transition	[3,2] transition
A	-921.83880	-921.30794	
B	-1185.51181	-1184.89436	-754.84449
C	-1048.47158	-1097.84717	-667.59562
D	-1333.29771	-1332.76779	-902.92760
E	-1188.42893	-1188.08245	-757.93338
F	-1070.90123	-1070.51381	-640.30503
G	-1220.42615	-1220.04703	-789.87065
H	-1369.95272	-1369.57194	-939.40397
I	-1186.10137	-1185.84261	-695.15638
J	-1099.77732	-1094.21170	-608.75693
K	-1333.86165	-1333.63879	-842.88917
L	-1189.04341	-1188.66940	-698.09505
M	-1071.57004	-1071.03613	-580.56144
N	-1221.01523	-1220.55085	-730.04681
O	-1370.54770	-1370.07064	-879.57396

Table A.16. Optimised ab initio energies (in a.u.) of substituted rearrangements from Chapter 7.

		[1,2]	[3,2]
B	UHF/6-31G(d)	-225.340276	-341.697863
	ROHF/6-31G(d)	-225.336284	
F	UHF/6-31G(d)	-172.644976	-289.024225
	ROHF/6-31G(d)	-172.640852	
I	UHF/6-31G(d)	-208.203485	-341.755364
	ROHF/6-31G(d)	-208.174262	
	UMP2/6-31G(d)	-208.811419	-342.856946
	ROMP2/6-31G(d)	-208.828686	
M	UHF/6-31G(d)	-155.504277	-289.032183
	ROHF/6-31G(d)	-155.478389	